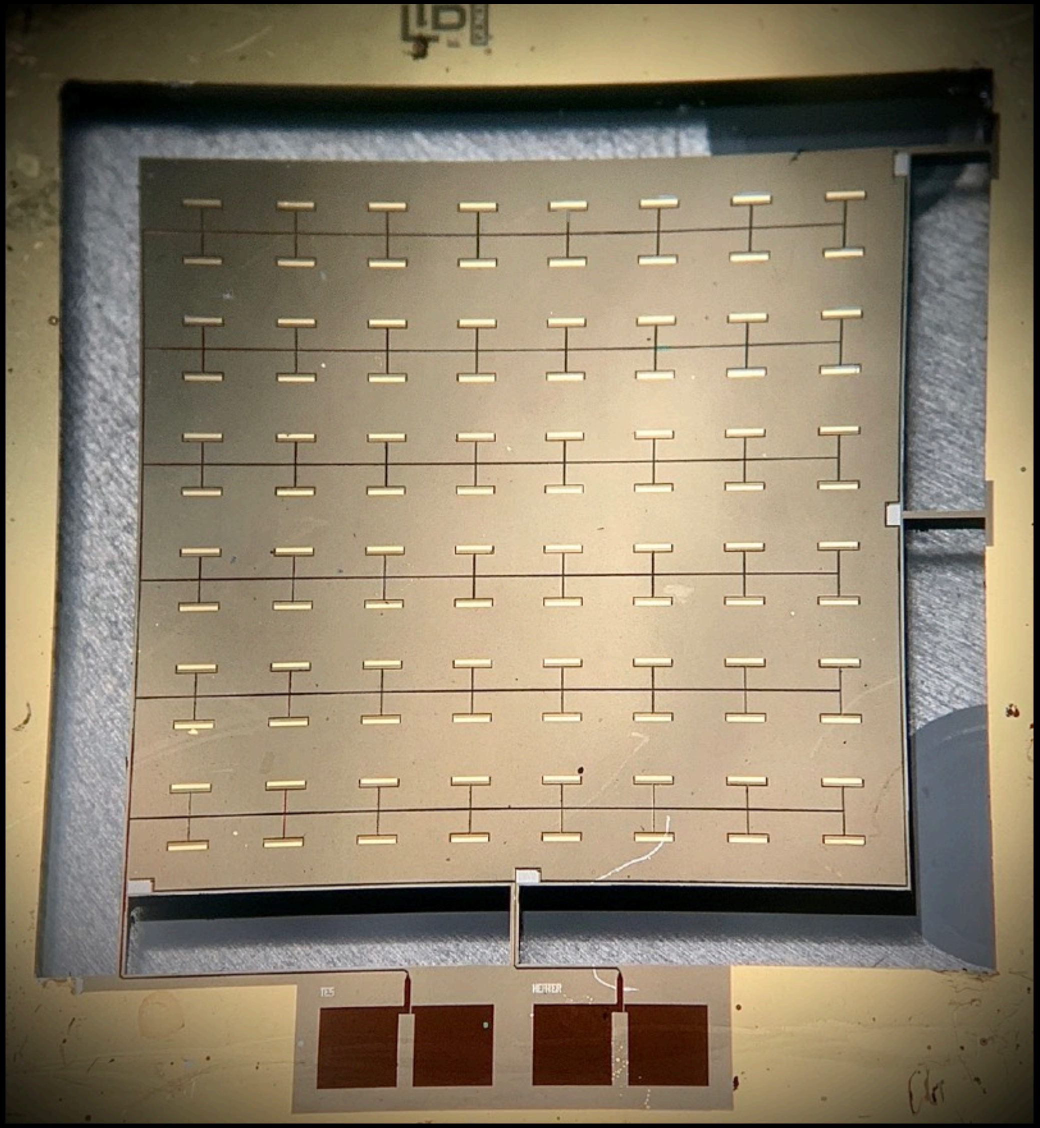

Superconduting radiation detectors

F.Gatti
University and INFN of Genova

EASIS School 3, Genoa - Setember 30, 2020

Origins of thermal radition detectors

S. Langley, "The Bolometer," *Nature*, vol. 25, p. 14, 1881.

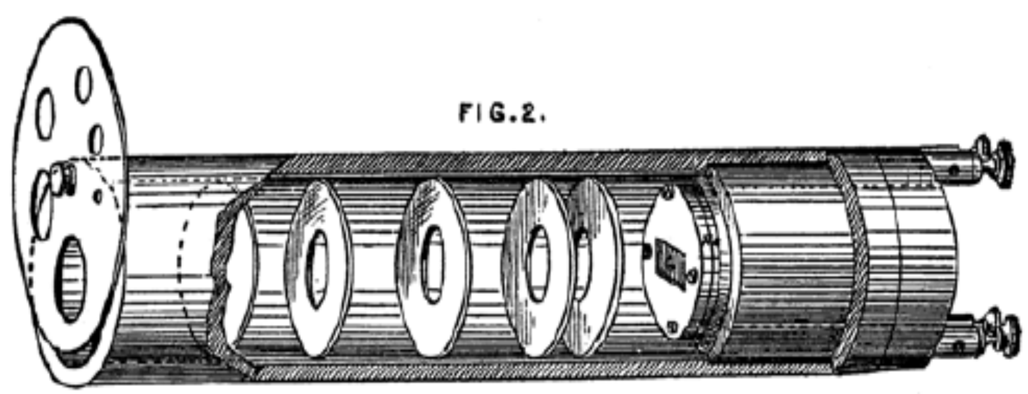

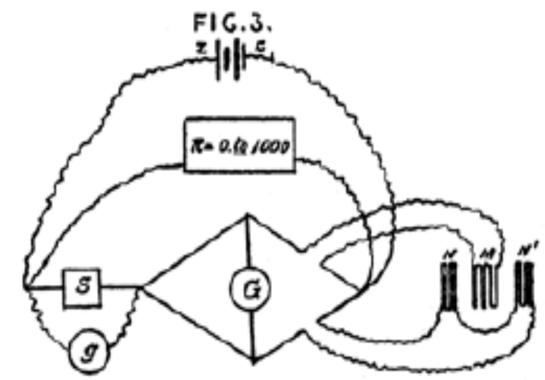

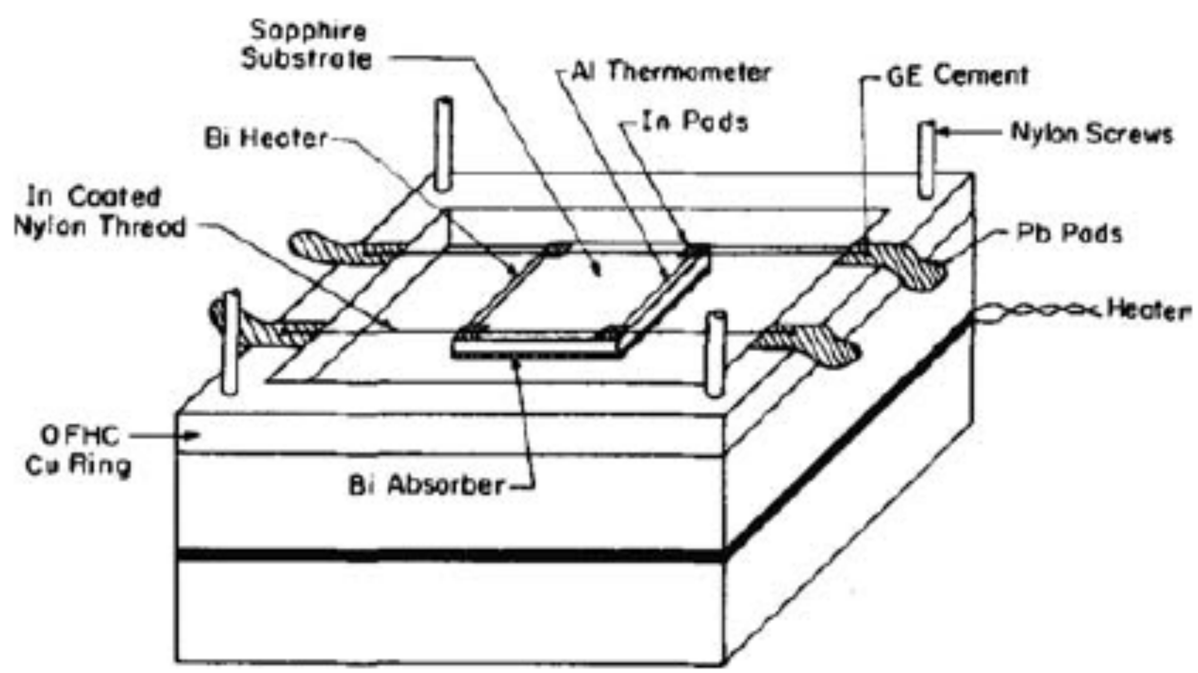

Clarcke et al. 1977

NEP $10^{-13} – 10^{-12}$ W/Hz

Origins of thermal radition detectors

Single particle detection with thermal detector in1949: a technique incredibly similar to the present TES detectors

The Effect of Alpha-particles on a Superconductor*

D. H. Andrews, R. D. Fowler and M. C. Williams
Chemistry Department, The Johns Hopkins University, Baltimore, Maryland

May 9, 1949

Superconducting bolometers have been bombarded with alpha-particles from a polonium source, and it is found that countable electrical pulses are produced, one for each particle impact. The bolometer used in the experiment reported here was made of a strip of columbium nitride, approximately $3.5\times 0.4 \times 0.006$ mm, mounted with bakelite lacquer on a copper base, and maintained at the operating temperature of 15.5°K in a cryostat, as previously described;[1] its time constant was about 10^{-3} sec.

To provide a mounting for the polonium source, a glass tube *ca.* 30 cm long and 3 cm diameter was sealed to the cryostat nose facing the bolometer. The source could be slid back and forth in this tube, placing it at distances from the bolometer ranging from 2 cm to 20 cm.

The source consisted of polonium on a nickel disk 1 cm diameter, attached to the face of a steel cylinder. A vacuum of better than 10^{-6} cm was maintained in the source tube and around the bolometer by a charcoal trap at liquid nitrogen temperature aided by the many contiguous surfaces at 15°K, so that the α-particles traveled from the source to the bolometer with no significant loss

Table I. Comparison of α-particle counts with ionization chamber and bolometer.

Distance from source to defining area: Average counts per second:	20 cm	2 cm
(a) Ionization chamber	40	740
(b) Bolometer	32	660

of energy. The bolometer was protected from general heat radiation by a shield held at 90°K. The α-particles passed through a hole in this shield, the opening being 7 mm diameter, in alignment with the bolometer.

The bolometer was connected to a direct current supply, and by potential leads to the primary of an audio transformer, the secondary of which led to a pulse amplifier, and thence to an oscilloscope, and scale-of-1000 counter.

The rate of counting was at a maximum when the CbN was maintained in the center of the transition, half-way between normal and super conductivity; it was relatively constant over a central interval 0.04° wide and fell sharply both above and below this temperature zone, being reduced approximately to noise level by an increase or decrease of 0.1°K. The electrical resistance of the strip was 2ω in the normal state at 15°K.

The number of counts per second was also a function of the direct current flowing through the CbN, being at a maximum for a current of 40 ma.

The number of α-particles counted with the bolometer agreed, as shown in Table I, with the number counted with an ionization chamber and linear amplifier when the ionization chamber was exposed to the source through a slit system similar in geometry to that in the bolometer experiments. The ionization chamber slit was covered with a thin mica window, and the air pressure in the source tube kept at 0.01 mm.

From photographs of the peaks on the oscilloscope it is estimated that each individual pulse from the bolometer is about 10^{-7} volt high and 10^{-4} second wide. The maximum signal to noise ratio was 3 to 1. Since the pulse height may be expected to be proportional to the energy of the α-particle, experiments are being continued to increase the signal to noise ratio, in order to evaluate the precision with which the energy of individual particles can be measured by this method, and to determine the kind of pulses produced when superconducting bolometers of this and other materials are exposed to different kinds of particle radiation. The authors wish to thank Professor Walter Koski and Mr. Carl Thomas for valuable advice and assistance.

* This work was supported in part by contract N5-ORi-166, Task IV, ONR U. S. Navy, and in part by a grant from Dr. H. A. B. Dunning.
[1] Andrews, Milton, and DeSorbo, J. Opt. Soc. Am. **36**, 518 (1946).

Origins of thermal radiation detectors

A Superconducting Bolometer as a High Sensitivity Detector for Molecular Beams

M. Cavallini, G. Gallinaro, and G. Scoles

Istituto di Fisica Sperimentale dell'Università, 16132 Genova, Italy

Gruppo Nazionale di Struttura della Materia del C.N.R.

(Z. Naturforsch. 24 a, 1850—1851 [1969]; received 31 July 1969)

The construction, operation and calibration of a superconducting bolometer is reported. Operated as a molecular beam detector the bolometer has, for Argon, a maximum sensitivity of $7 \cdot 10^6$ molecules sec^{-1} corresponding to a N.E.P. of $3 \cdot 10^{-13}$ Watt Hz$^{-\frac{1}{2}}$.

The use of a liqu… as a high sensitivity… beams has been rec… in molecular scatteri…

The present note … struction, operation … ing bolometer which … detector, showed an … in signal to noise r… used Ge bolometer.

A superconducting … most ten years ago, … showed a noise equ… $3 \cdot 10^{-12}$ Watt Hz$^{-\frac{1}{2}}$ … a time constant of … element was an eva…

… resistance that can be used to transduce a chopped power imput to a voltage output which may then be integrated with standard techniques.

Up to the present time the superconducting bolometer has not been widely adopted in infrared spectroscopy for two main reasons. The first is the difficulty of thermo-regulating the sensitive element within 10^{-5} °K, and the second is the extreme delicacy of its construction.

Taking into account that the N.E.P. of Martin and Bloor's bolometer was reported to be limited by the electronics available at that time, we undertook the development of a superconducting bolometer with the …

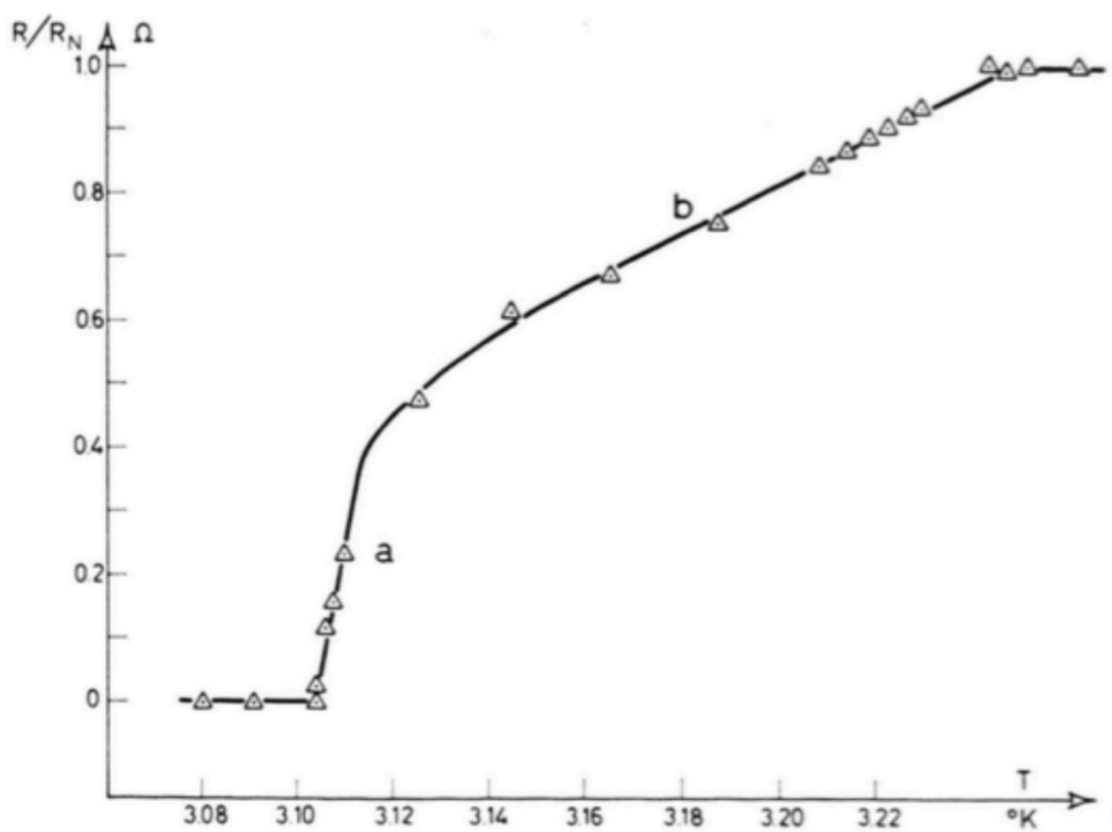

Fig. 1. Transition curve of a typical bolometer.

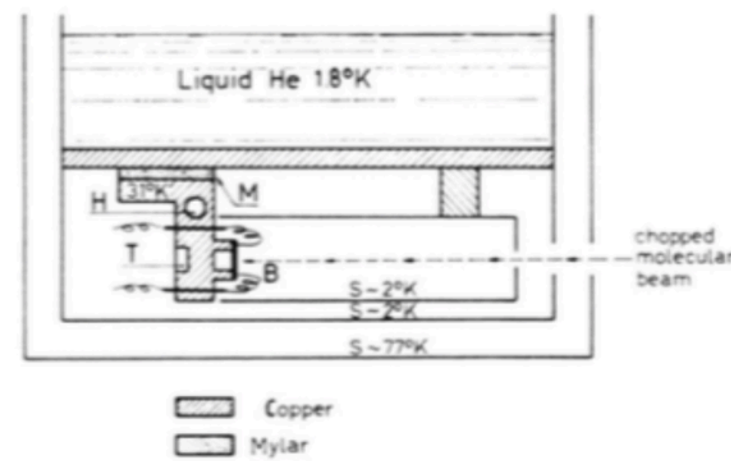

Fig. 2. Schematic experimental set-up.

How superconducting TES based detector works.

High quality film with “steep” superconducting to normal transition is needed

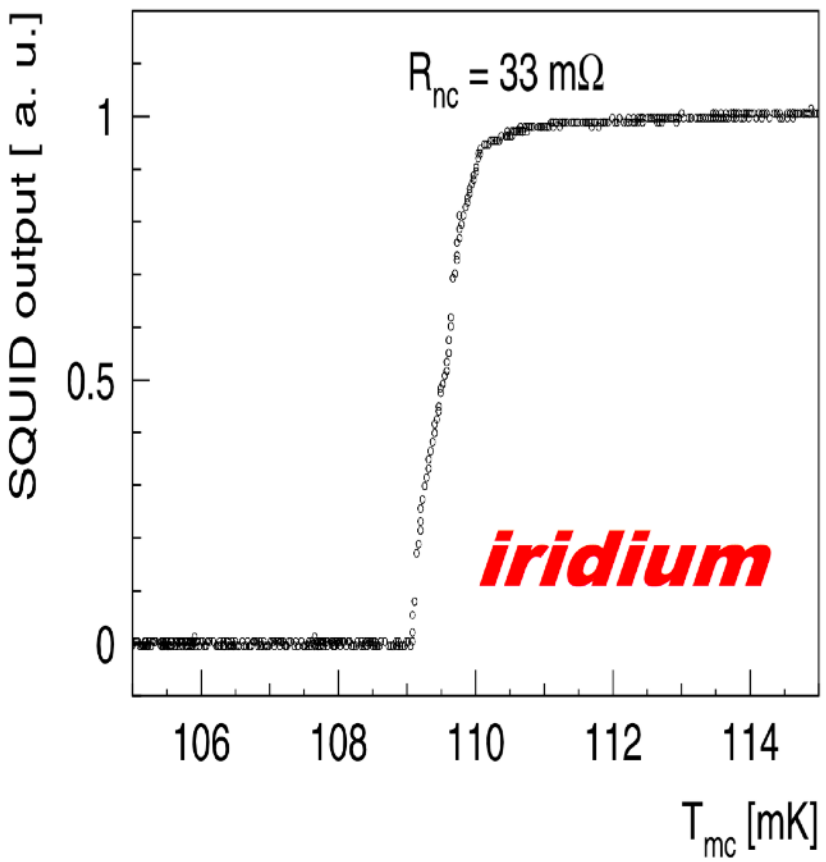

	ρ_{el}[1] ($\mu\Omega$·cm)	n[2] ($10^{28}/m^3$)	v_F[2] (10^6m/s)	γ[1] (mJ/mole·K^2)	ρ/A (mole/cm^3)	T_c[1] (K)	$\lambda_L(0)$ (nm)
Al	2.74	18.1	2.03	1.35	0.100	1.140	16[1]
Ti	43.1	10.5	.041[4]	3.35	0.0944	0.39	310[4]
Mo	5.3	38.6	0.60[4]	2.0	0.107	0.92	
W	5.3	37.9	0.70[4]	1.3	0.105	0.012	82[5]
Ir	5.1	63.4	0.36[6]	3.1	0.117	0.140	29[6]
Nb	14.5	27.8	0.62[3]	7.79	0.0922	9.5	39[7], 88[8]
Cu	1.70	8.47	1.57	0.695	0.141	-	-
Ag	1.61	5.86	1.39	0.646	0.0974	-	-
Au	2.20	5.90	1.40	0.729	0.0983	-	-
Bi	116.	14.1	1.87	0.008	0.0468	-	-

TES films are usually in the dirty limit: coher. lenght ξ~1 μm , electron mean free path L~ 10 -100 nm (almost a 2D system)

G-L parameter k_{GL} ~ 0.7 λ_L/L(t), where t is the film thickness.

k_{GL} moves over the full range of the G-L value for Type I and Type II superconducors depending on the tickness t used for specific apllication.

In both cases a finite transition width is expected (and obsevated), even if the phenomena underlying the TES operation with current bias are different and complex to be fully exploited in precision models.

How superconducting TES based detector works.

The listed pure elements have only few Tc, but the actual detetctor must worrk at a temperature that is the best compromise among input power, overall noise and best operating temperrature of the cooler: Tc must be adjusted !

A first method is the proximization effect in multilayer structure Superconductind Metal - Normal Metal. Usadel Theory is often used (K.D. Usadel, Phys. Rev. Lett. **25**, 507 (1970)).

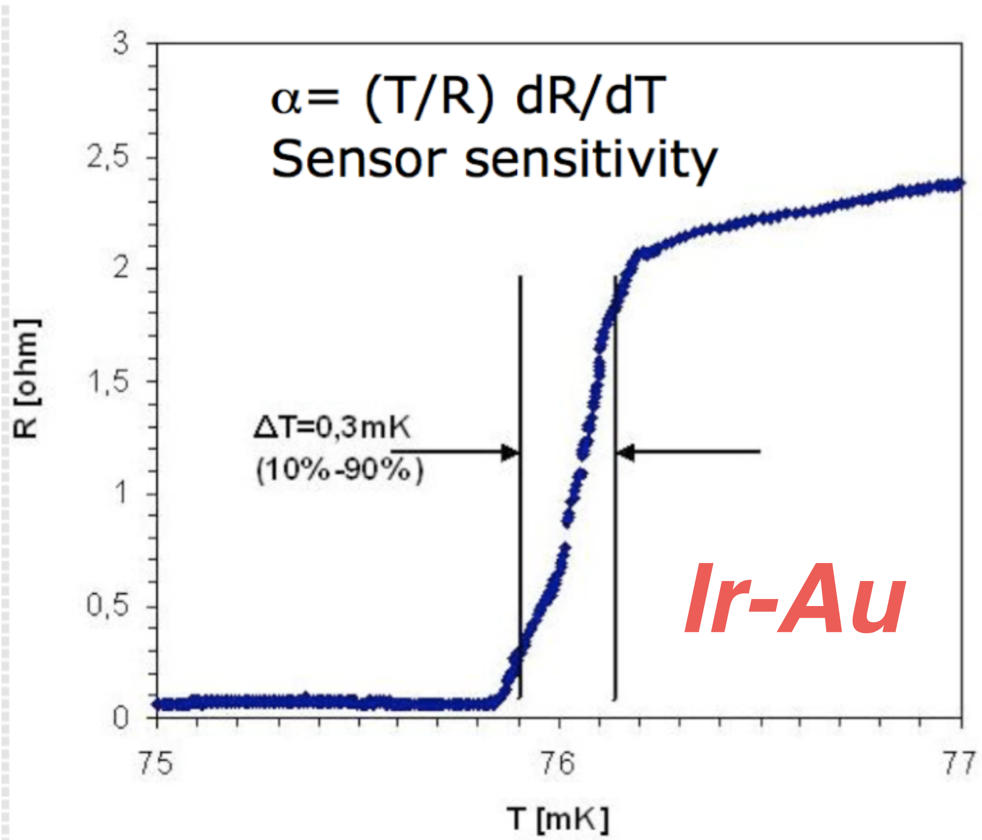

$$
\begin{aligned}
T_c &= T_{c0}\left[\frac{d_s}{d_0}\frac{1}{1.13(1+1/\alpha)}\frac{1}{t}\right]^{\alpha} \\
\frac{1}{d_0} &= \frac{\pi}{2}k_B T_{c0}\lambda_f^2 n_s, \\
\alpha &= d_n n_n / d_n n_s.
\end{aligned}
$$

d, film tickness; n, electron density at Fermi level; 0< t <1, electron interface transmission; Tco, superconductor transition temperature; λ_f , Fermi wavelenght.

.

How superconducting TES based detector works.

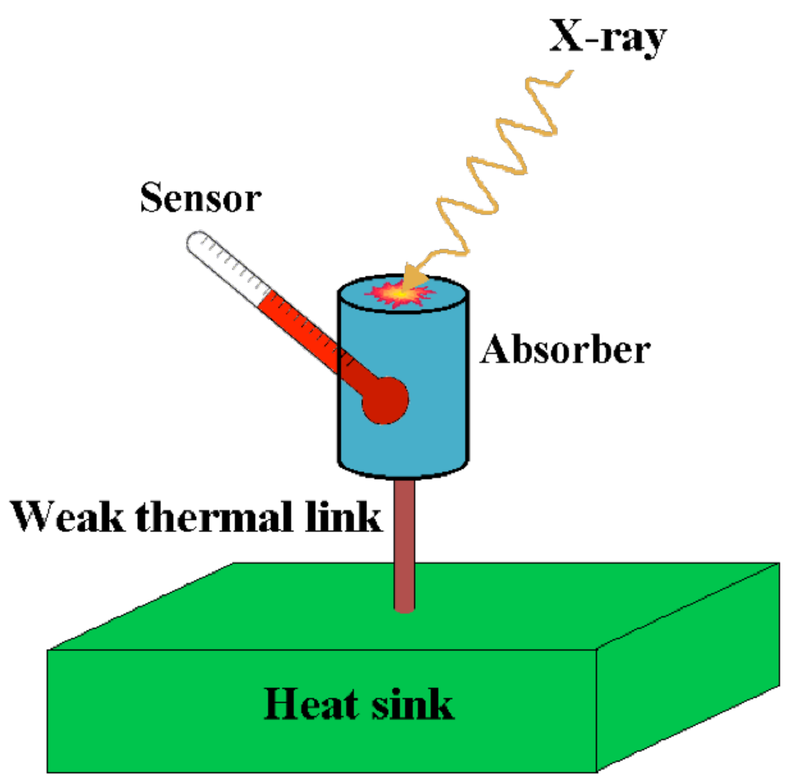

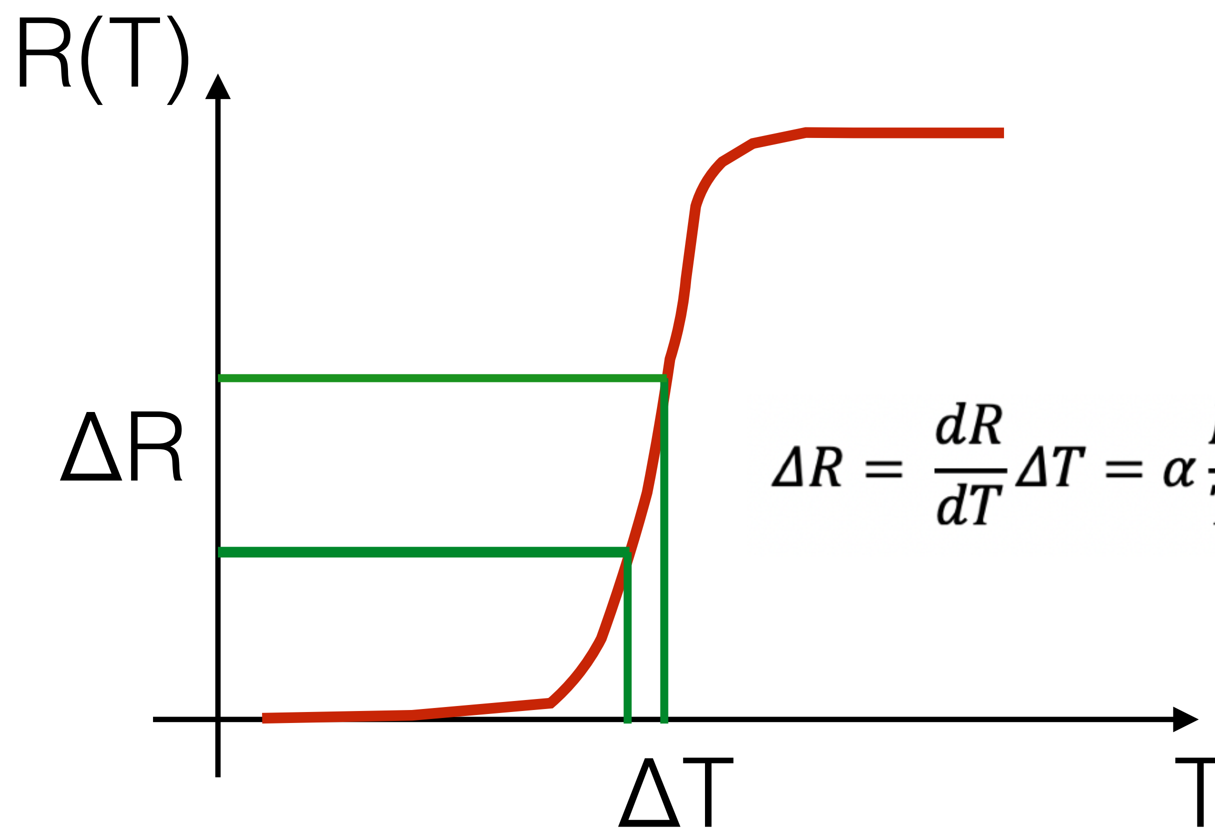

$$\Delta R = \frac{dR}{dT}\Delta T = \alpha \frac{R}{T}\Delta T \qquad \alpha = \frac{T}{R}\frac{dR}{dT}$$

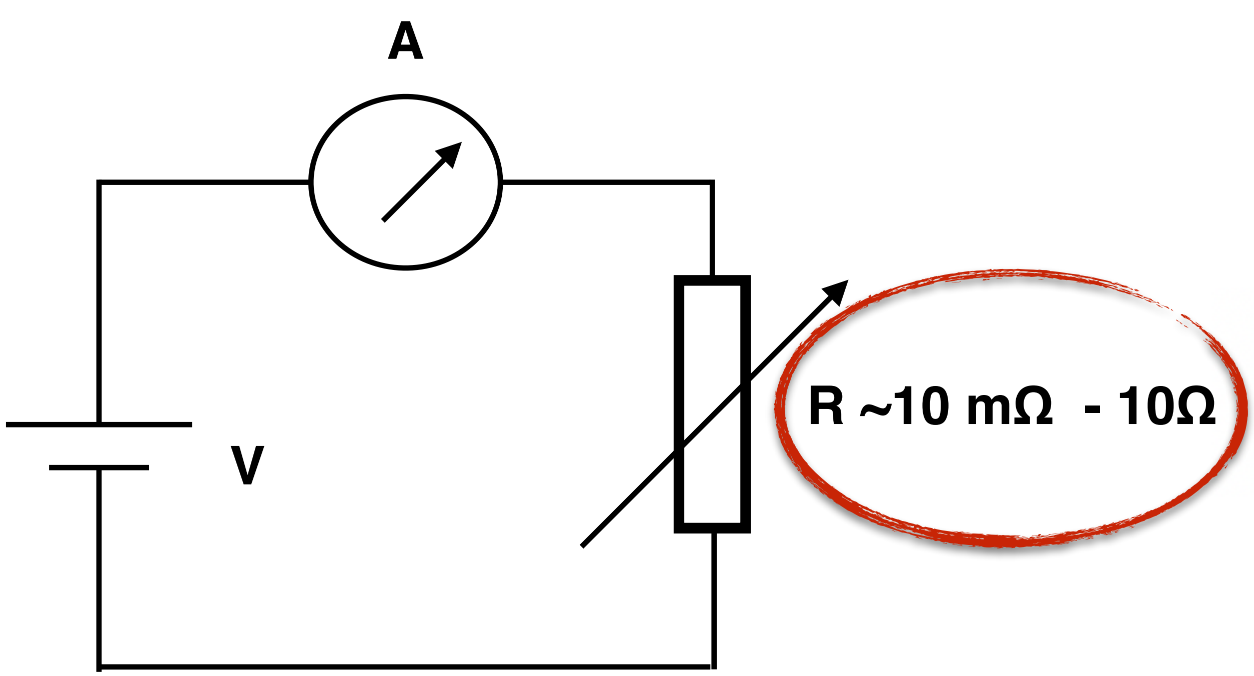

$$\Delta I = -\frac{V}{R^2}\frac{dR}{dT}\Delta T = \alpha I \frac{\Delta T}{T}$$

How superconducting TES based detector works.

- The thermal detector has a weak link the the thermal bath for rerstoring the initial conditions

- The effect of a thermal link is easily described within the first principle of thermodinamics in the approximation of <u>small signal</u>:

$$C\frac{d\Delta T}{dt} + G\Delta T = P_J$$

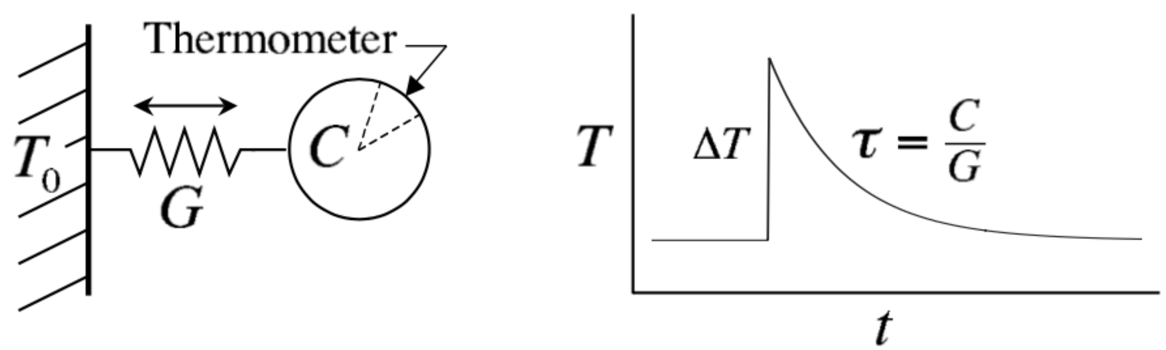

Picture from D. Mc Cammom

- Combining electrical and tharmal equations, and moving in frequency domaıv, it can be seen that the “responsivity parameter” S(ω) - approximation of the classical responsivity dI/dP- mixes termal and electric parameters (the following holds for large L_G, much grater than 1)

$$S_I(\omega) \approx -\frac{1}{IRL_G}\frac{1}{1+i\omega\tau/L_G}$$

$$L_G = \frac{\alpha P_j}{G\Delta T}$$

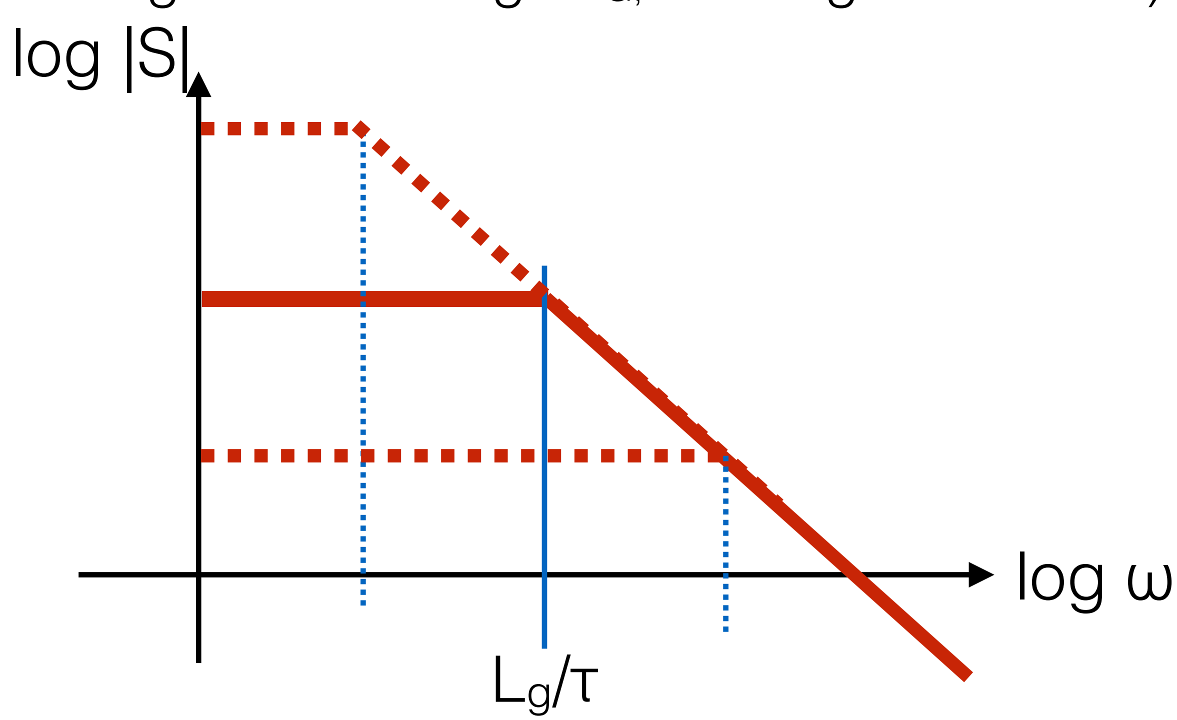

How superconducting TES based detector works.

- Finally the redout circuit must matches the source impedance (very small respect to the one require by standard electronics) and the detector noise
- A DC SQuiD in the configurartion of trans-impedance amplifier is the best choice in almost all cases.

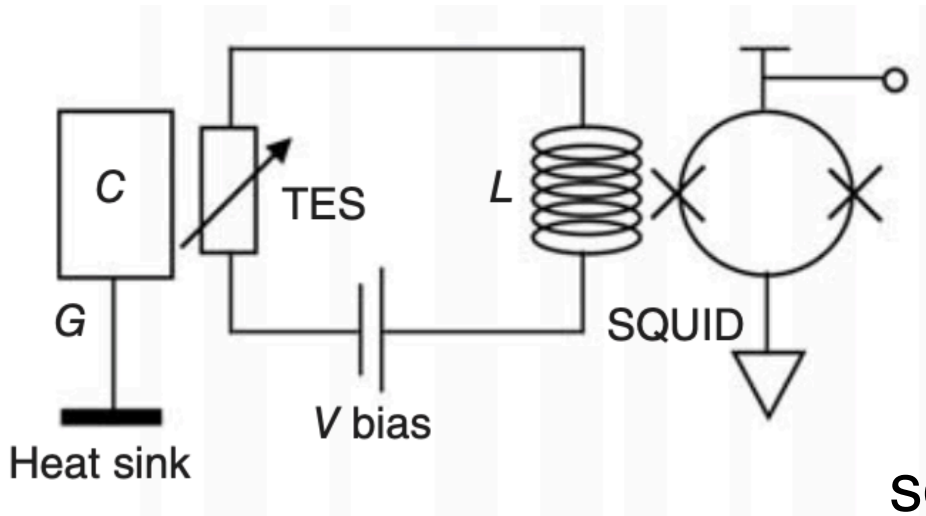

see M. Kiviranta's lecture tomorrow

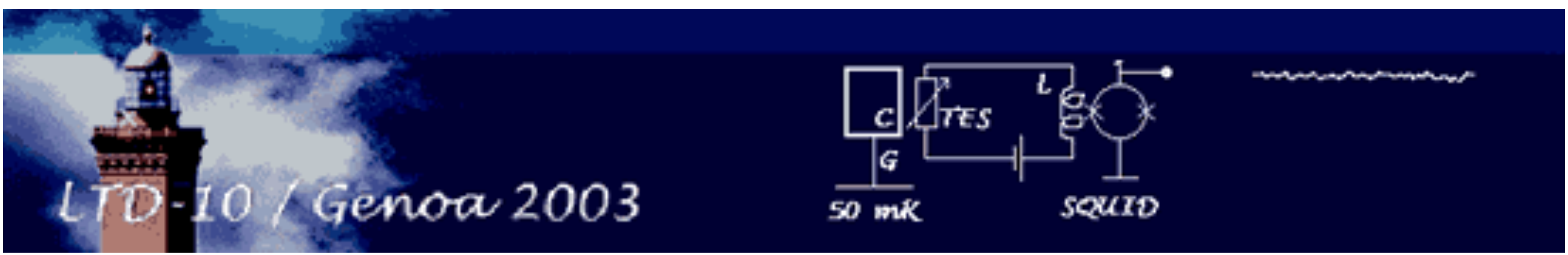

How superconducting TES based detector works.

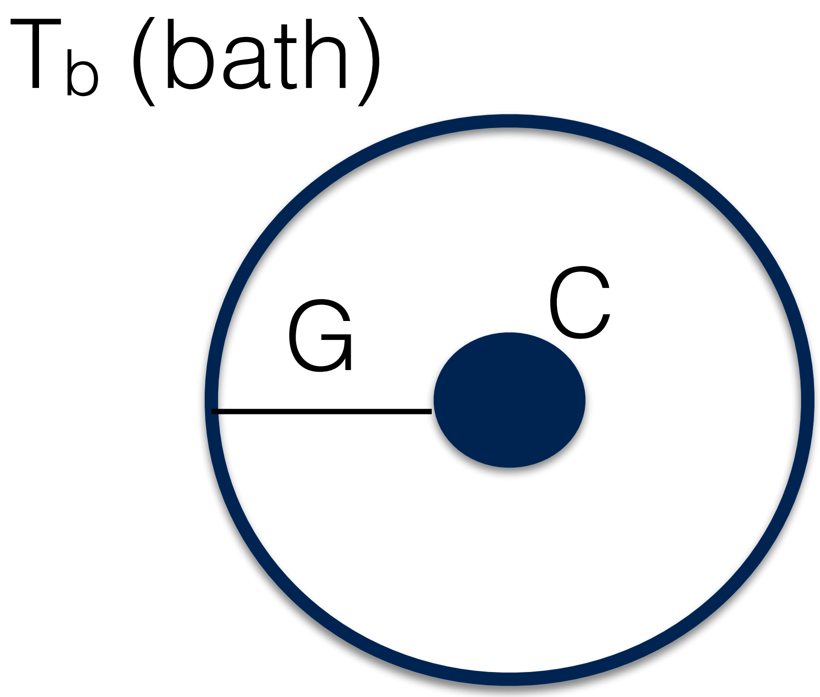

- Statistical thermodinamics gives the energy fluctuation of the body C at equilibrium with the bath
- A simple argument can help in remembering the finale formula
- Suppose the body have a number n of phonons with thermal energy kT
- They move randomly amomg the ling G ginving statistic fluctuations

$$n = C/k \qquad \Delta n = \sqrt{\frac{C}{k}} \qquad \Delta E = kT\,\Delta n = \sqrt{kT^2 C}$$

- The fluctuations are produced by a noise power flow over the thermal link G, and the power in a unit bandwidth at frequency ω
- If we assume that the power spectrum is "shot-noise-like", the noise is independent of frequency,
- This can be integrated over all frequencies to give the total energy fluctuation, which requires the spectral density :

$$P^2(TFN) = 4kT^2G \qquad W^2/Hz$$

How superconducting TES based detector works.

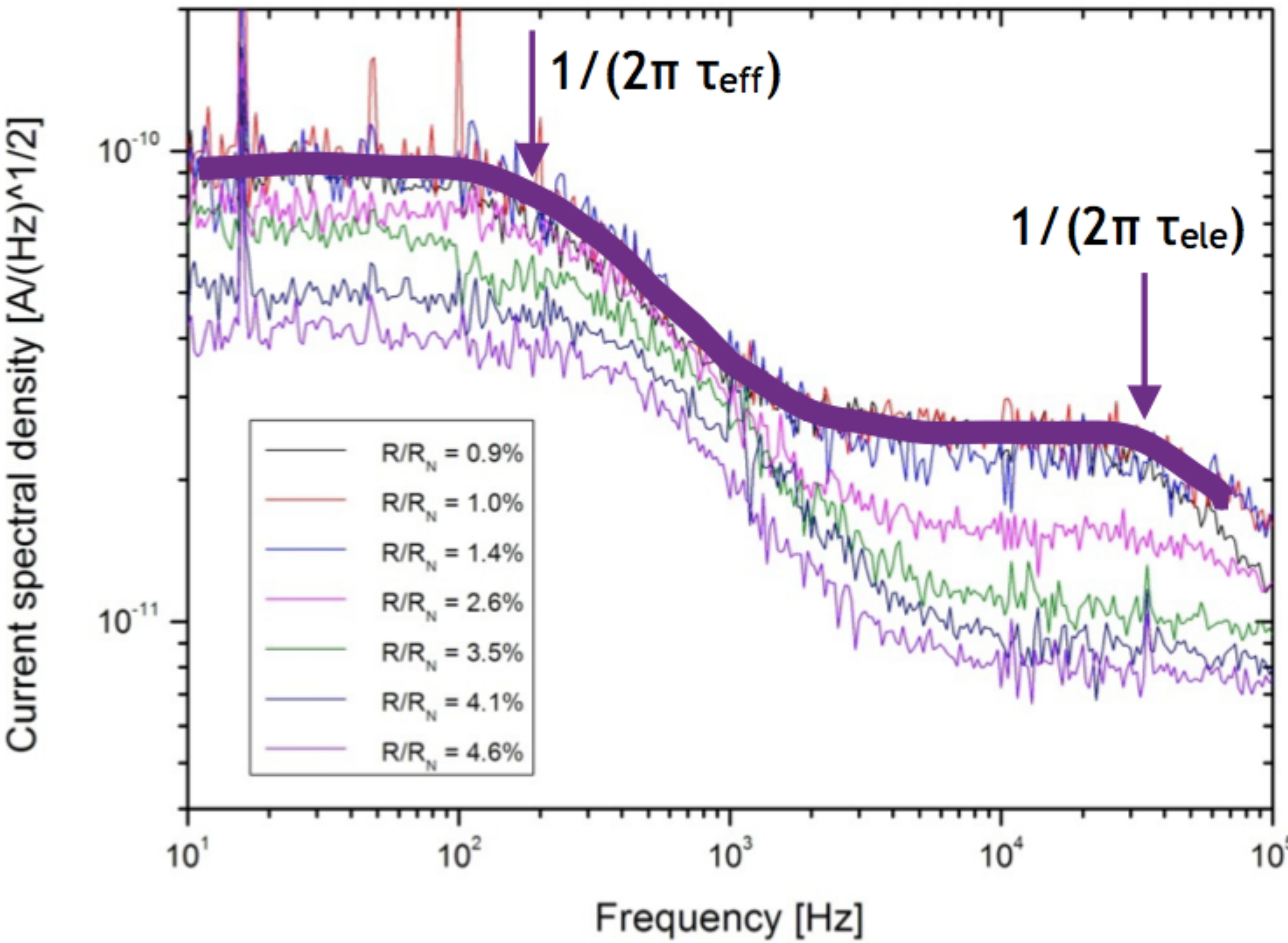

Build the minimal model: set of non linear equation→ numerical solution is required

$$
\begin{cases}
C_{TES}\dfrac{dT_{TES}}{dt} = K_2\left(T_{Abs}{}^{n} - T_{TES}{}^{n}\right) - K_1\left(T_{TES}{}^{n} - T_h{}^{n}\right) + R_x\left(T_{TES}\right)I_b{}^{2} \\[2ex]
C_{Abs}\dfrac{dT_{Abs}}{dt} = -K_2\left(T_{Abs}{}^{n} - T_{TES}{}^{n}\right) + P_\beta\left(t\right) \\[2ex]
R_{st}\left(I_0\left(t\right) - I_b\right) = R_x\left(T_{TES}\right)I_b + L_p\dfrac{dI_b}{dt} + \dfrac{q}{C} \\[2ex]
I_b = \dfrac{dq}{dt}
\end{cases}
$$

Results: ETF clearly visible

- ETF: the bias power act as negative feedback reducing thermal swing and time response.
- ETF: Linearize and sped-up the response
- ETF: becomes important if L ranges is~ 10-10²

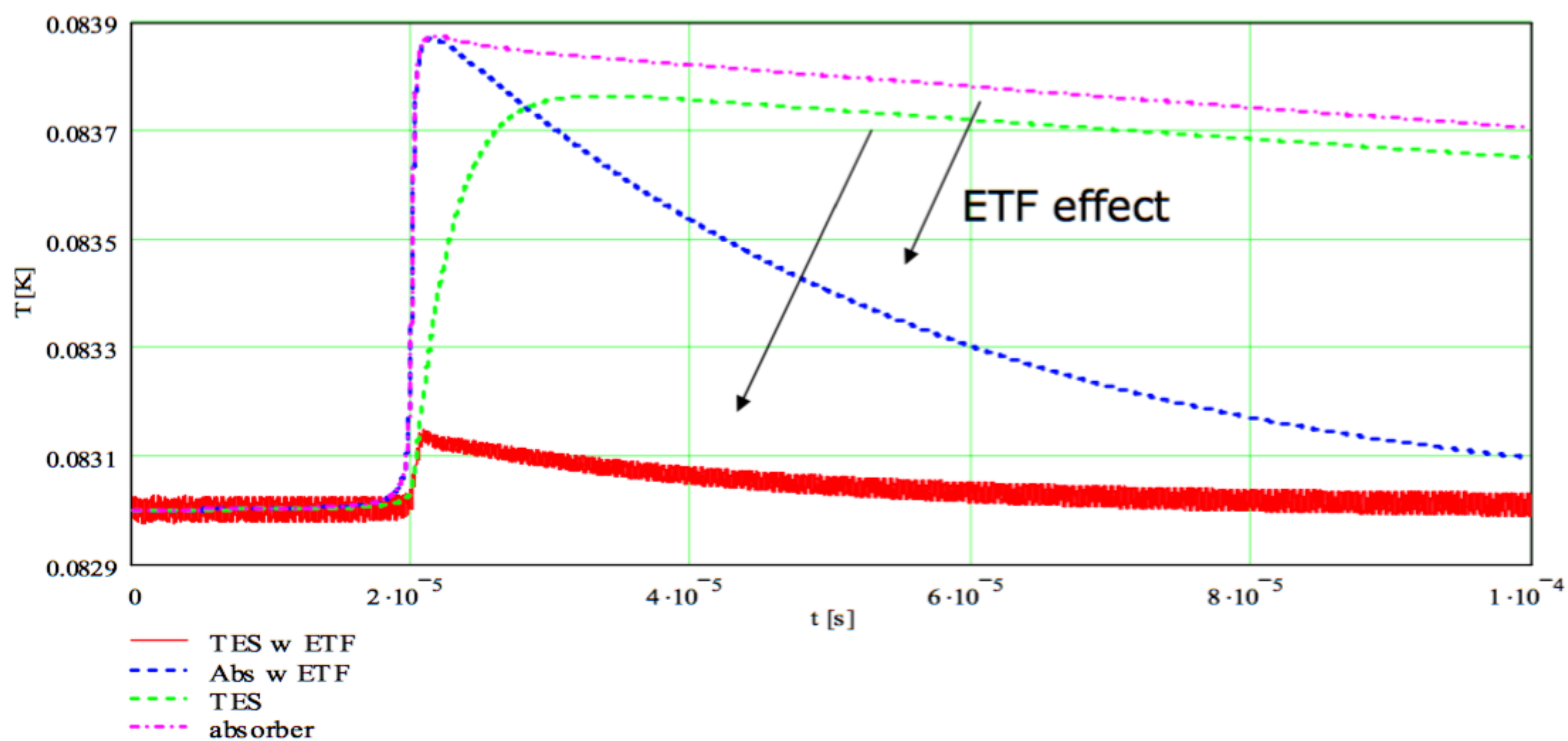

TES-Transition edge sensor

- Real TES sensor have T and I dependence

$$R(T,I) \approx R_0 + \left.\frac{dR}{dT}\right|_I \delta T + \left.\frac{dR}{dI}\right|_T \delta I \qquad R(T,I) \approx R_0 + \alpha \frac{T}{R} \delta T + \beta \frac{T}{R} \delta I$$

- Dynamical performance much more complex to be evaluated

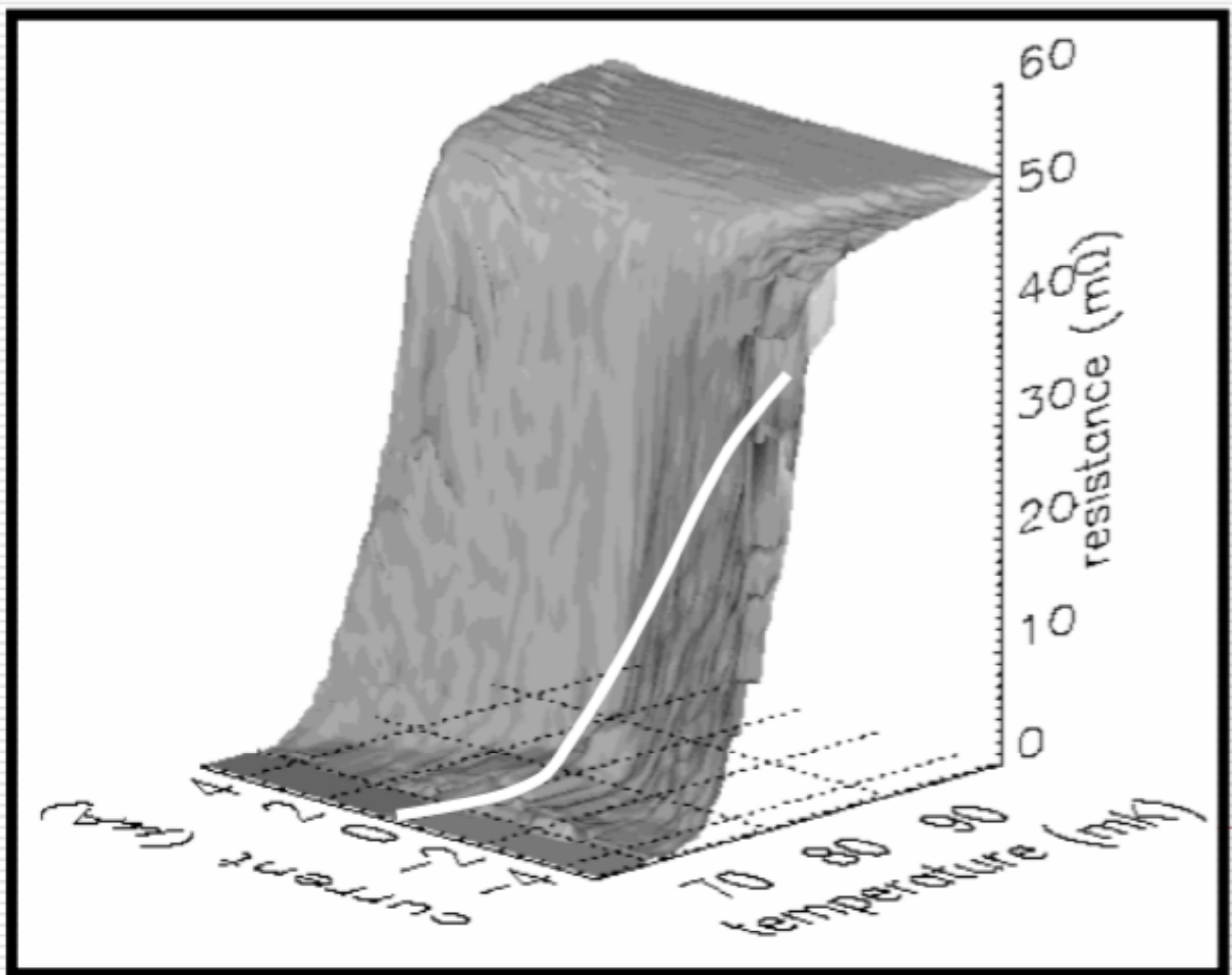

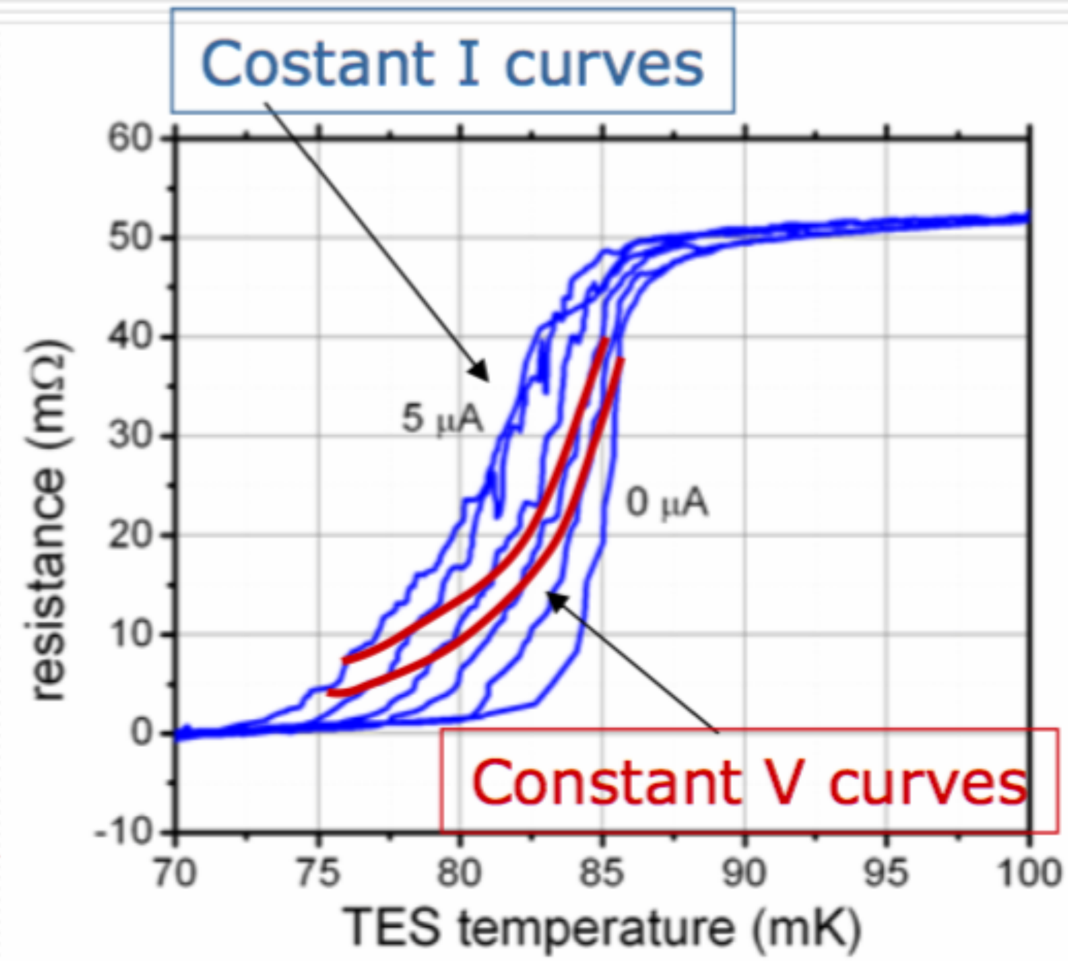

Whole model for the energy resolution for TES

- Including all the noise sources (Phonon, Johnson…), the intrinsic thermal resolution contains sensor and conductance parameters: α and n (→G~T^n)

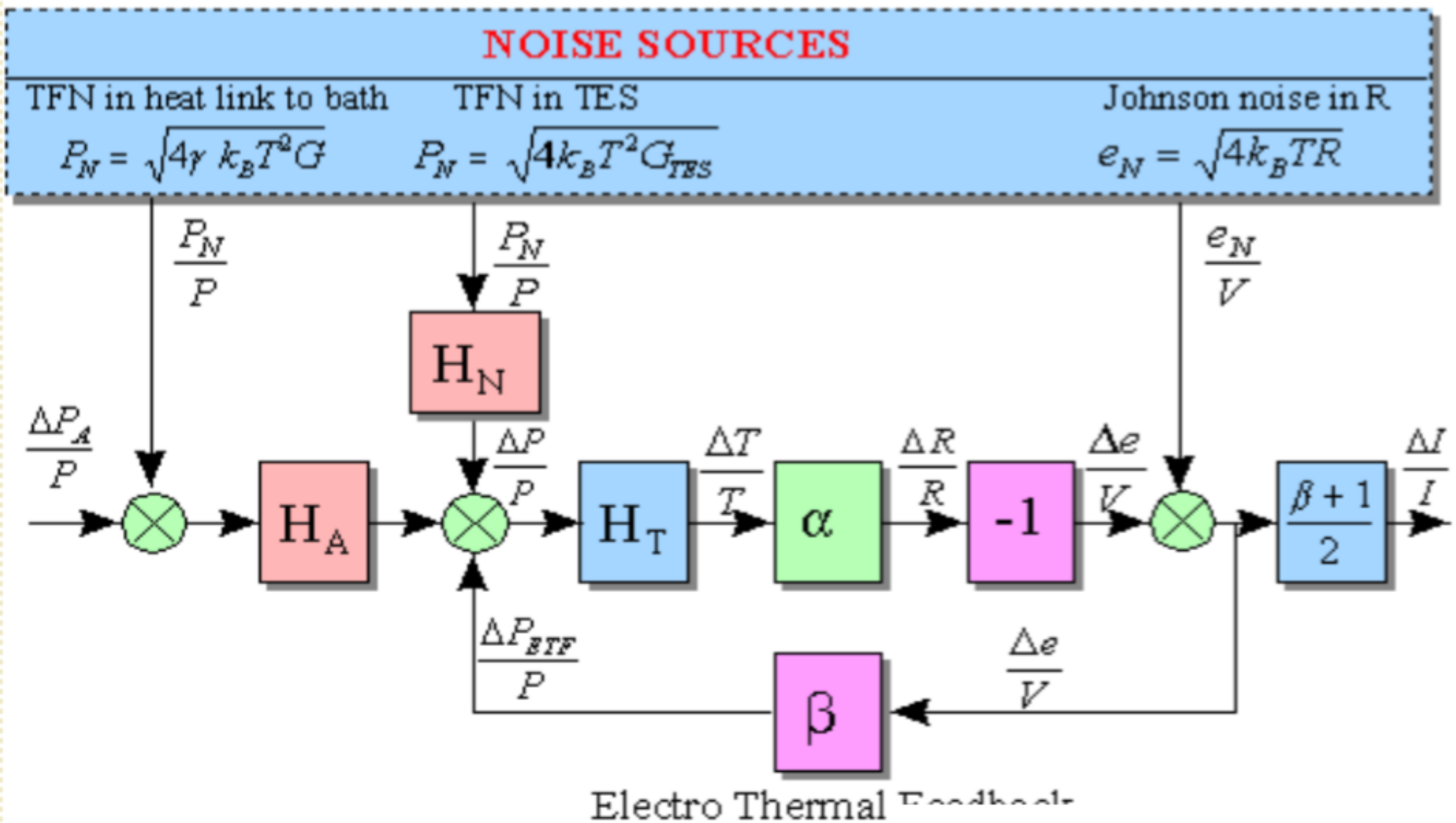

Calculated ETF L parameter

$$\delta E_{\mathrm{FWHM}} = 2\sqrt{2\ln 2}\sqrt{4k_{\mathrm{B}}T_0^2\frac{C}{\alpha_I}\sqrt{n/2}}\,,$$

TES detector configurations

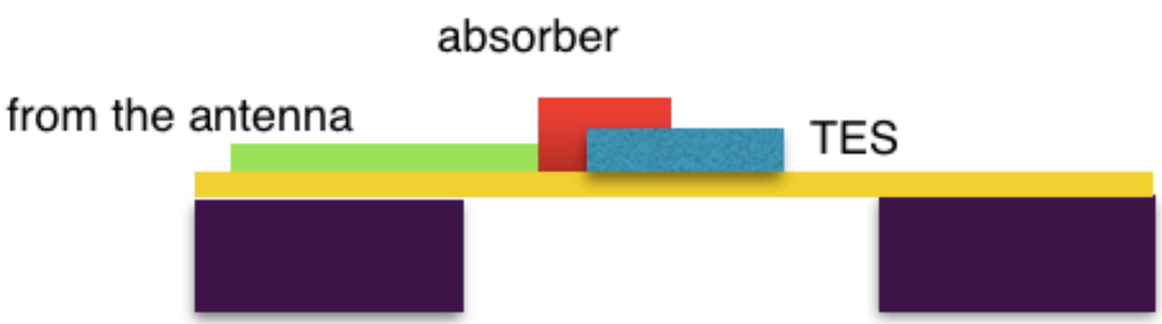

Simple Ir TES on suspended membrane

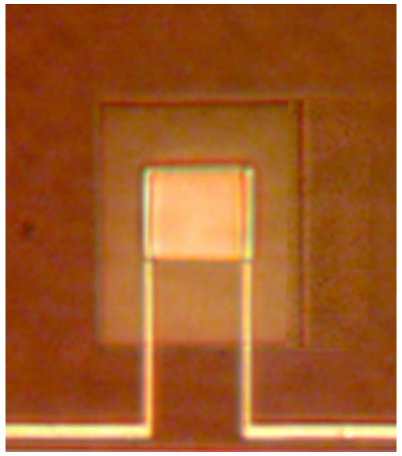

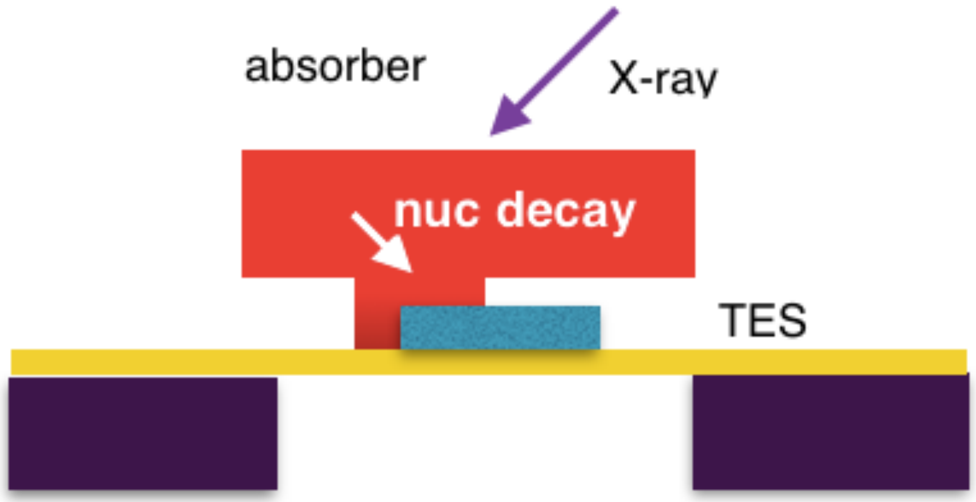

Re-Crystal TES microcalorimeter for Re-187 beta decay Presently changed to gold absorber for Ho-163 (ERC- HOLMES)

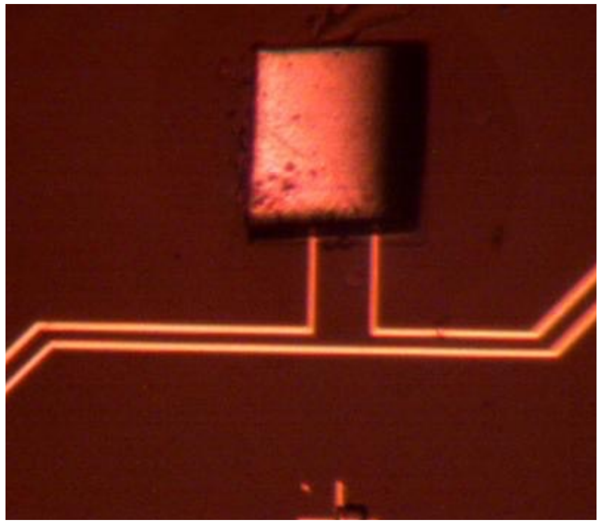

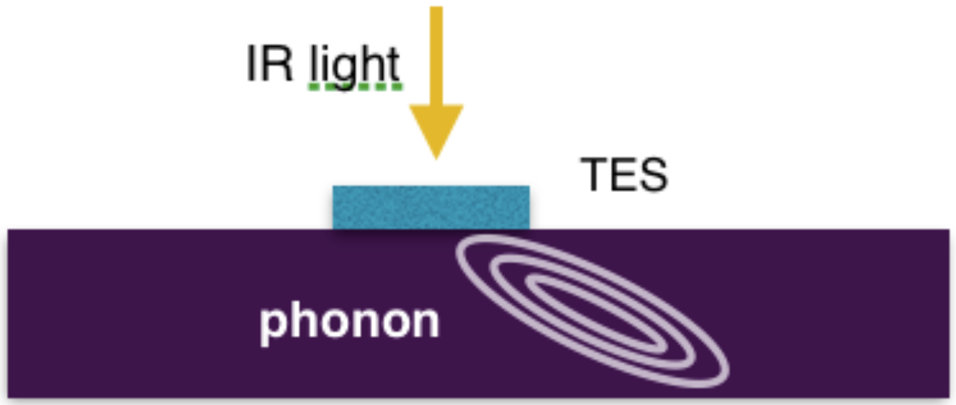

Anti coincidence Xray Space Telescope ATHENA

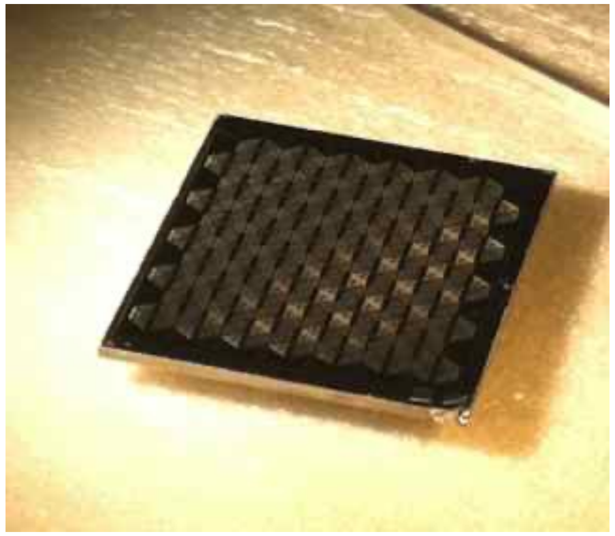

Soft X-ray Photon

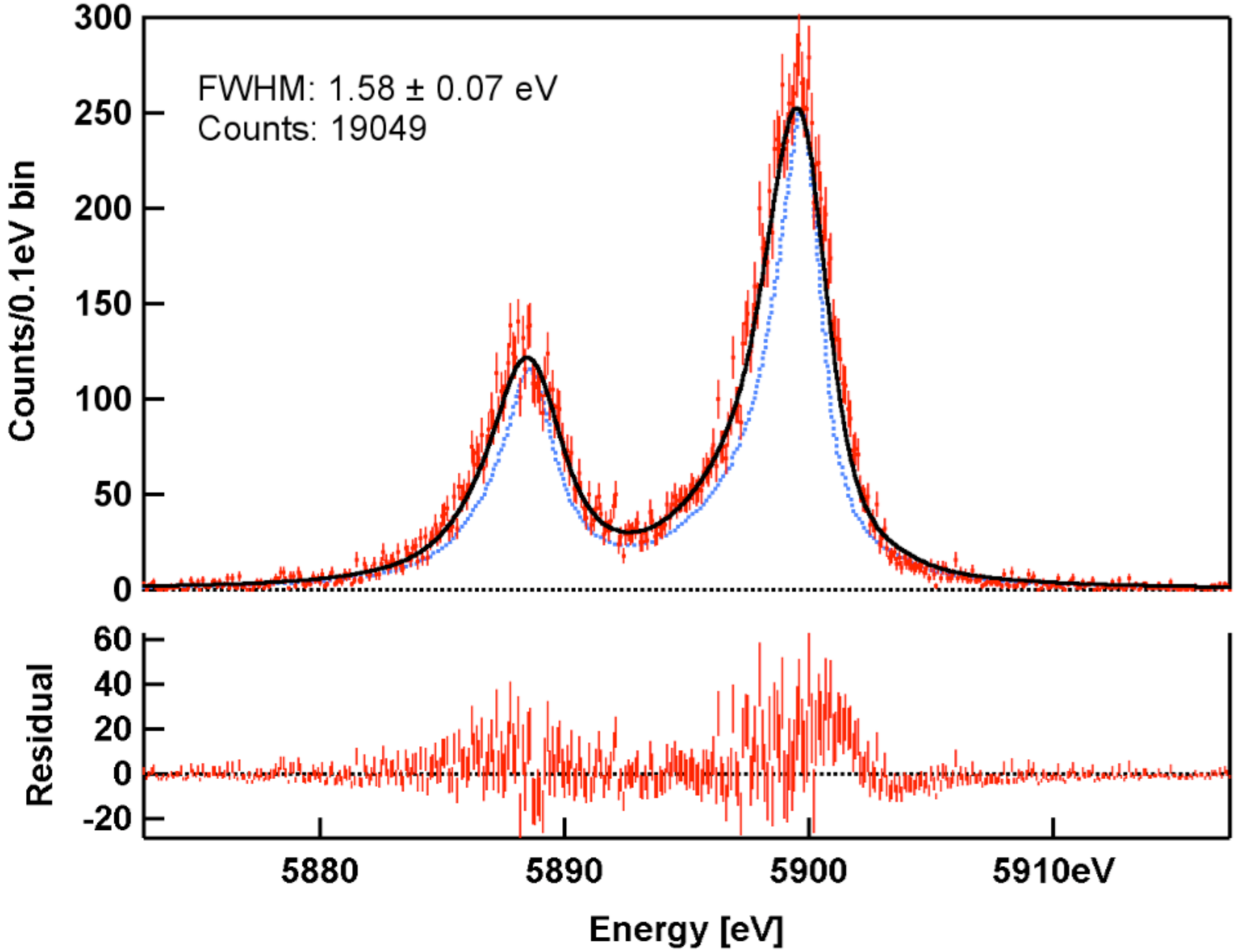

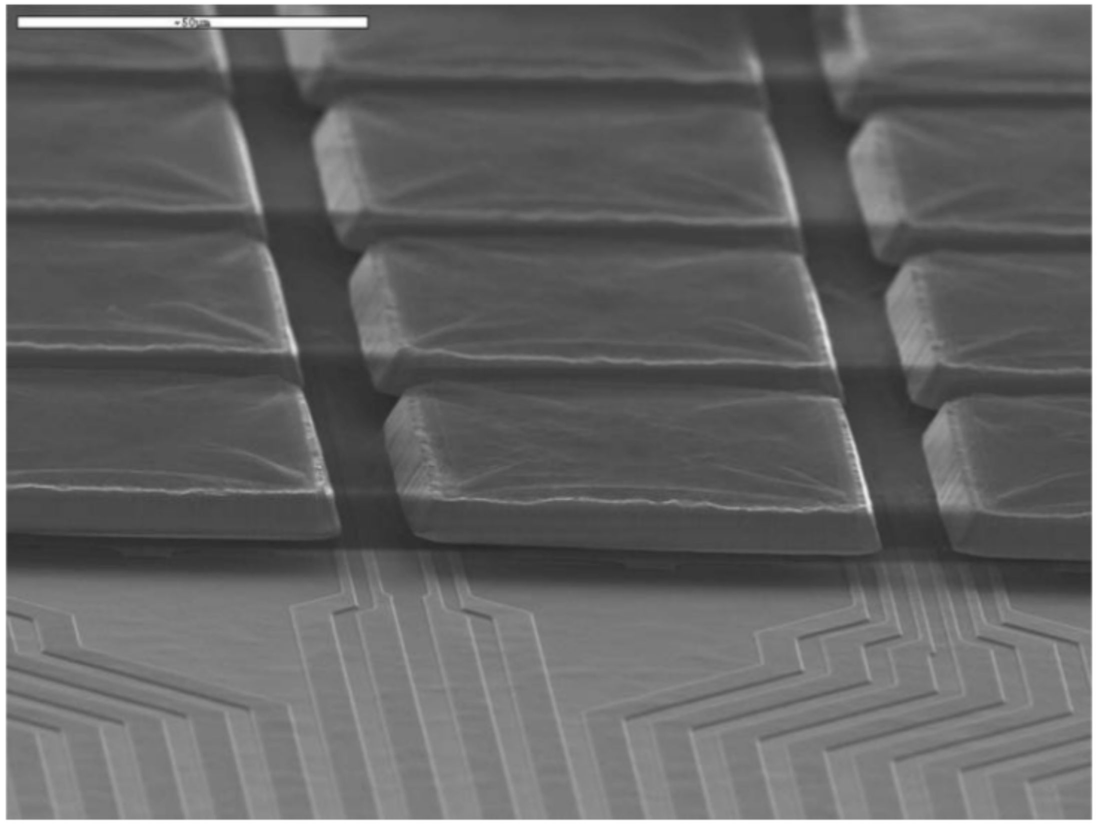

57 μm pixel with 30 μs time constant

Courtesy of S.Bandler GSFC NASA

Soft X-ray Photon

Courtesy of S.Bandler GSFC NASA

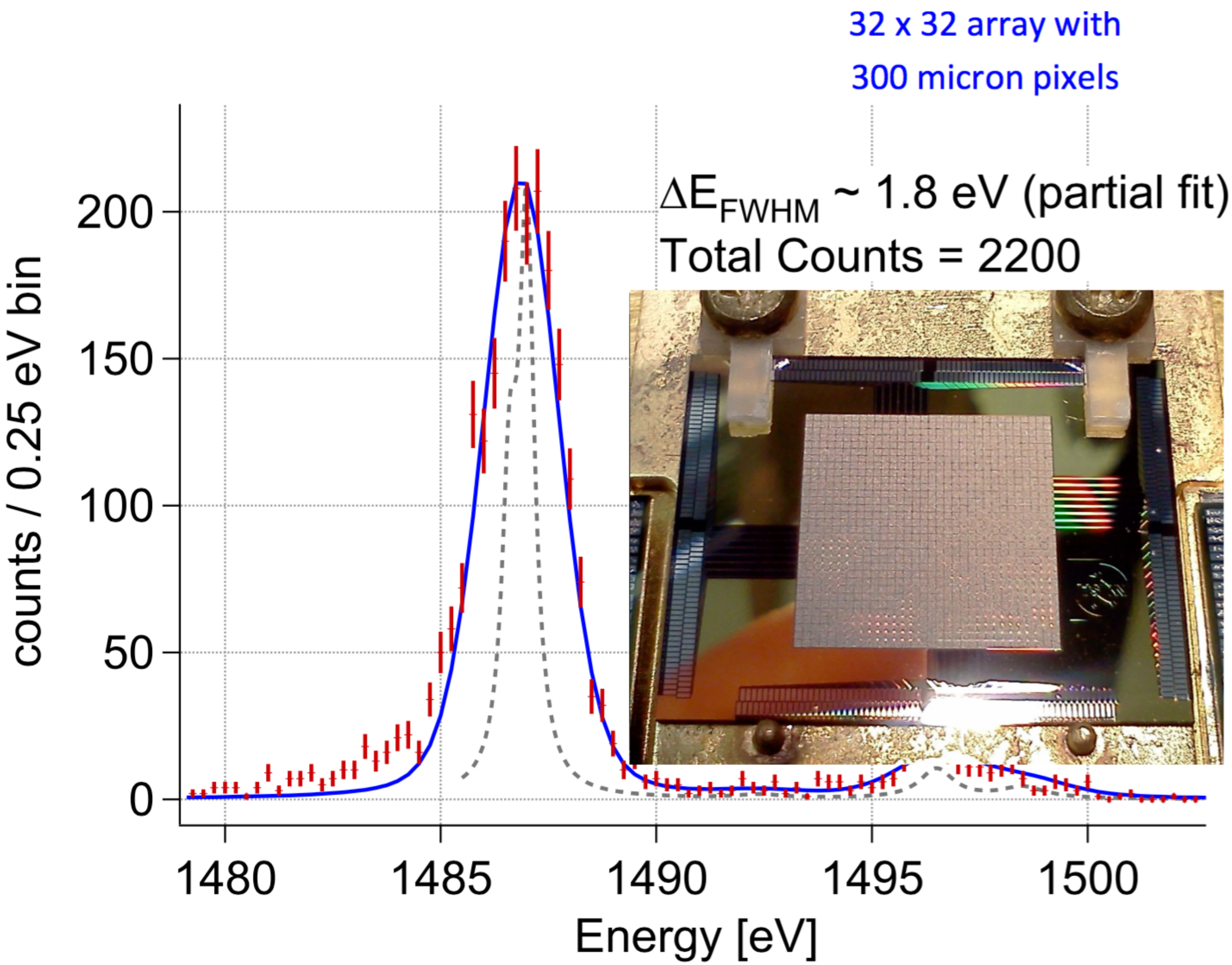

High Energy Photons

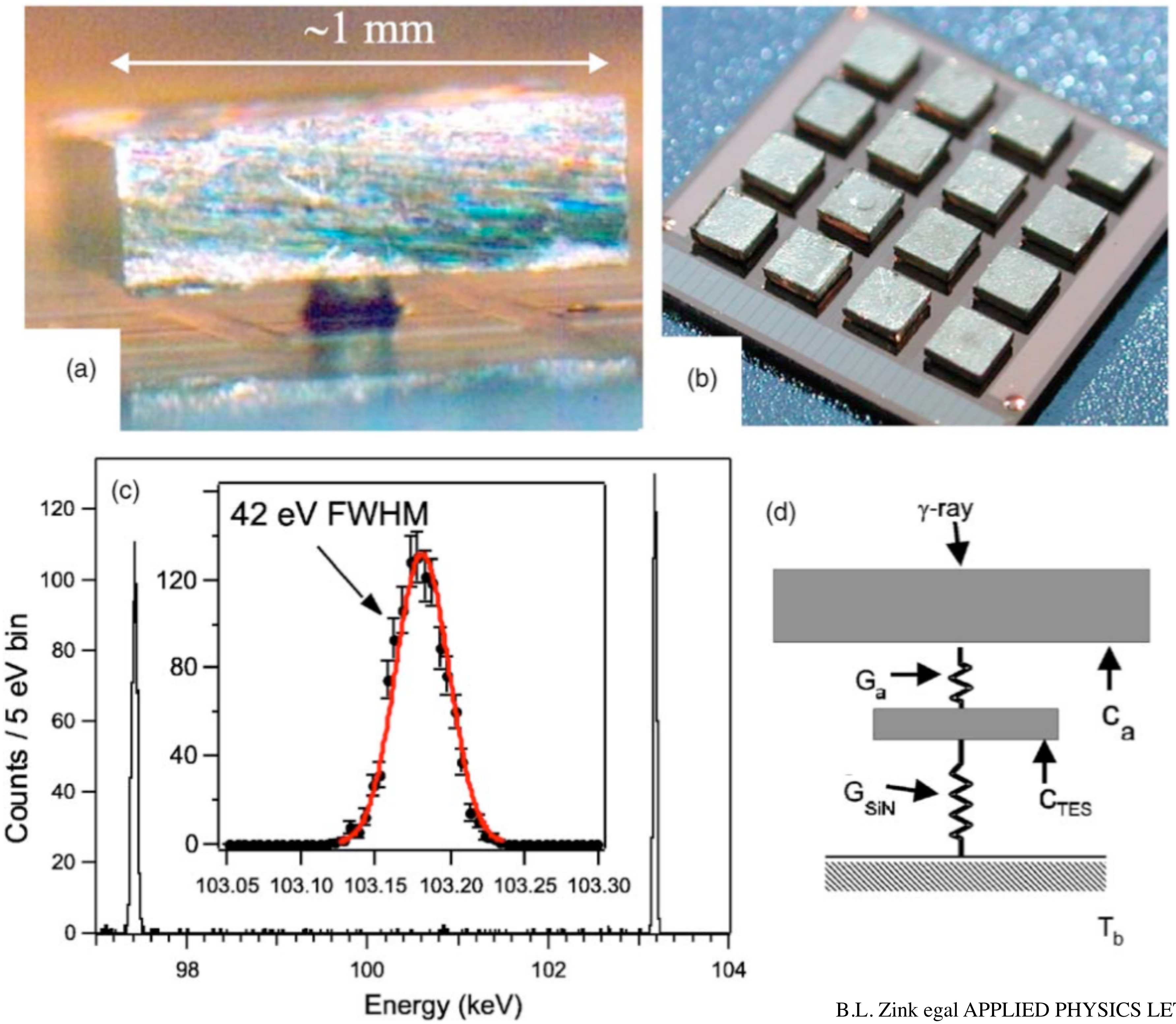

B.L. Zink egal APPLIED PHYSICS LETRS **89**, 124101 2006

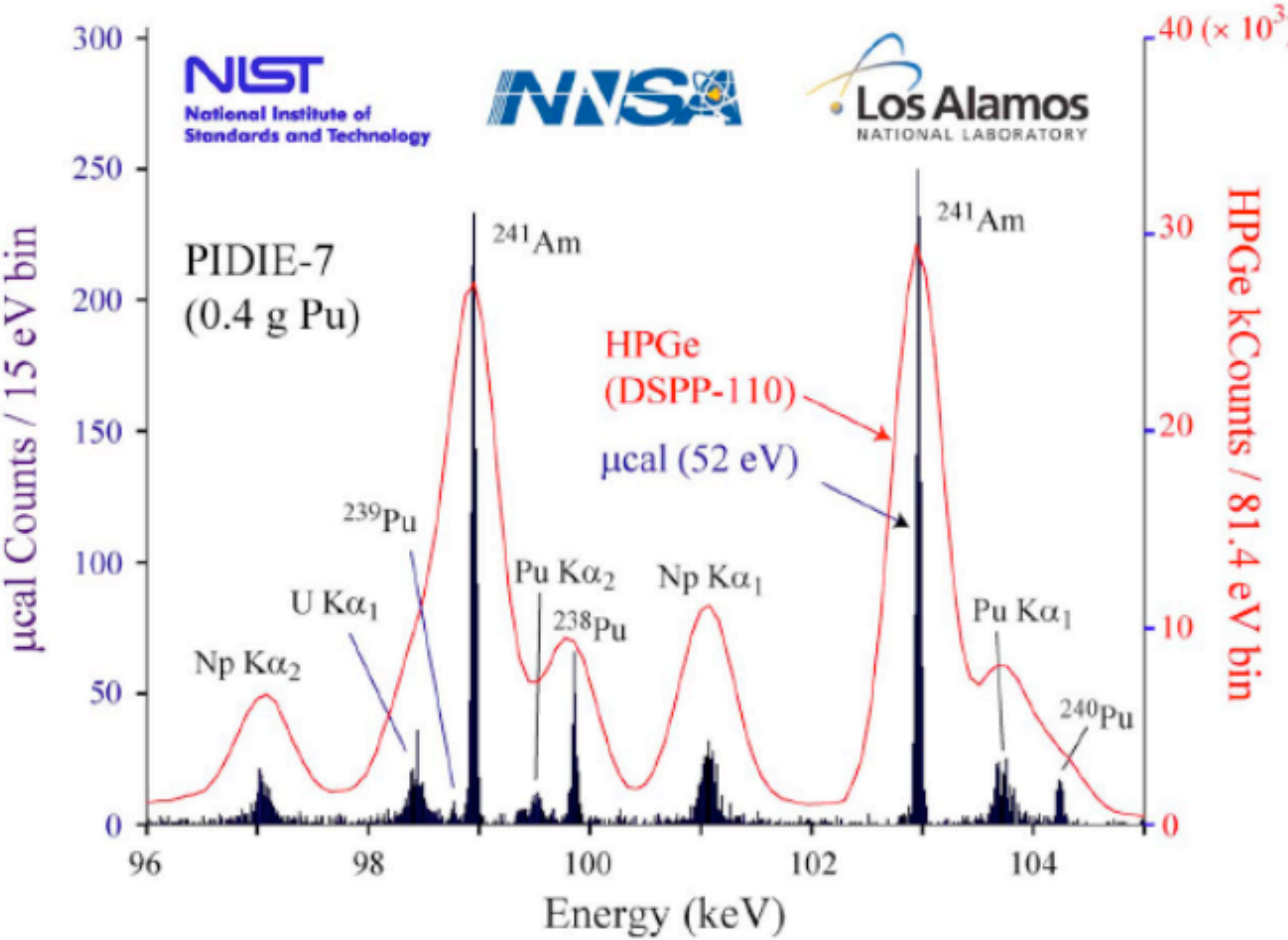

National Institute of Standards and Technology
Los Alamos NATIONAL LABORATORY
PIDIE-7
(0.4 g Pu)
241Am
241Am
239Pu
U Kα1
Np Kα2
Pu Kα2
238Pu
Np Kα1
Pu Kα1
240Pu
HPGe
(DSPP-110)
μcal (52 eV)
μcal Counts / 15 eV bin
HPGe kCounts / 81.4 eV bin
40 (× 10^3)
Energy (keV)

Soft x-ray Photon Resolution

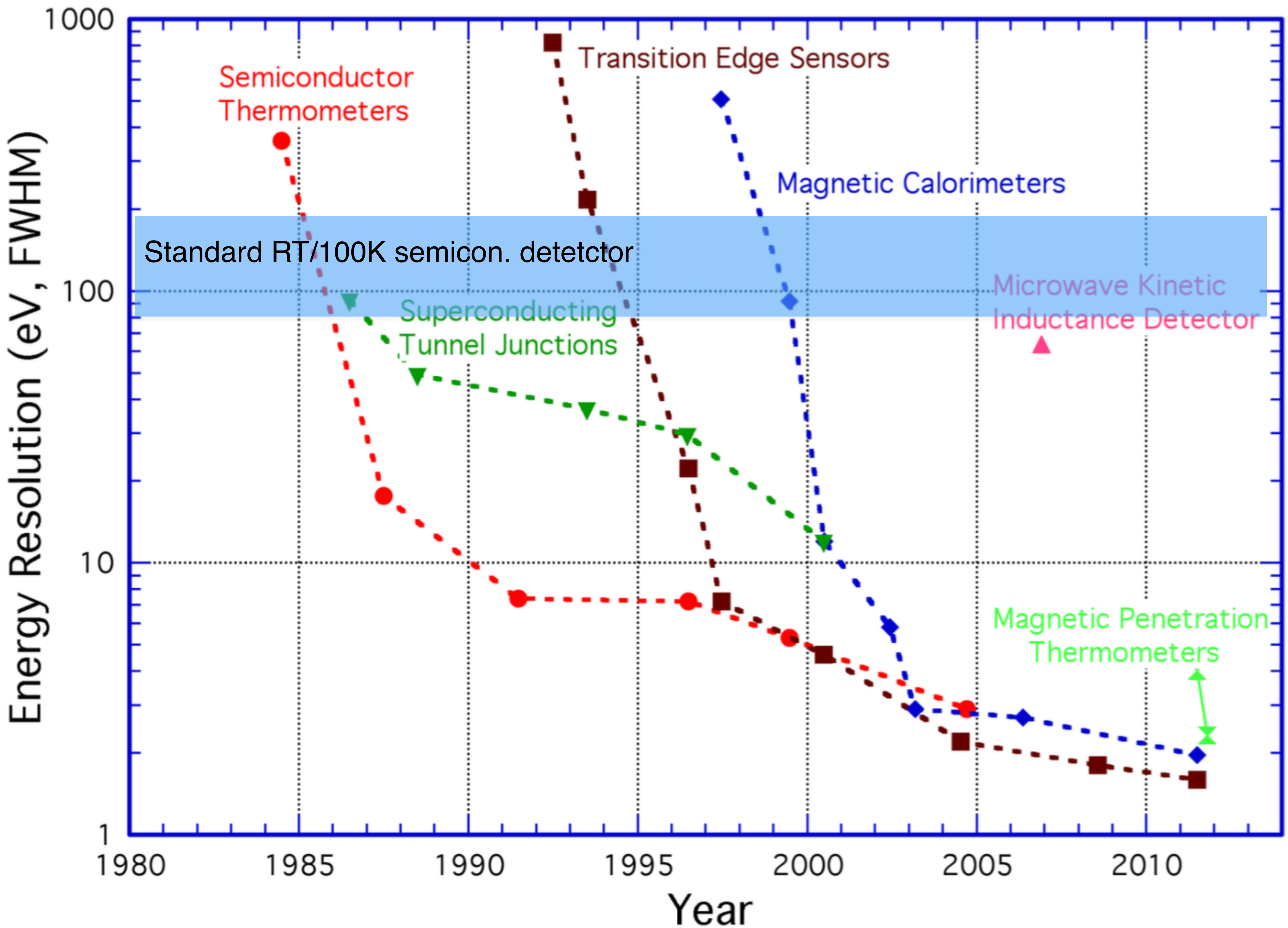

Blue Light TES SPD

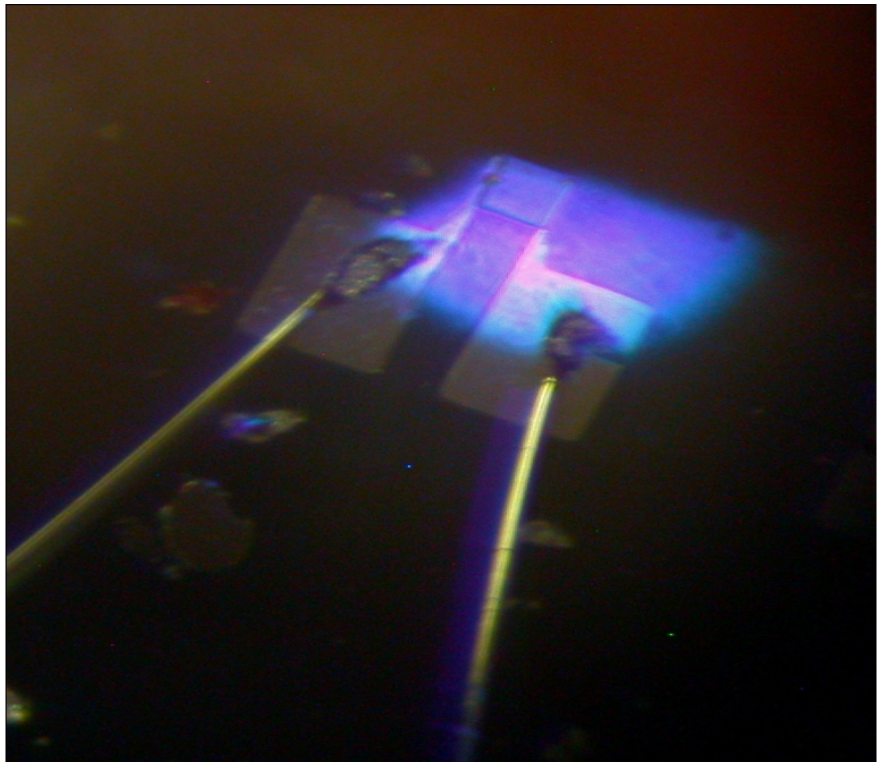

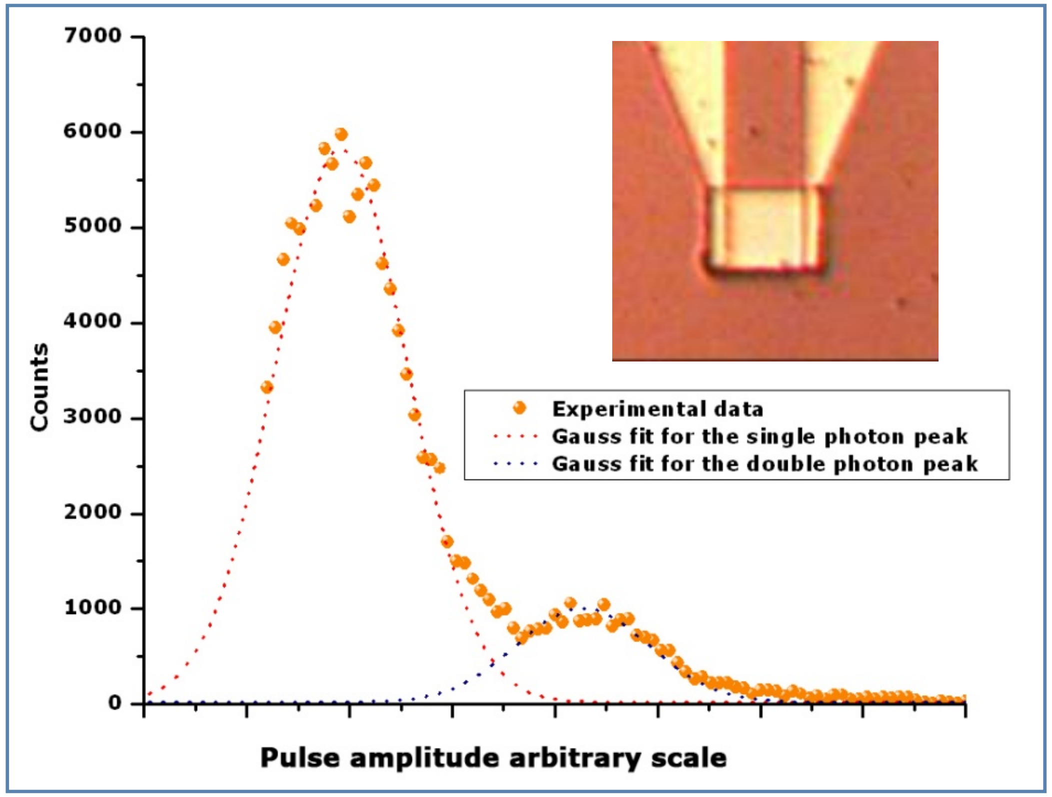

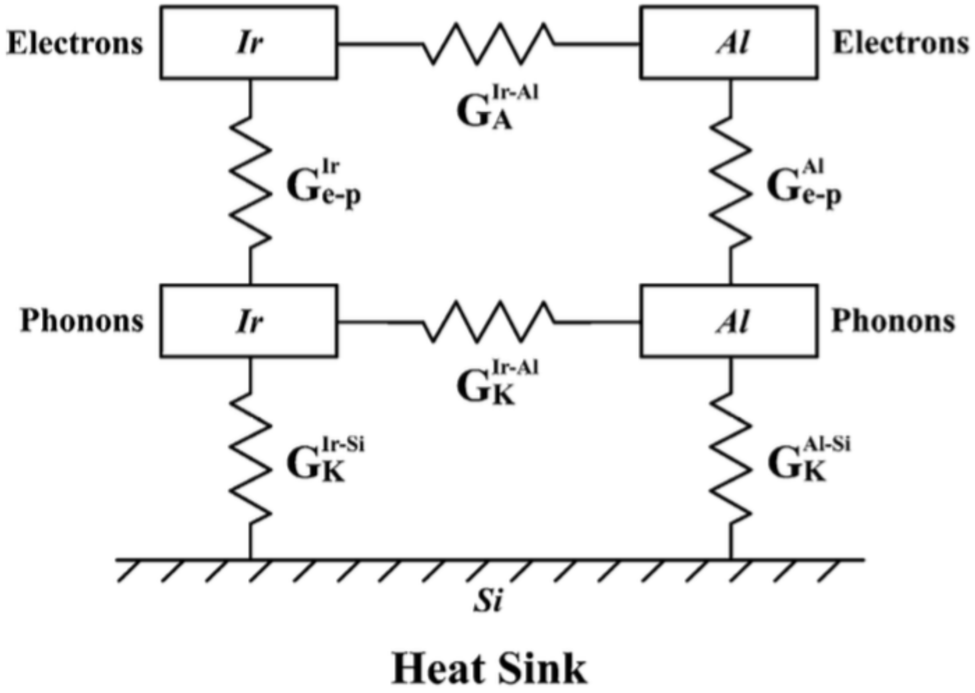

1550 nm TES SPD

M.Rajteri et , INRIM Torino

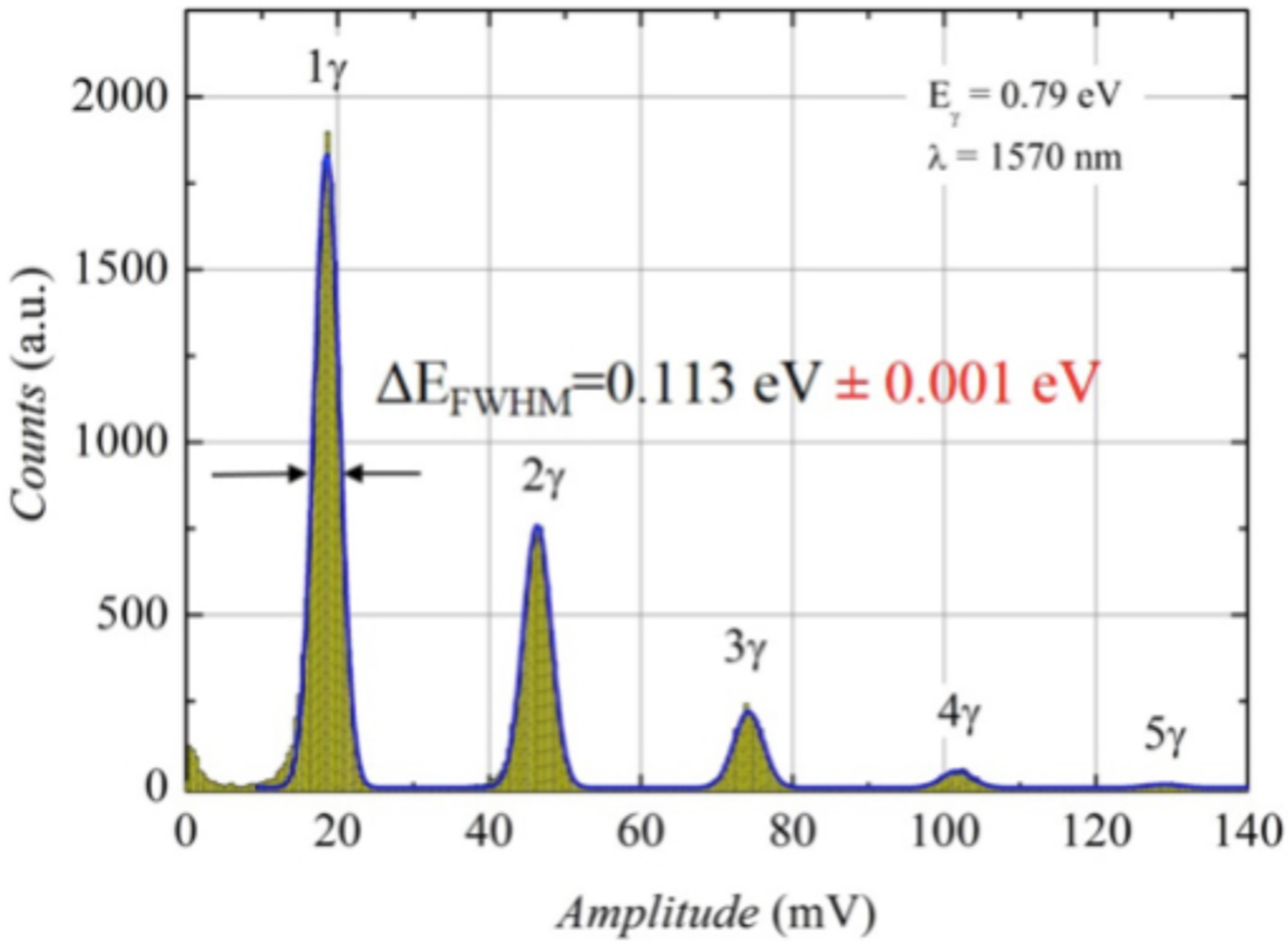

Antenna Coupled TES

- Wide Band Antenna Coupled TES Bolometer

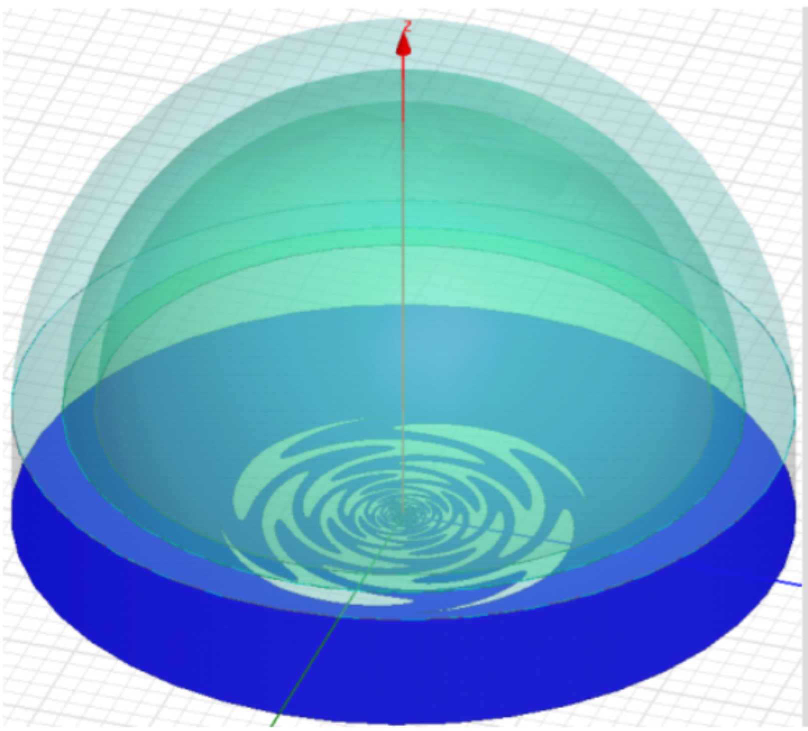
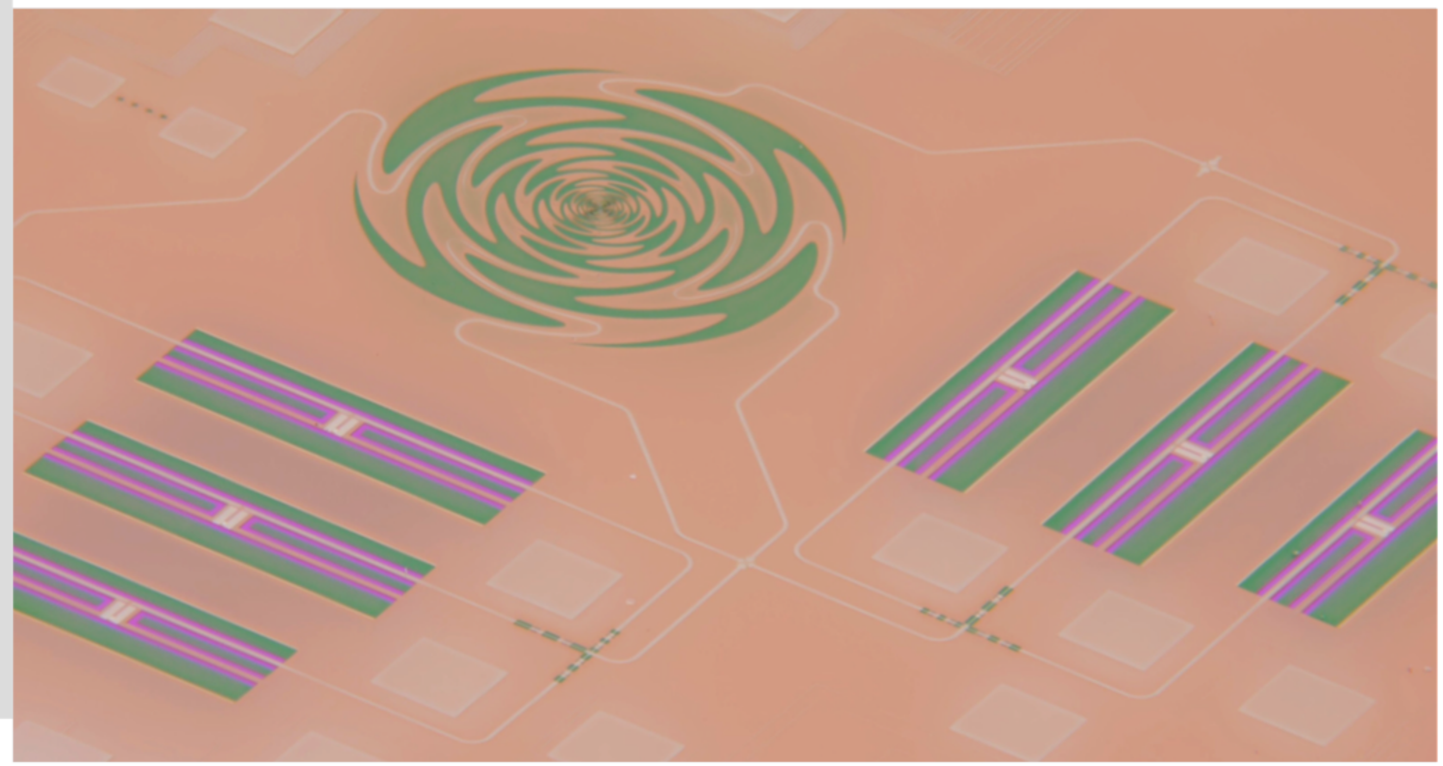

A. Lee, UCB, “Workshop CMB from Space”

Microwave Antenna Coupled Bolometer

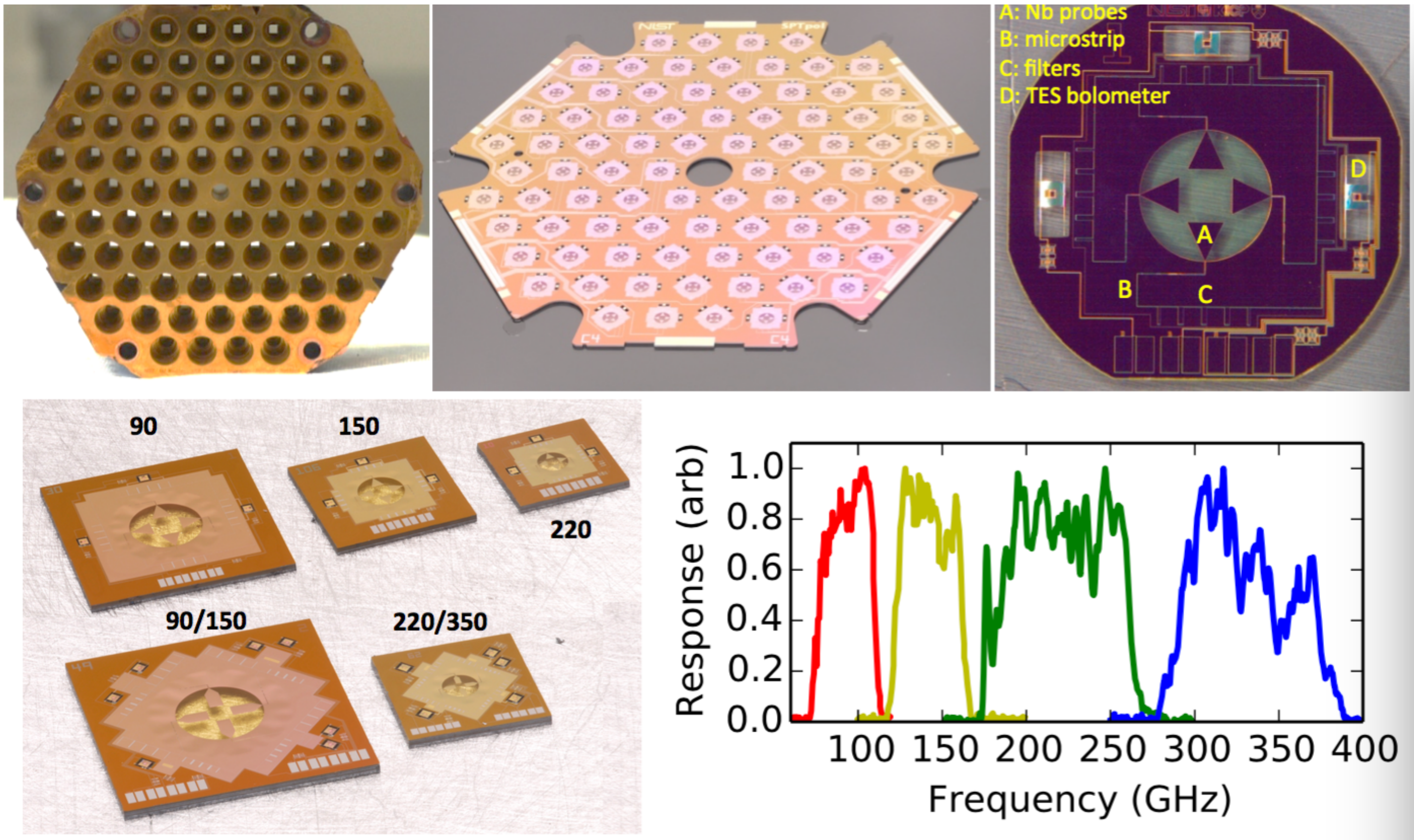

A. Lee, UCB, “Workshop CMB from Space”

Large Array

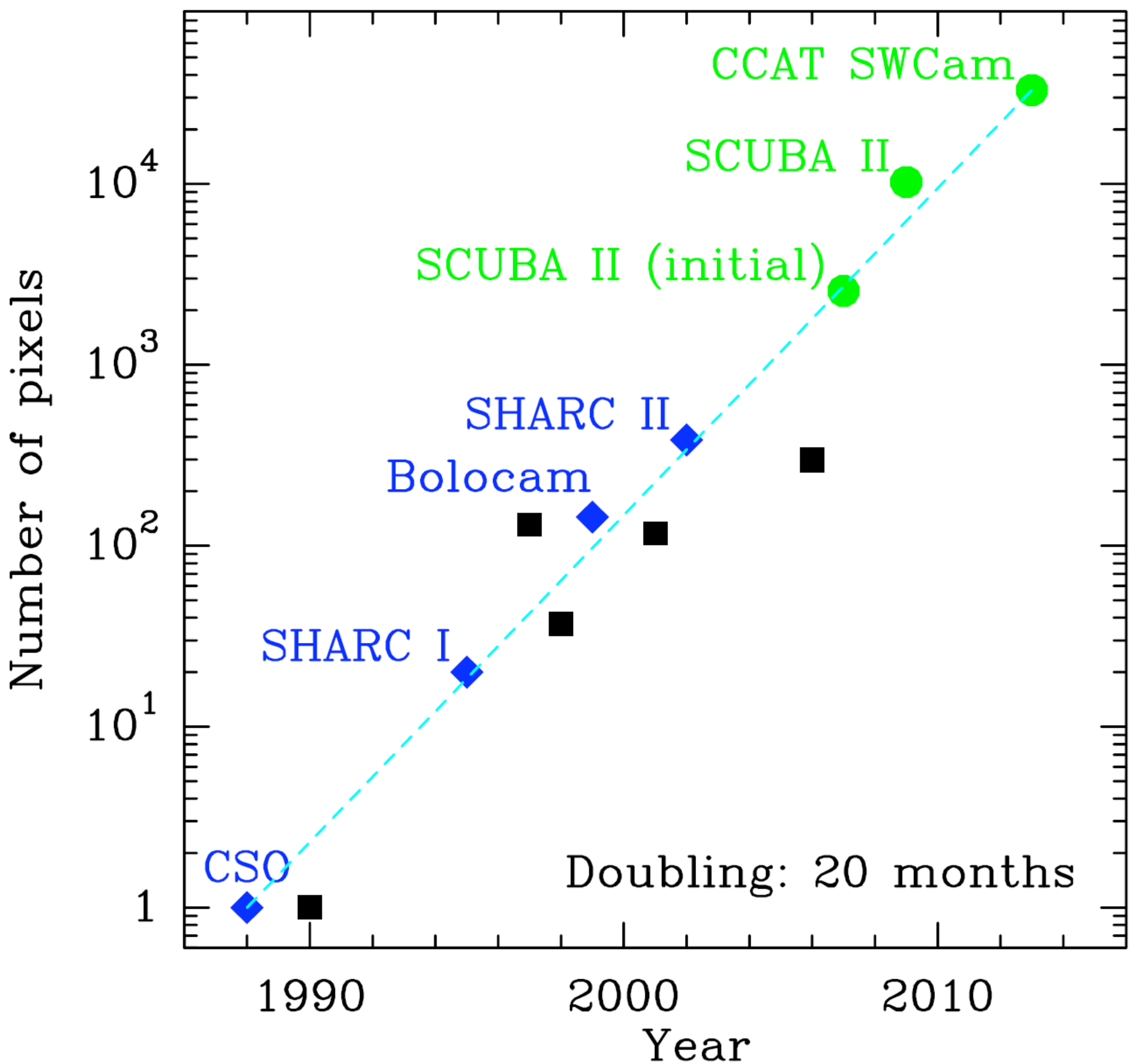

CCAT SWCam
SCUBA II
SCUBA II (initial)
SHARC II
Bolocam
SHARC I
CSO
Doubling: 20 months
Number of pixels
1
10^1
10^2
10^3
10^4
1990
2000
2010
Year

The NEP Challenge

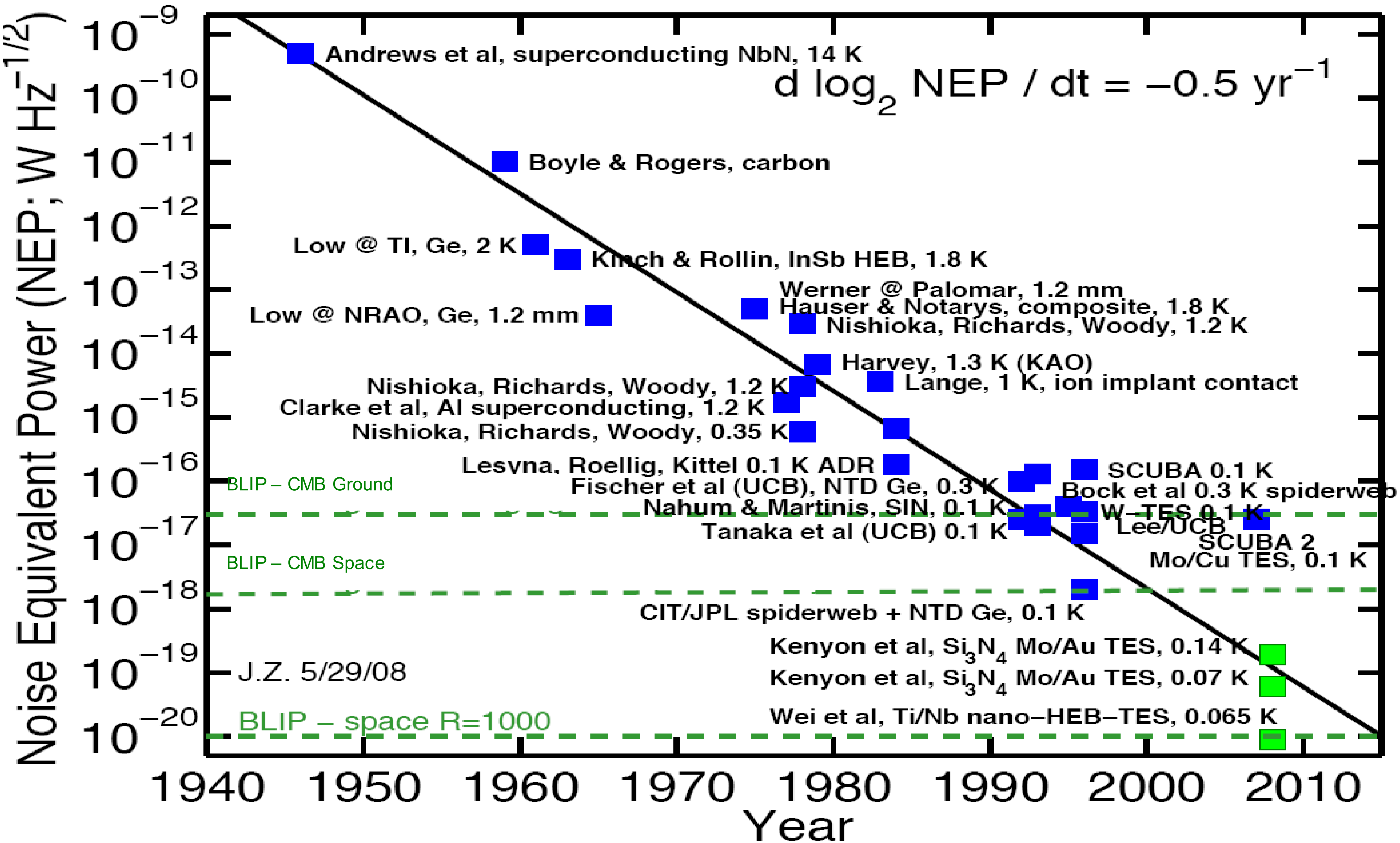

Dark Matter

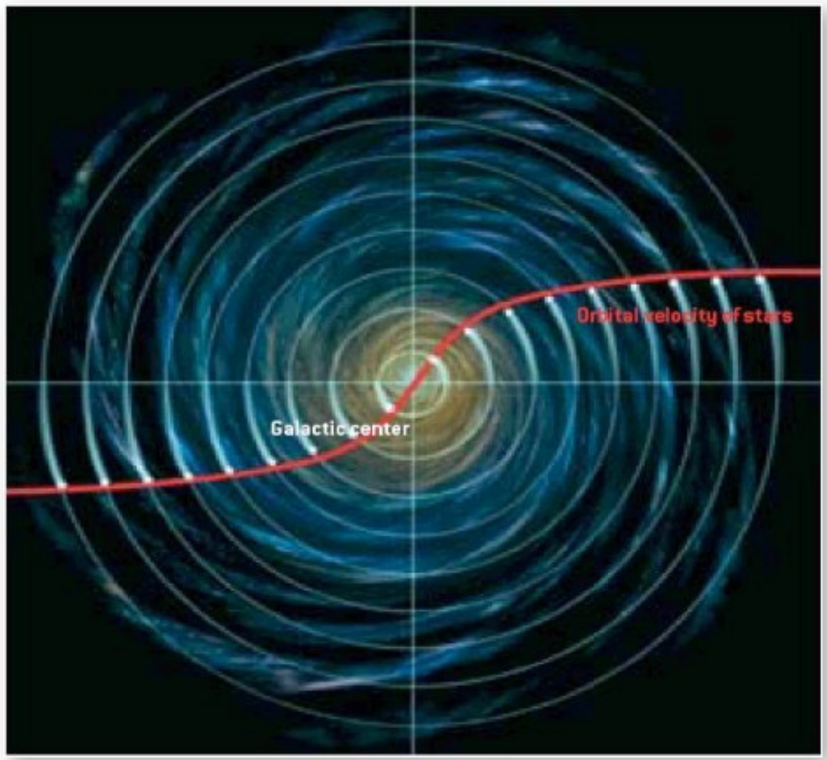
Orbital velocity of stars
Galactic center

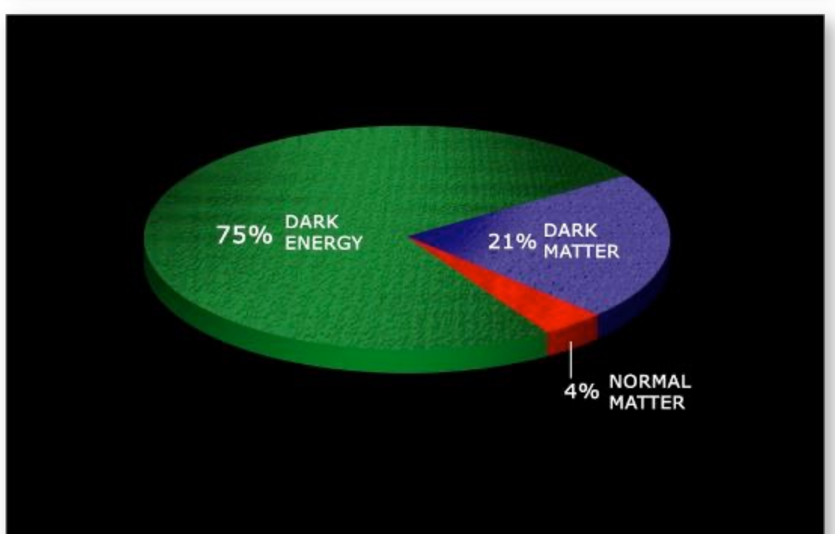
75% DARK ENERGY
21% DARK MATTER
4% NORMAL MATTER

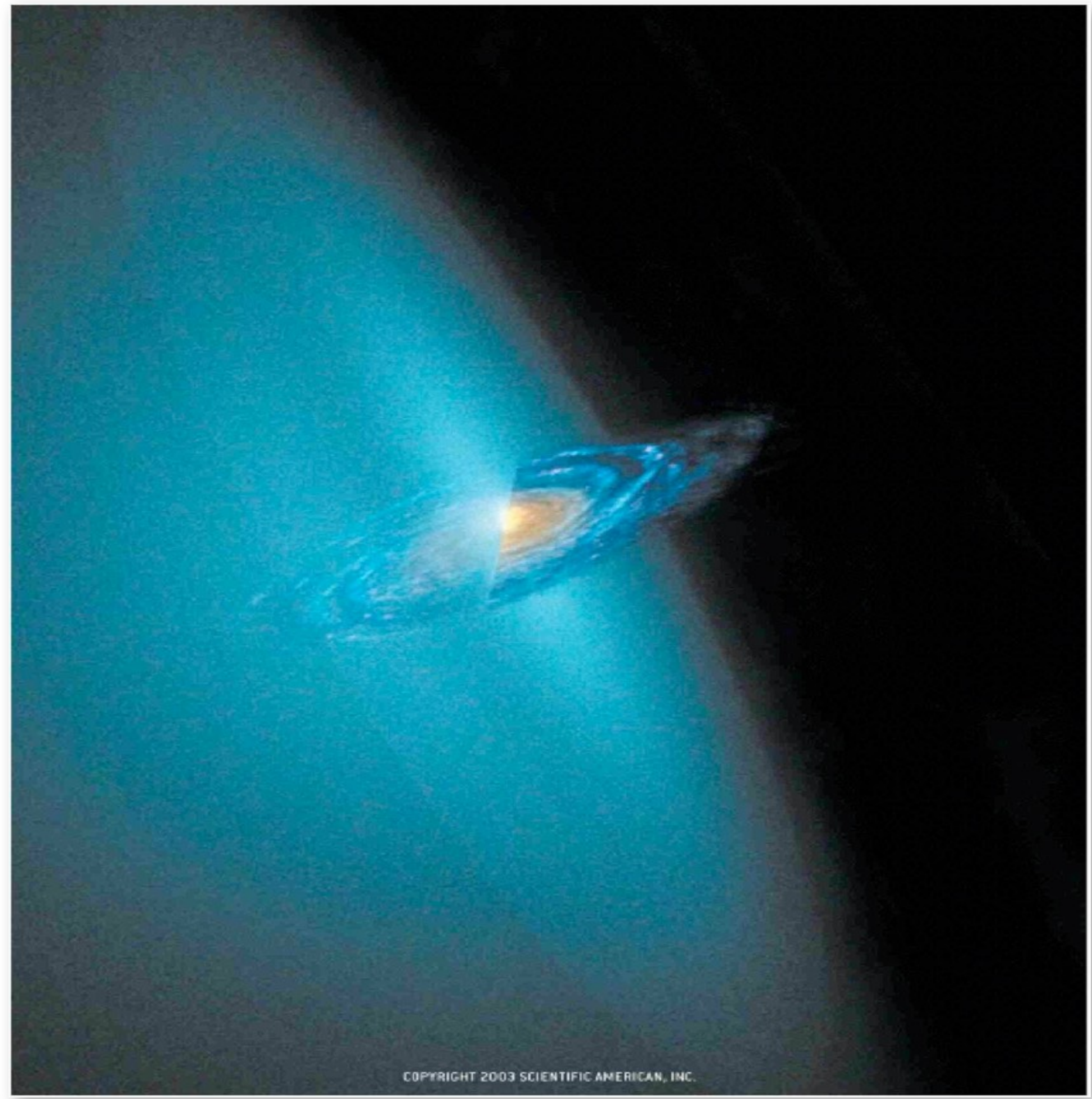
COPYRIGHT 2003 SCIENTIFIC AMERICAN, INC.

If DM is composed by relic particle: WIMP

- Neutralino LSP produce naturally cosmological WIMP density
- Annihilation $\sigma \rightarrow$ relic density $\rightarrow$ WIMP density (Ω_{DM})
- Scattering σ on proton $\rightarrow$ prediction for direct detection
- 10^{-8} pb is **experimentally at hand, and a very significant goal for direct detection**

Test of cosmologicaly + SUSY motivated “Focus Point” region

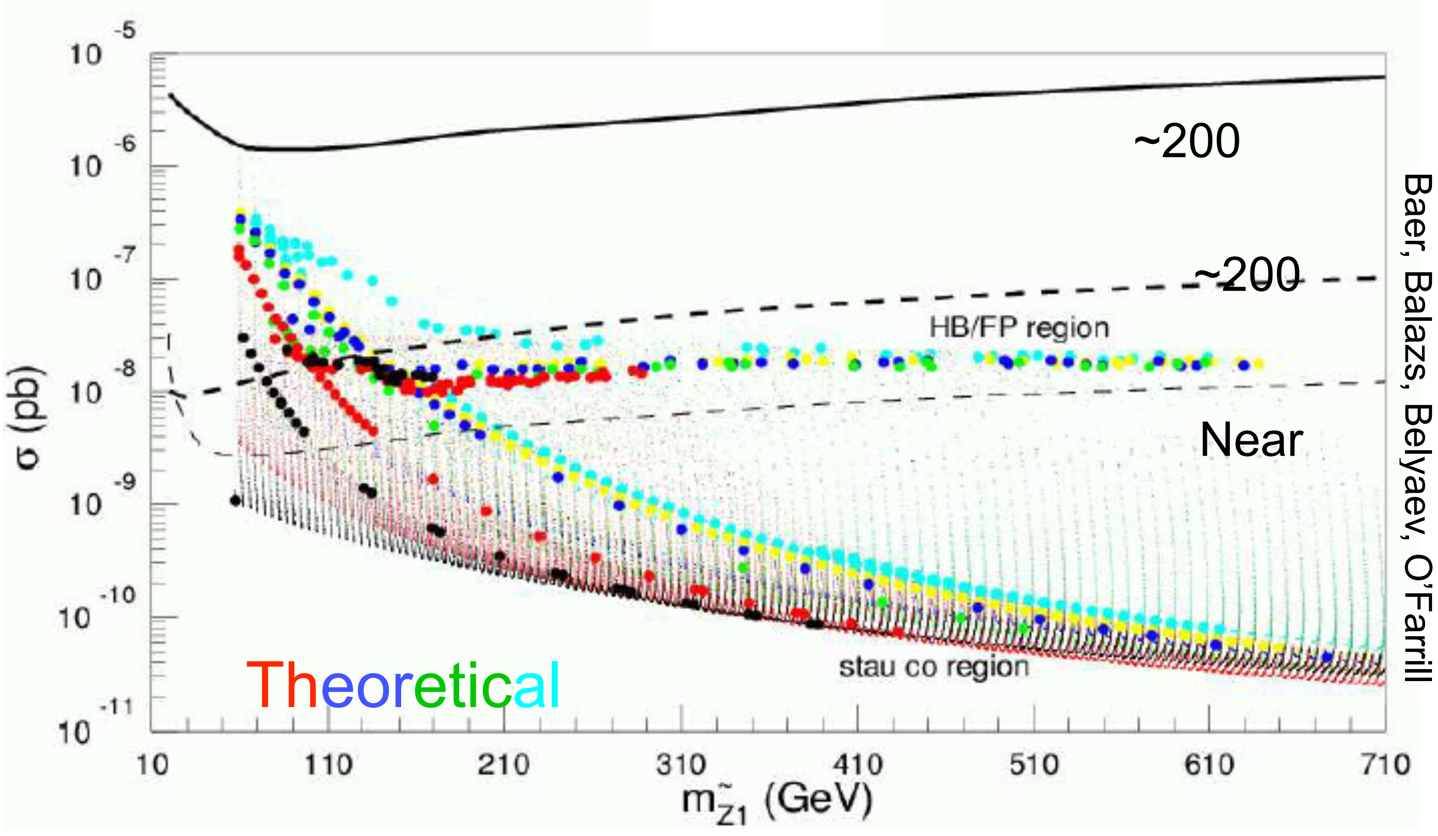

DM experiments

Solid state technology:		Detection:	Target:	Location:
SuperCDMS	current	Phonon/Ionization	Ge (Si)	Soudan (US)/SNOLab (Canada)
EDELWEISS	current	Phonon/Ionization	Ge	Modane (France)
CRESST	current	Phonon/Scintillation	CaWO4	LNGS (Italy)
EURECA	planned	Phonon/Ionization/Scintillation	Ge, CaWO4, ...	Modane (France)
CoGeNT	current	Ionization	Ge	Soudan (US)
C-4	planned	Ionization	Ge	Soudan (US)
TEXONO	current	Ionization	Ge	KSNL (Taiwan)
CDEX	current	Ionization	Ge	CJPL (China)
Liquid Xenon:				
LUX	current	Ionization/Scintillation	Xe	SURF
LZ	planned	Ionization/Scintillation	Xe	SURF
PandaX	current	Ionization/Scintillation	Xe	CJPL (China)
XENON100kg-10T	current/planned	Ionization/Scintillation	Xe	LNGS (Italy)
XMASS1T-20T	current/planned	Scintillation	Xe	Kamioka (Japan)
Liquid Argon:				
DarkSide	current	Ionization/Scintillation	Ar	LNGS (Italy)
ArDM	current	Ionization/Scintillation	Ar	Canfranc (Spain)
MiniCLEAN	current	Scintillation	Ar	SNOLab (Canada)
DEAP	current	Scintillation	Ar	SNOLab (Canada)
Crystals for annual modulation:				
DAMA/LIBRA	current	Scintillation	NaI	LNGS (Italy)
ELEGANT	current	Scintillation	NaI	(Japan)
DM-Ice17	current	Scintillation	NaI	(Southpole)
Princeton NaI	planned	Scintillation	NaI	LNGS (Italy)
CINDMS	planned	Scintillation	CsI(Na)	(China)
KIMS	current	Scintillation	CsI	(Korea)
Superheated liquids:				
COUPP	current	Bubbles	CF3I	SNOLab (Canada)
PICASSO	current	Bubbles	C4FIO	SNOLab (Canada)
SIMPLE	current	Bubbles	C_2ClF_5	Canfranc (Spain)
Directional detection:				
DRIFT	current	Ionization	CS2 CS4	Boulby (UK)
DMTPC	current	Ionization	CF4	WIPP
D^3	planned	Ionization	iC4H10	
MIMAC	planned	Ionization	CF4	Modane (France)
Newage	planned	Ionization	CF4	(Japan) ?

Goal: Detect **WIMP-induced** nuclear recoil in an earth based target material

Standard assumptions:

- WIMP density (ρ_D) at the Earth: ~0.3 GeV/c²/cm³
- Spectral shape: exponential towards lower energies
- Wide range of WIMP masses: 10 – 1000 GeV/c²
- Expected signature: nuclear recoil (of a few keV)
- Expected scattering behaviour: coherent, i.e. ~ A^2
- Single scatters distributed uniformly in target volume
- Extremely rare interaction rate with baryonic matter **(< 0.1 evts/kg/d)**

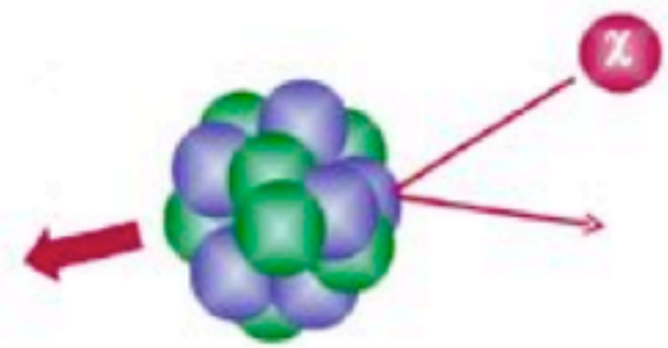

$$\frac{\partial R}{\partial E_R} \propto NF^2(\vec{q})\frac{\rho_D}{M_D}\sigma_\chi e^{-\frac{E_R}{E_0}}$$

R measured rate in detector
M_D mass of WIMP
N number of target nuclei
E_R recoil energy of target nucleus
σ_χ WIMP nucleus cross section
F^2 nuclear Form factor

→ suppress natural radioactivity and cosmic radiation by orders of magnitude:

- Deep **underground facilities**
- **Additional shielding** with selected materials
- Detectors with very **low energy threshold** and excellent **background discrimination** capability

9

CRESST II

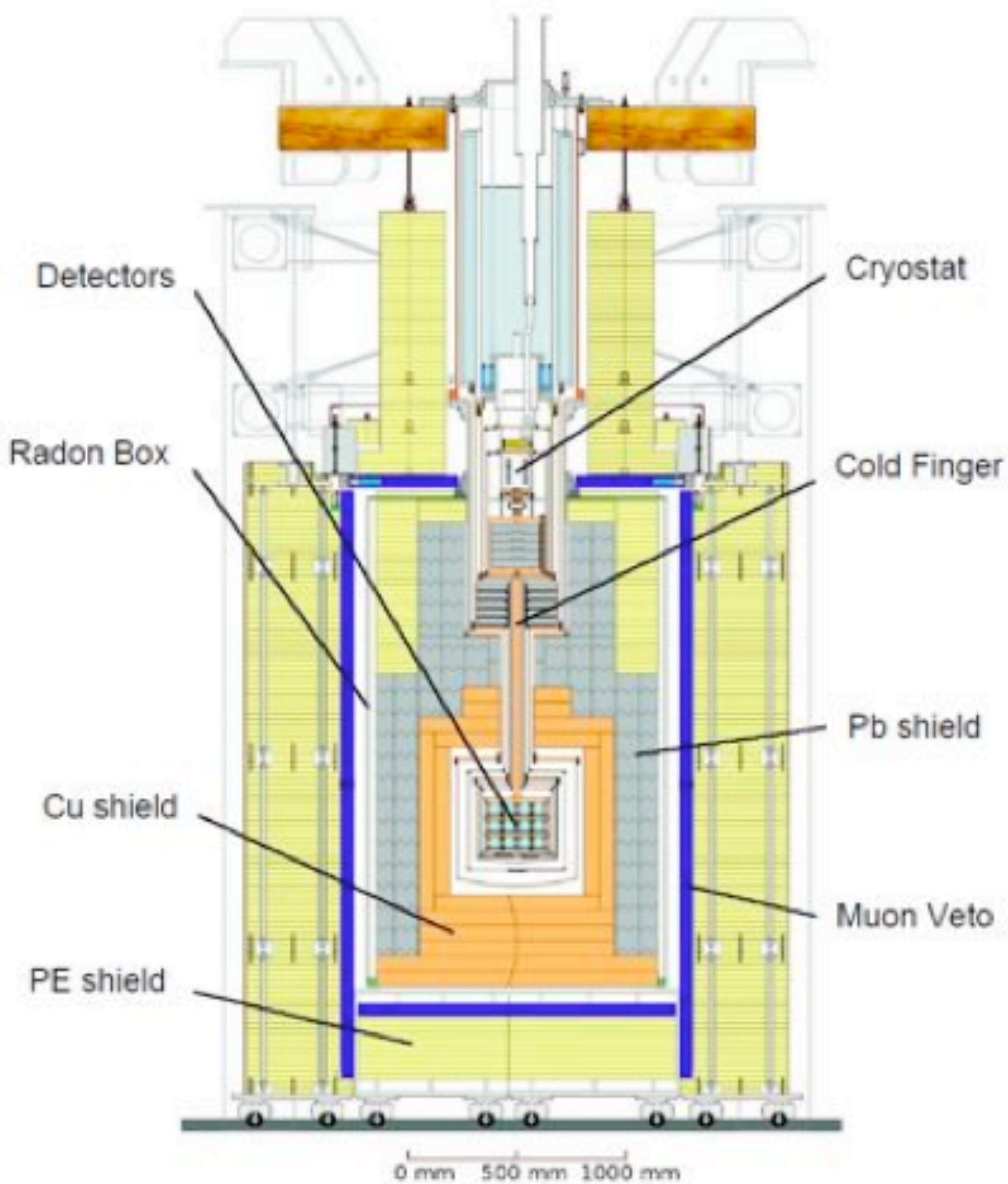

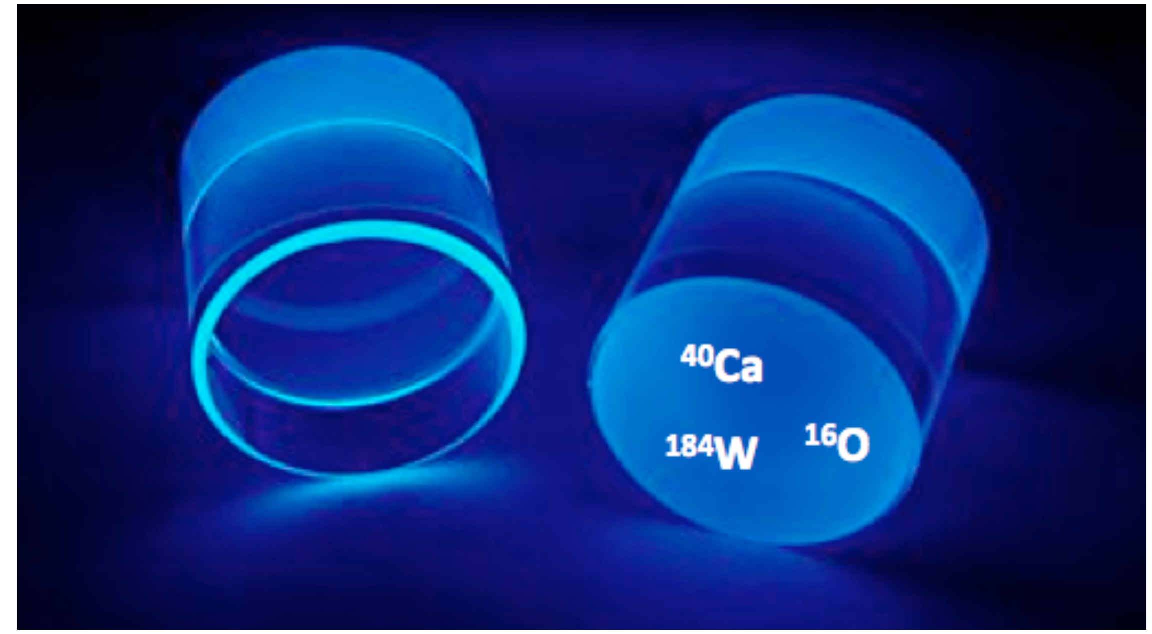

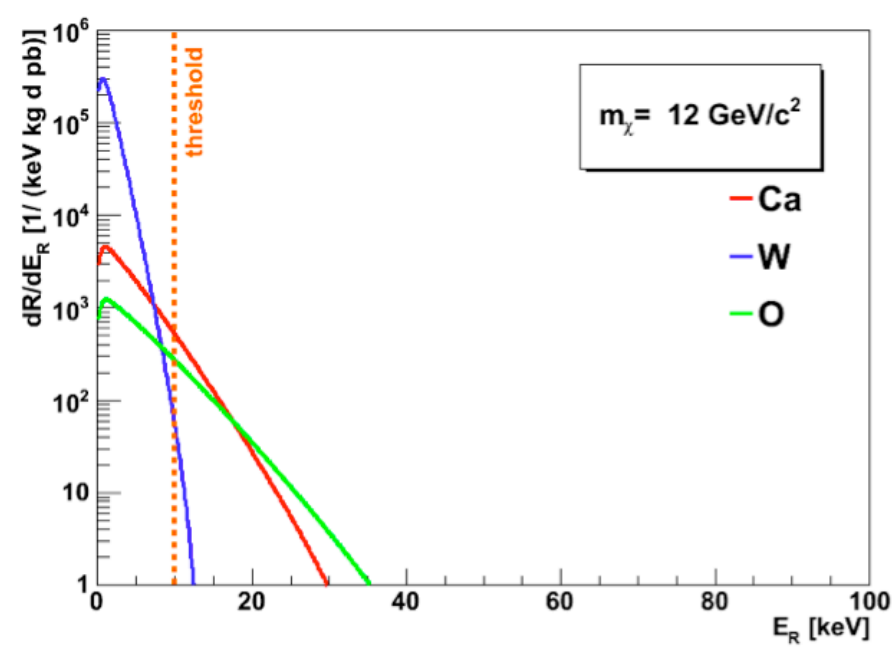

Light-mass WIMP (12 GeV): contribution of O and Ca, W just above threshold

A-thermal phonon detection

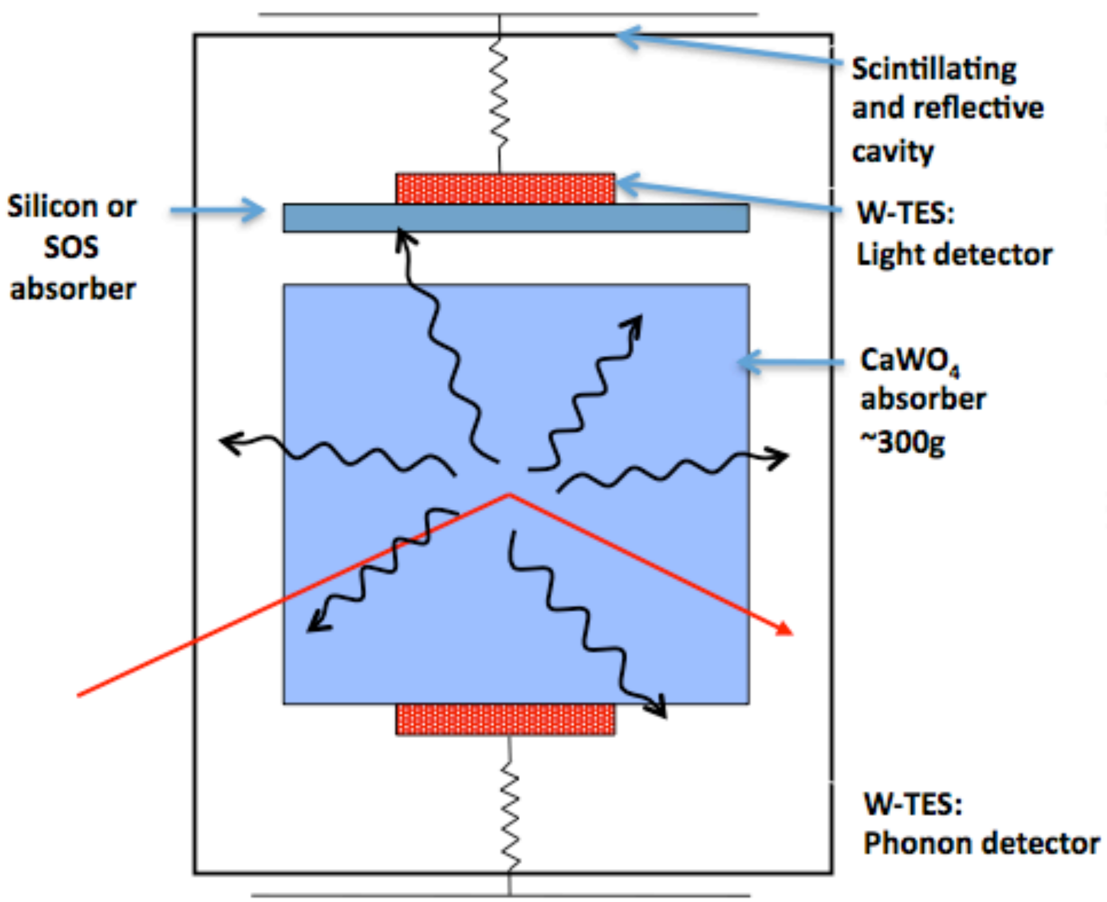

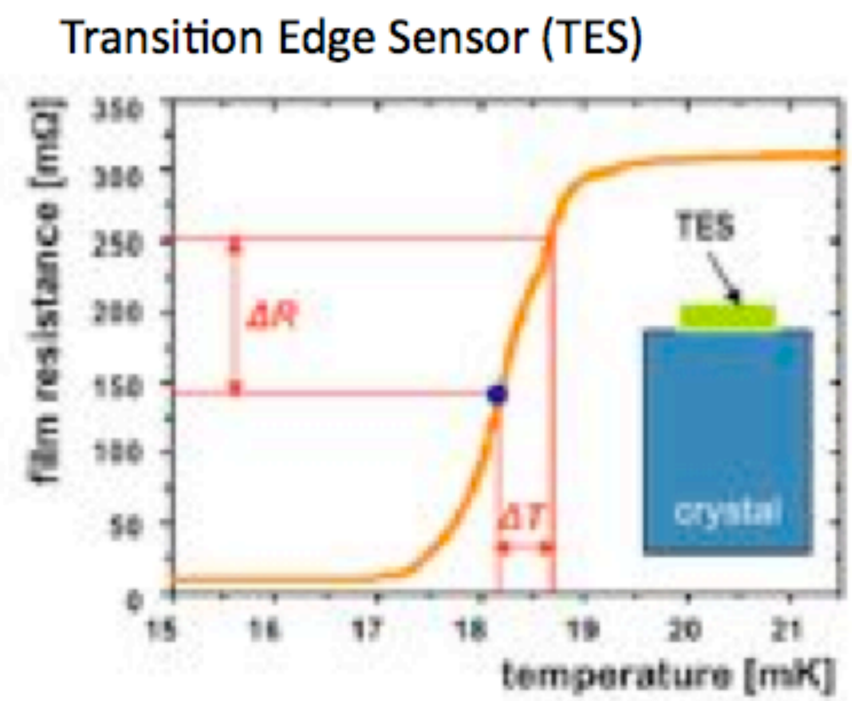

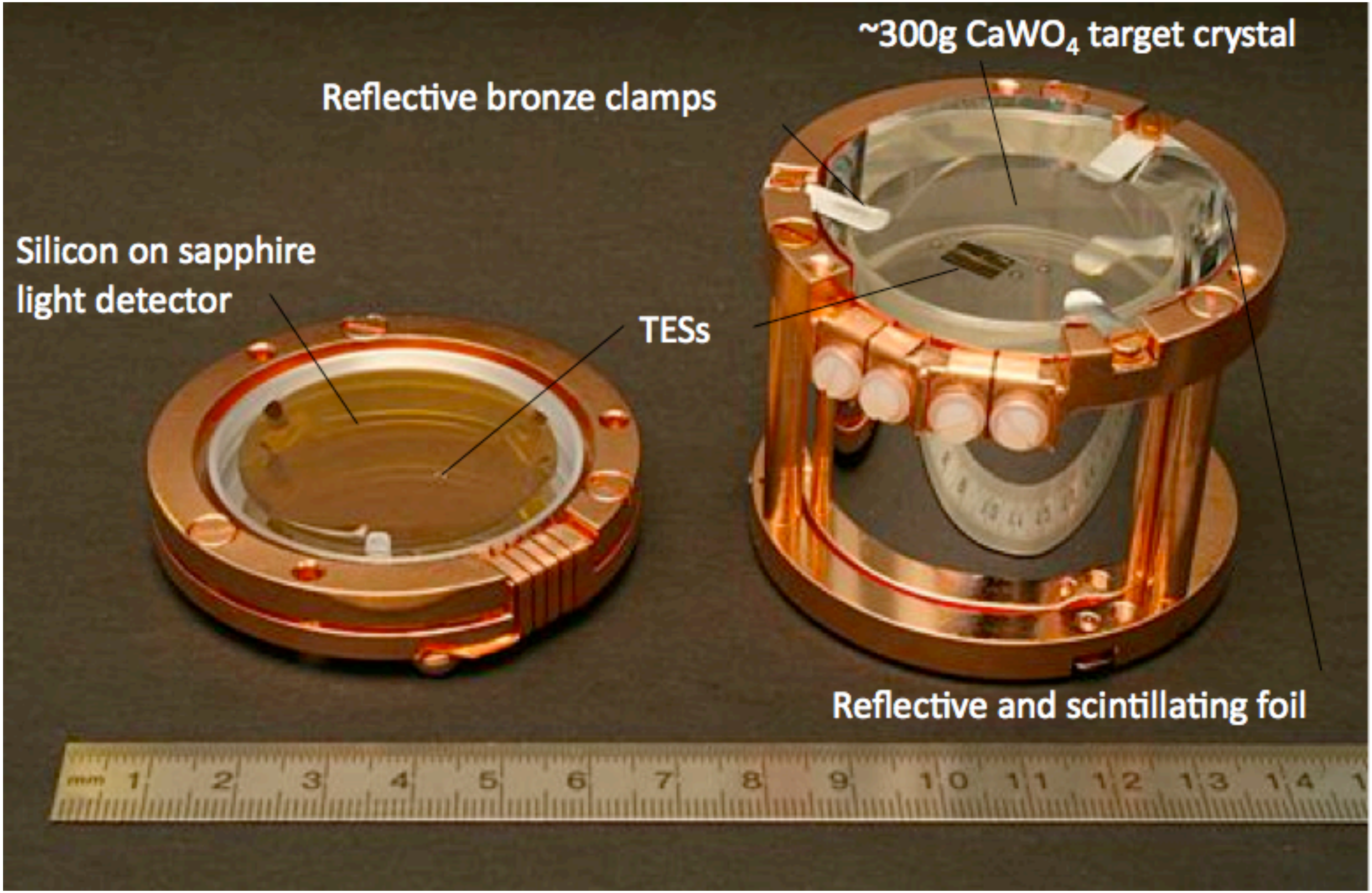
~300g $CaWO_4$ target crystal
Reflective bronze clamps
Silicon on sapphire
light detector
TESs
Reflective and scintillating foil

Data of one single 300g detector module in Run32:

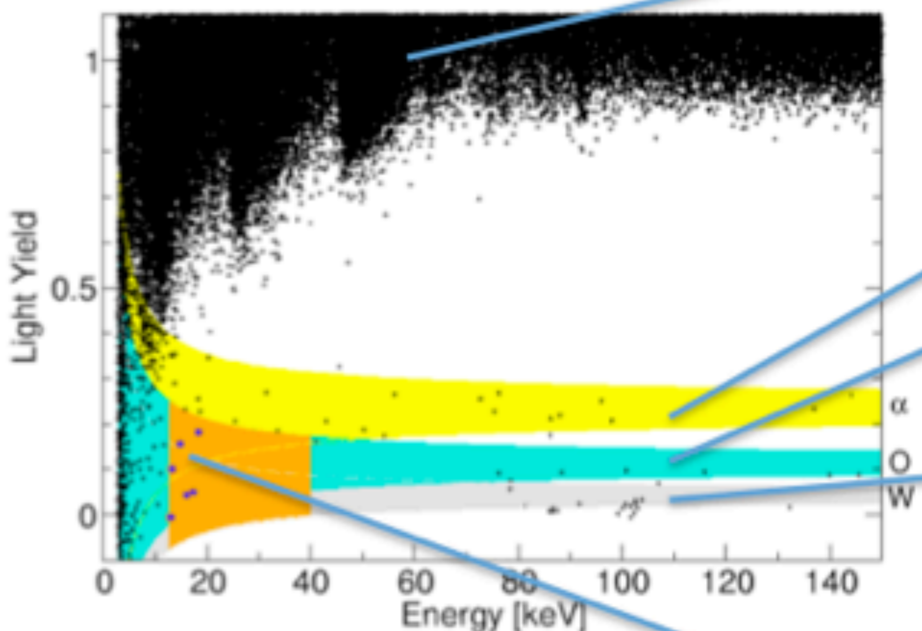

Electron recoils: γ, β

α–events: from surfaces

O-band: neutrons

W-band: expect „heavy"-WIMP interaction
-> contamination from ^{210}Po α-decays in clamps

67 events at low energy observed in O, Ca and W-bands in all detector modules (~730kg d)

Correlated background via sputtering effect in clamps?

M. Kuźniak et al. Astropart. Phys. 36 (2012) 77-82

Eur. Phys. J. C (2012) 72:1971
DOI 10.1140/epjc/s10052-012-1971-8

CDMS

Athermal Phonon Detection Principles

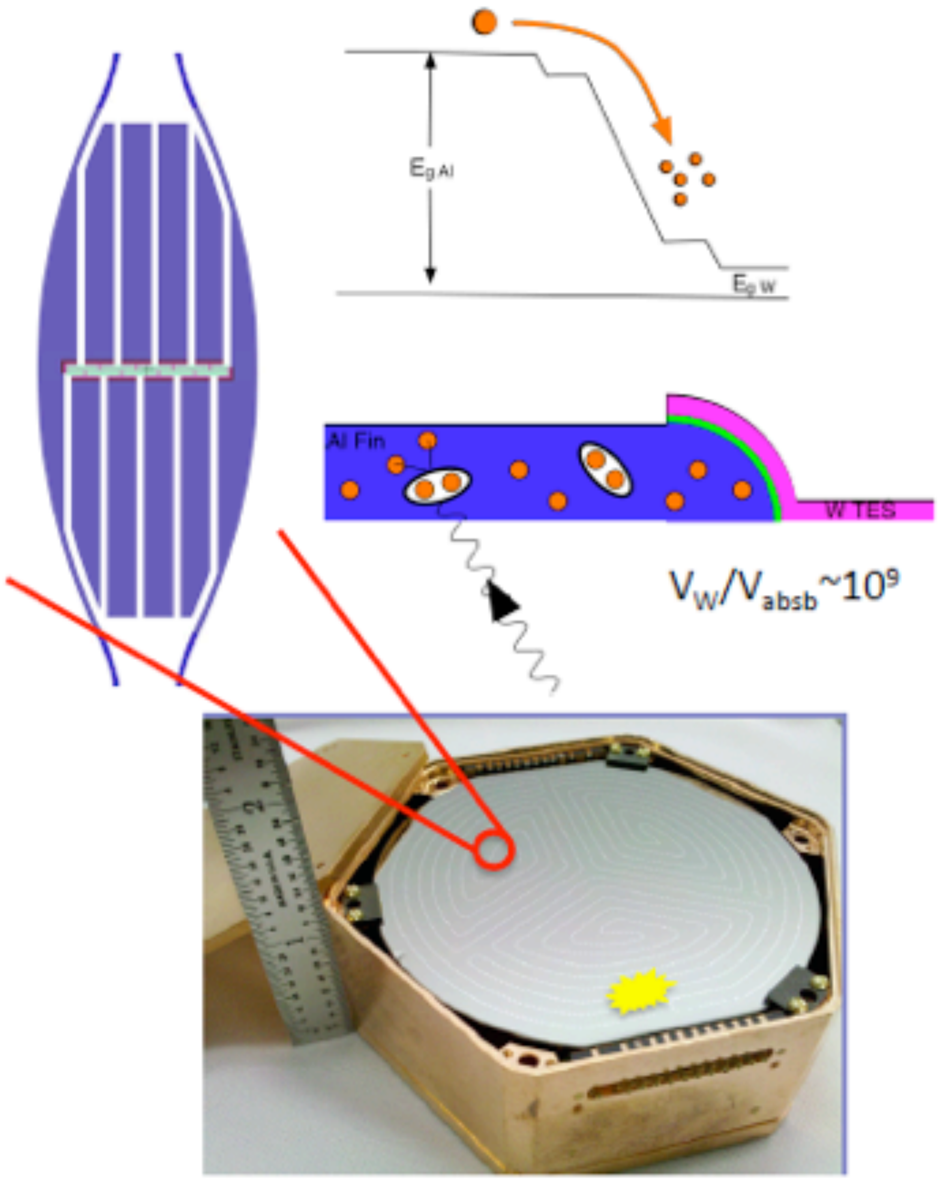

- Become insensitive to absorber heat capacity by collection and concentration of Phonons
- More Complex = More losses
  - Theoretical Max Efficiency: 40%
  - SuperCDMS Efficiency (ε_p): 10-15%

7

iZIP Pulse Shape

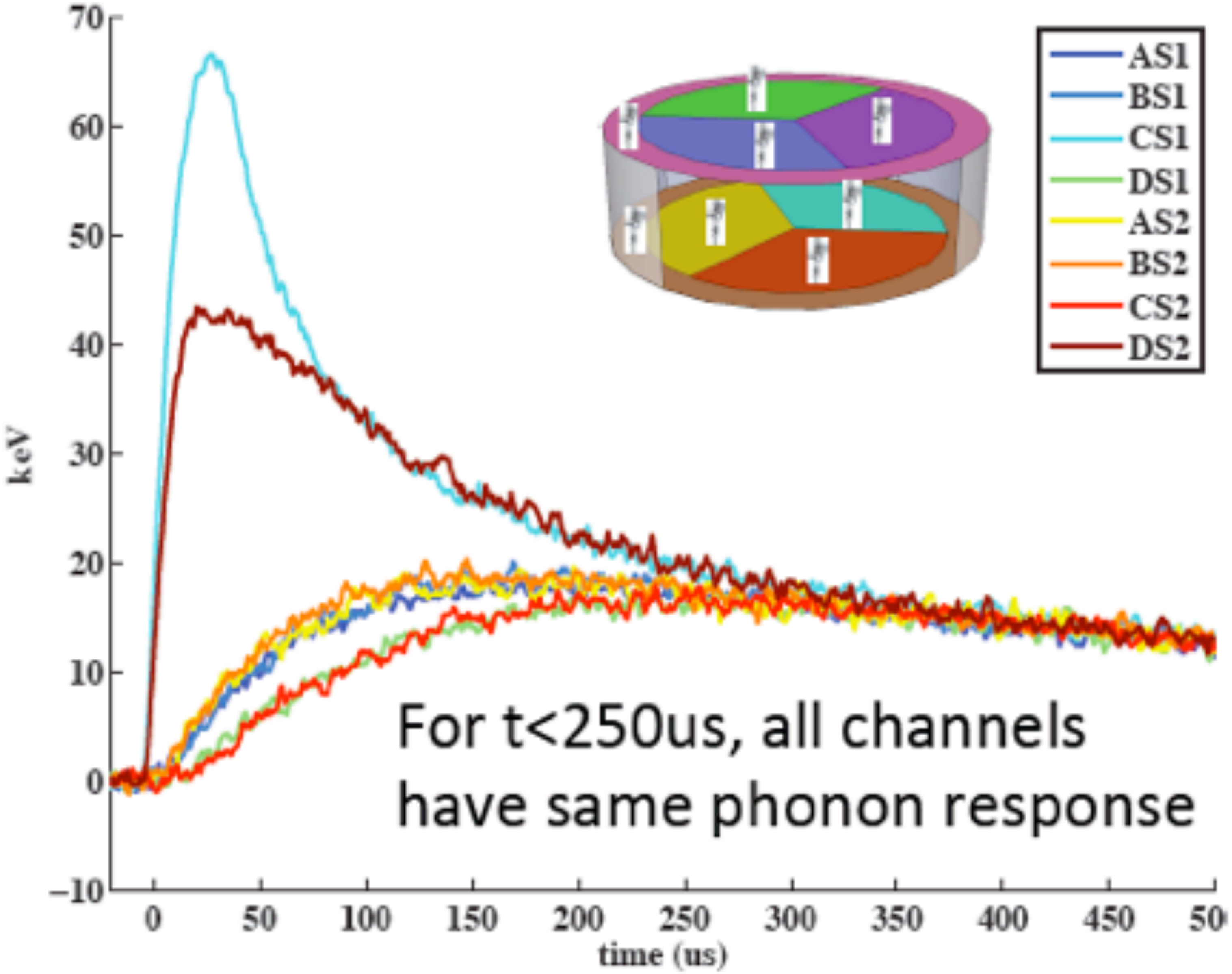

Model: at long time scales, homogenously distributed ballistic phonons bounce around in the crystal until they are collected by the Al collection fins

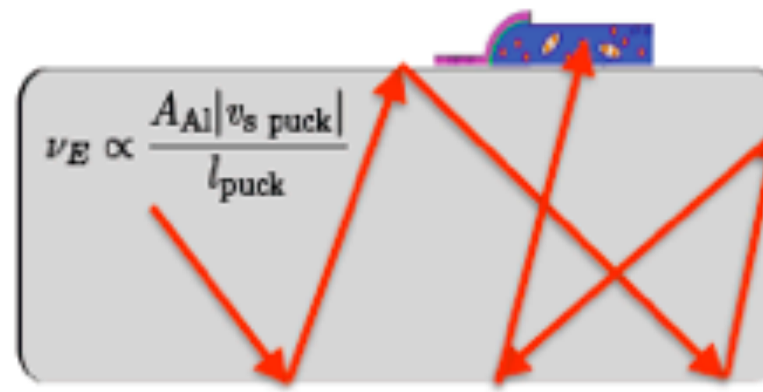

- **Ballistic phonon collection time >> TES fall time**
- **$\omega_{signal} << \omega_{eff}$**

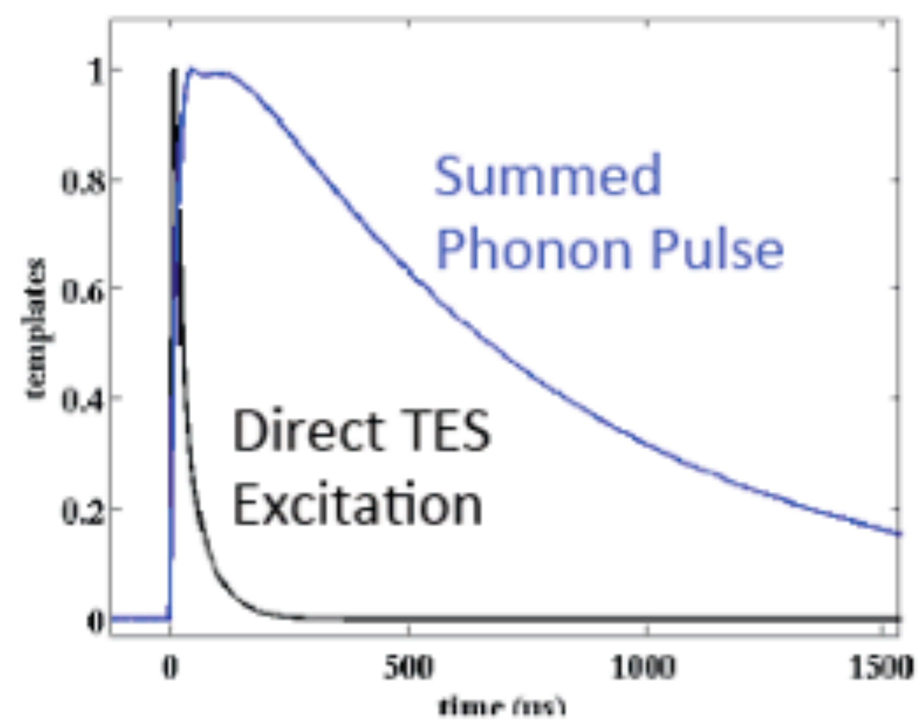

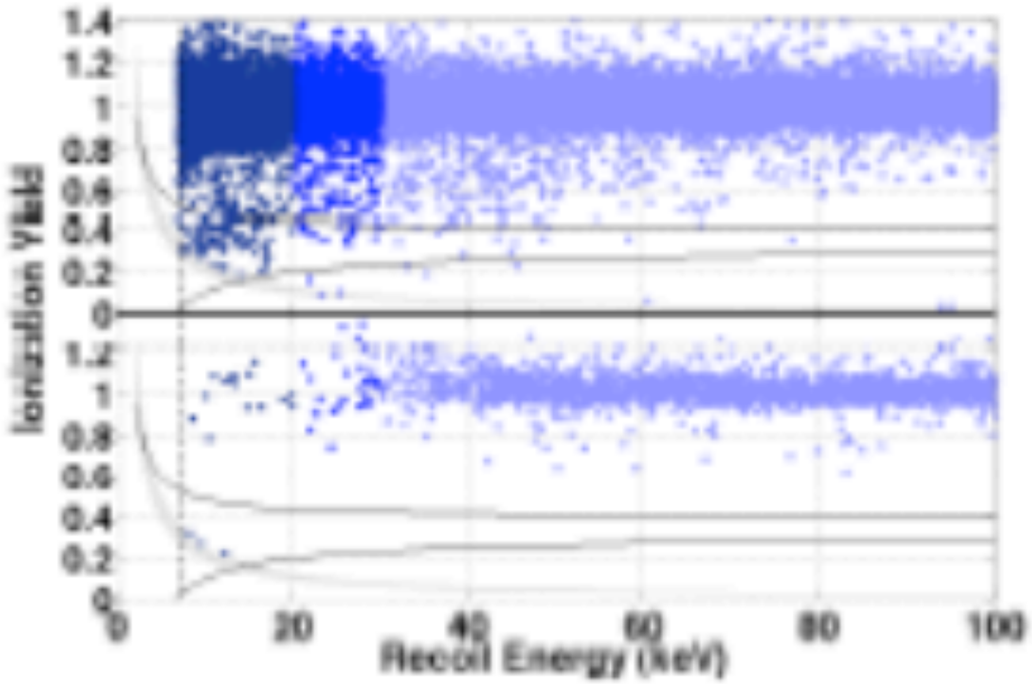

FIG. 2. Ionization yield versus recoil energy in all detectors included in this analysis for events passing all signal criteria except (top) and including (bottom) the phonon timing criterion. The curved black lines indicate the signal region (-1.8σ and +1.2σ from the mean nuclear recoil yield) between 7 and 100 keV recoil energies, while the gray band shows the range of charge thresholds. Electron recoils in the detector bulk have yield near unity. The data are colored to indicate recoil energy ranges (dark to light) of 7–20, 20–30, and 30–100 keV to aid the interpretation of Fig. 3.

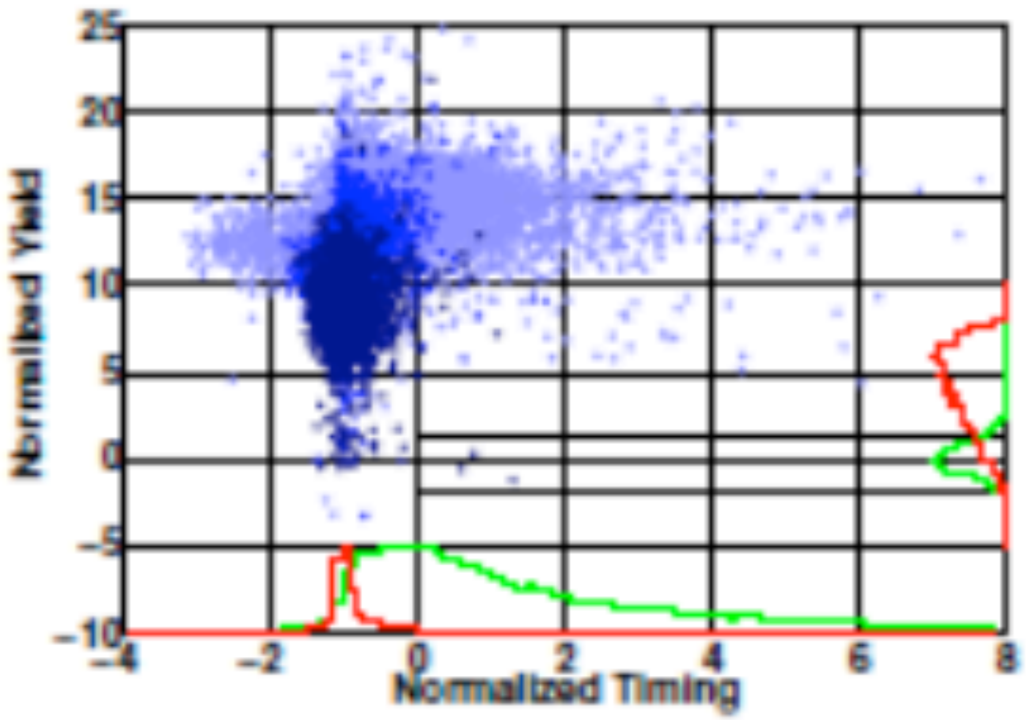

FIG. 3. Normalized ionization yield (standard deviations from the nuclear recoil band centroid) versus normalized phonon timing parameter (normalized such that the median of the surface event calibration sample is at -1 and the cut position is at 0) for events in all detectors from the WIMP-search data set passing all other selection criteria. The black box indicates the WIMP candidate selection region. The data are colored to indicate recoil energy ranges (dark to light) of 7–20, 20–30, and 30–100 keV. The thin red curves on the bottom and right axes are the histograms of surface events from ^{133}Ba calibration data, while the thicker green curves are the histograms of nuclear recoils from ^{252}Cf calibration data.

Precision Experiment: QCD Test

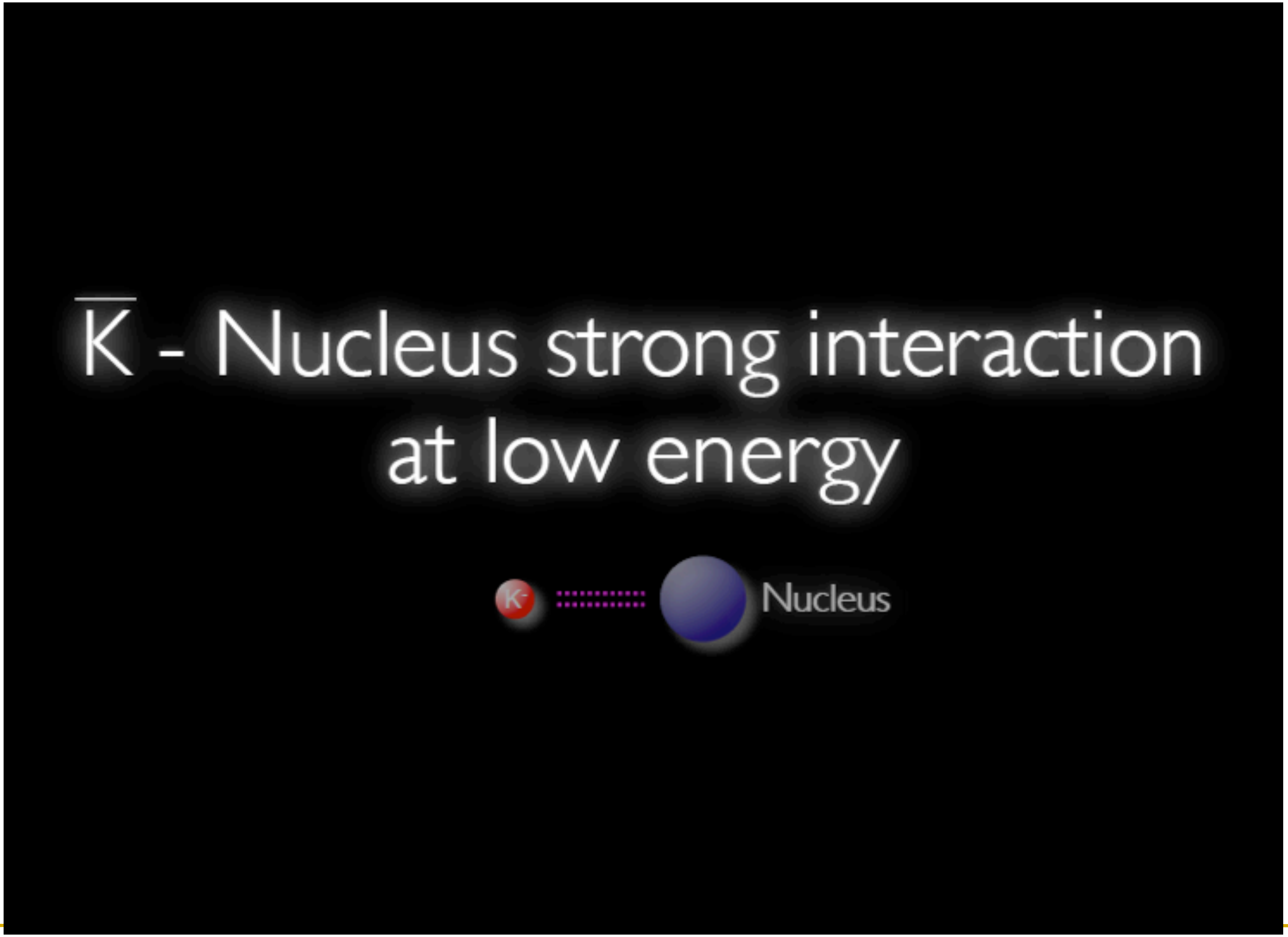

QCD tests

Quantum ChromoDynamics (QCD) becomes non-perturbative at low energy

➡ impossible to use perturbative methods

➡ (approximative) symmetries are good guidelines to understand the hadron dynamics

quark	mass [MeV]	symmetry	
up	~ 2	chiral symmetry	quark mass zero limit
down	~ 5		
strange	~ 100	intermediate	
charm	~ 1,300	heavy-quark symmetry	quark mass infinity
bottom	~ 4,200		
top	~ 170,000	weak decay w/o forming hadrons	

(K^- is the lightest hadron containing strange quark.)

➡ "K^--Nucl." systems are suitable testing grounds for investigating the interplay between spontaneous and explicit **chiral symmetry breaking**.

Strongly attractive!

✓ **Dense matter :** higher density beyond normal nuclear-matter density?

✓ **Neutron star :** Kaon is a strong candidate of hadrons composing inside of neutron star.

✓ **Origin of mass :** the in-medium mass modification effect as a function of matter density?

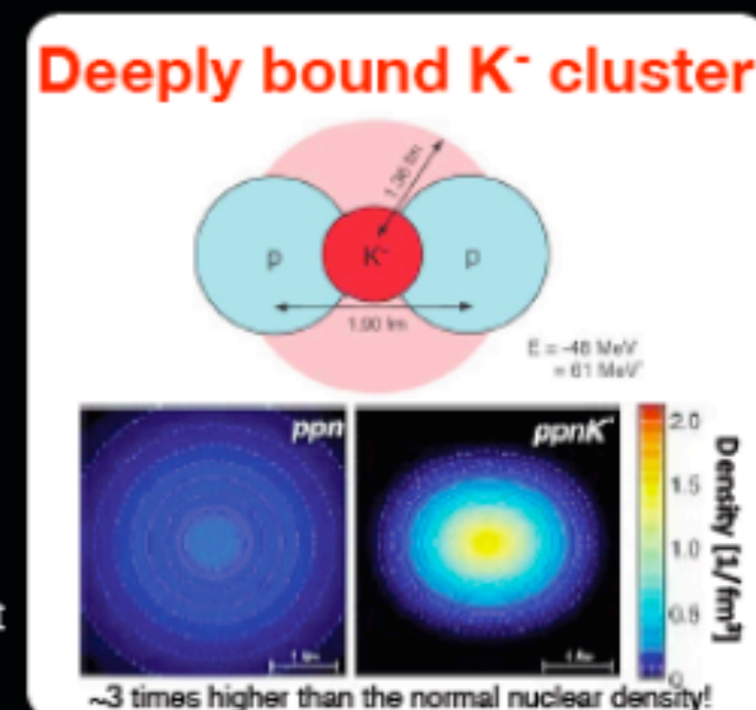

Phys. Lett. B587, 167 (2004)

QCD tests

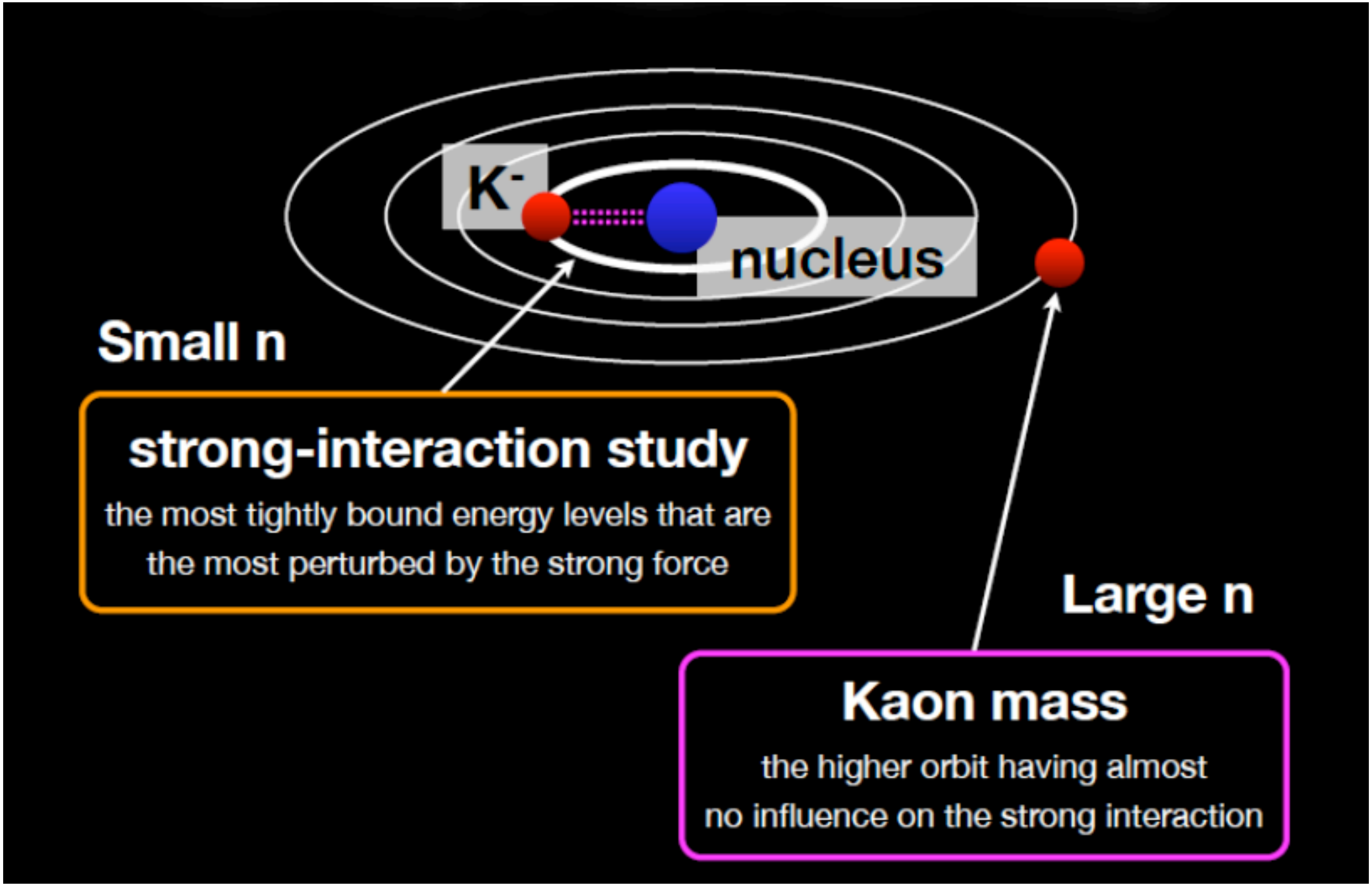

K-
nucleus
Small n
strong-interaction study
the most tightly bound energy levels that are
the most perturbed by the strong force
Large n
Kaon mass
the higher orbit having almost
no influence on the strong interaction

QCD tests: need high E resolution

	K-4He Kα events	detector resolution (FWHM)	stat. accuracy of determining the central value of 6 keV
KEK-E570 with SDD	1500 events	190 eV	2 eV = 190 / 2.35 / sqrt(1500)
TES Microcalorimeter	100 events (~ 4-day beam)	2 eV	0.09 eV
		3 eV	0.13 eV = 3 / 2.35 / sqrt(100)
		4 eV	0.17 eV

QCD tests: need high E resolution

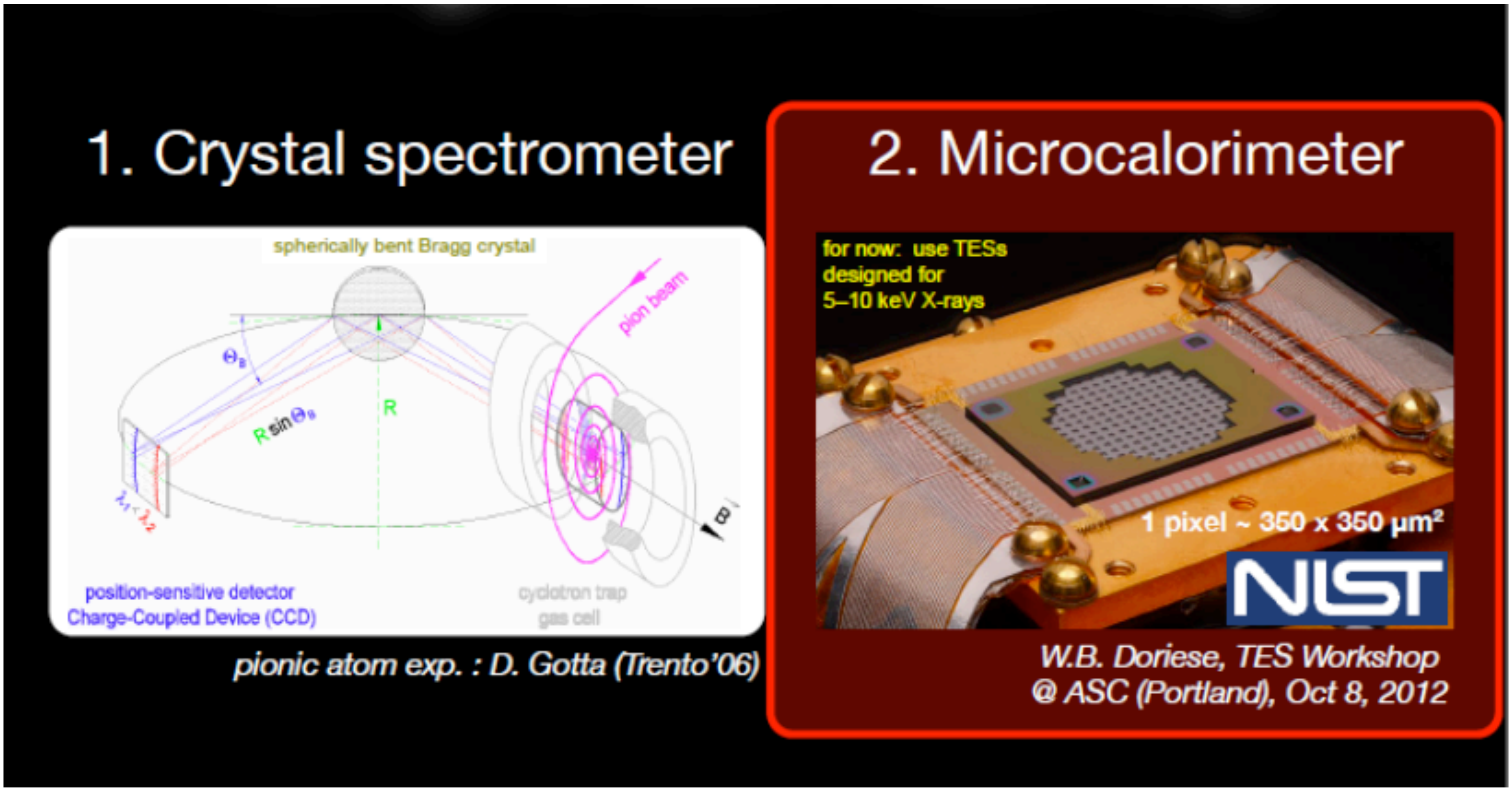

QED tests

- physics interest: precise test of QED
  - for H-atom: measured with high precision (10^{-6}-level)
    - → excellent agreement with prediction
  - for high Z: strong Coulomb fields
    - → $Z\alpha \approx 1$: sensitive test still missing

- idea of the experiment:
  measure transition energy of the Lyman-α line for hydrogen-like Au, U
  ⇒ energy resolution determines precision

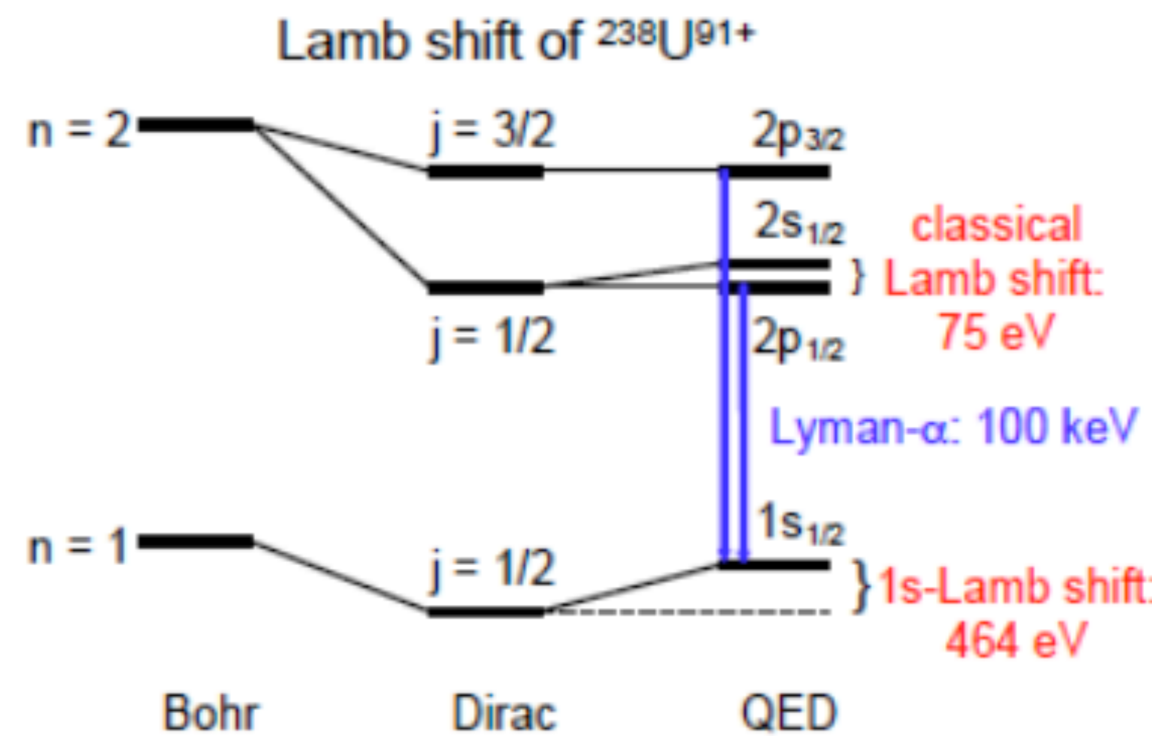

- theoretical prediction for $^{238}U^{91+}$:
  464.3 ± 0.5 eV (Yerochin et al., Phys.Rev.Lett **91** (2003) 073001)

- experimental value for $^{238}U^{91+}$ (measured at GSI with conventional Ge detectors): 460.2 ± 4.6 eV (Gumberidze et al., Phys. Rev. Lett. **94** (2005) 223001)
  - to improve experimental accuracy: new detector concept

Uranium exp. at GSI

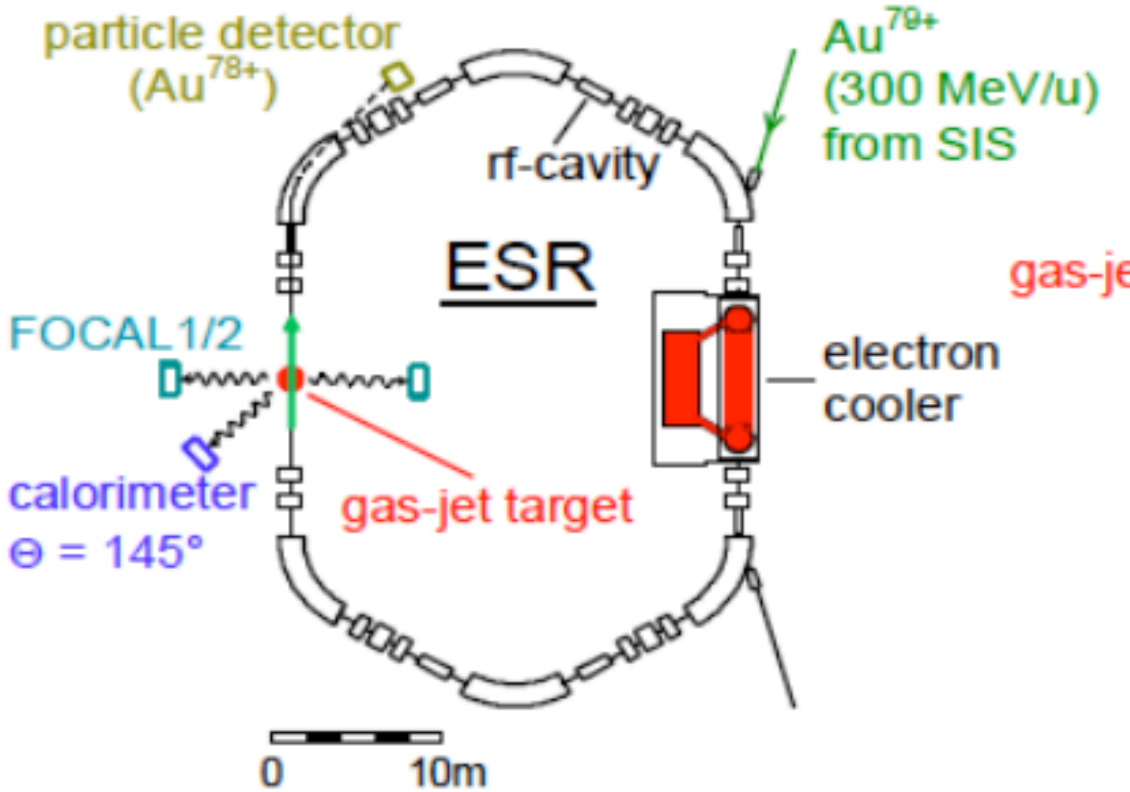

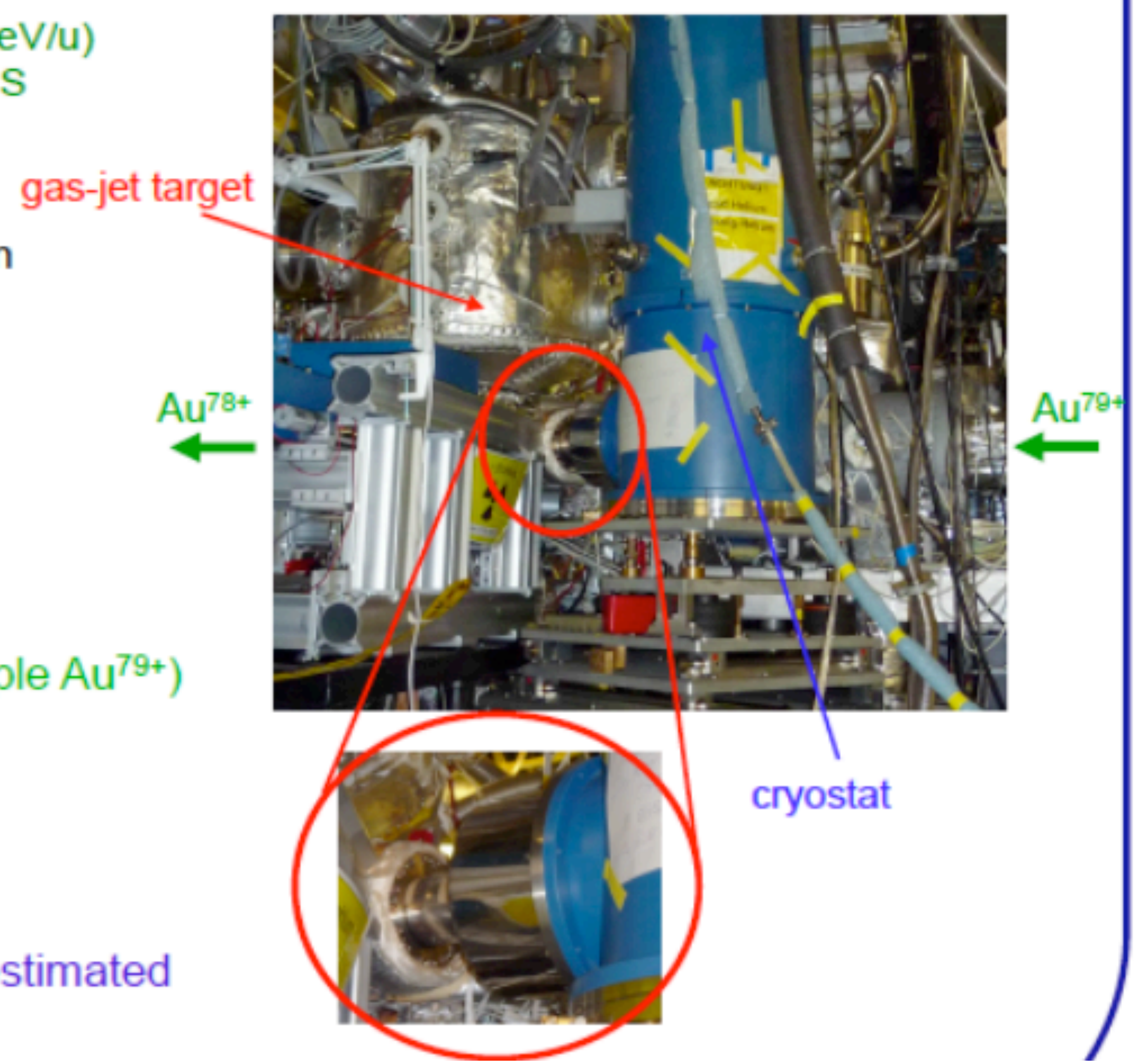

- injection of fully stripped ions (example Au^{79+})
- beam cooling and deceleration
- electron capture in the gas-jet target
- detection of the Lyman-α radiation
  Lyman-α rate in $4\pi = 2 \times 10^5\ s^{-1} \Rightarrow$ estimated count rate/pixel $= 3 \times 10^{-3}\ s^{-1}$

Measurement on $^{197}Au^{78+}$ (2012)

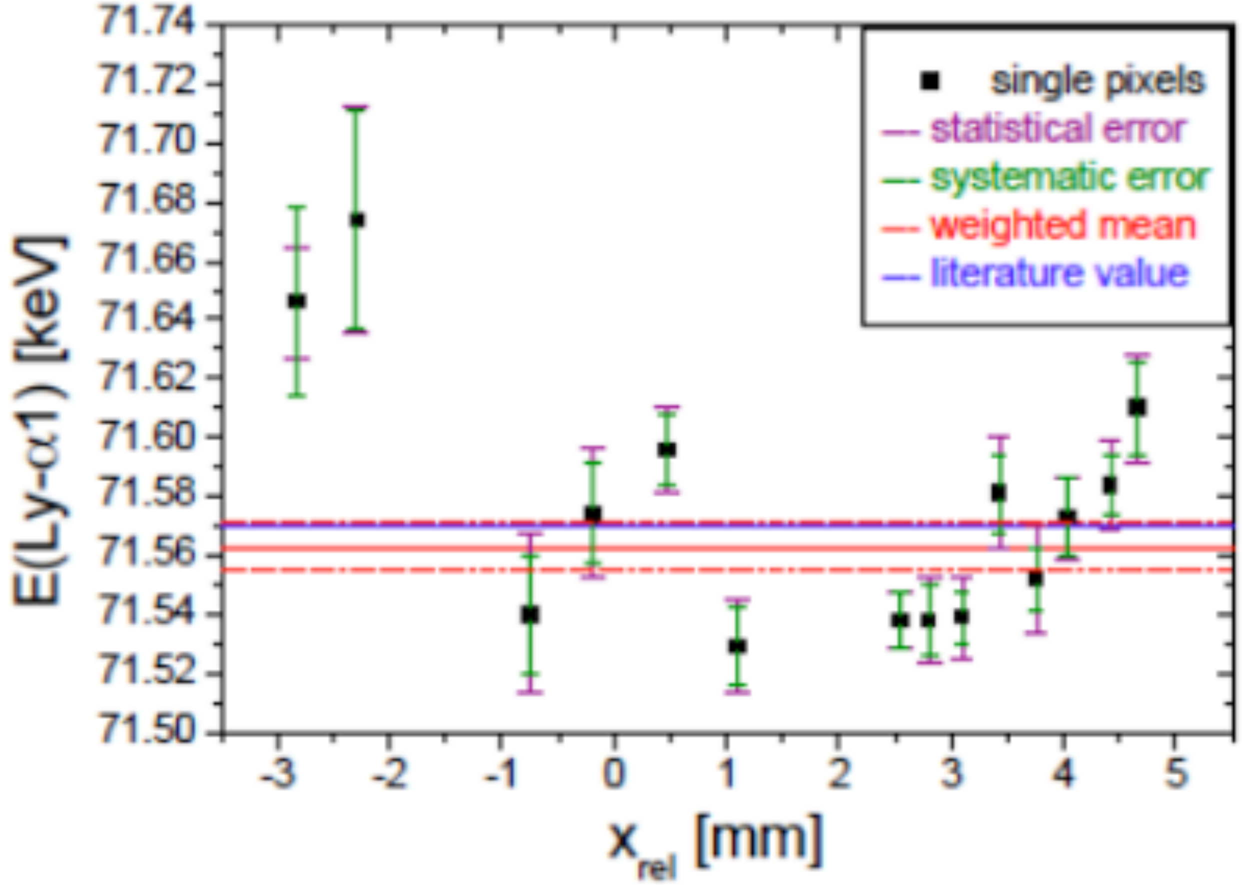

Result: **$E(Ly\text{-}\alpha 1) = (71563 \pm 4_{stat} \pm 7_{syst})$ eV**

- in good agreement with theoretical prediction $E(Ly\text{-}\alpha 1) = 71569.7(5)$ eV
- statistical and systematic uncertainities considerably reduced
- precision already comparable to best result with conventional Germanium detectors (± 4.6 eV)
- systematic uncertainity dominated by precision of determination of Θ (6 eV)

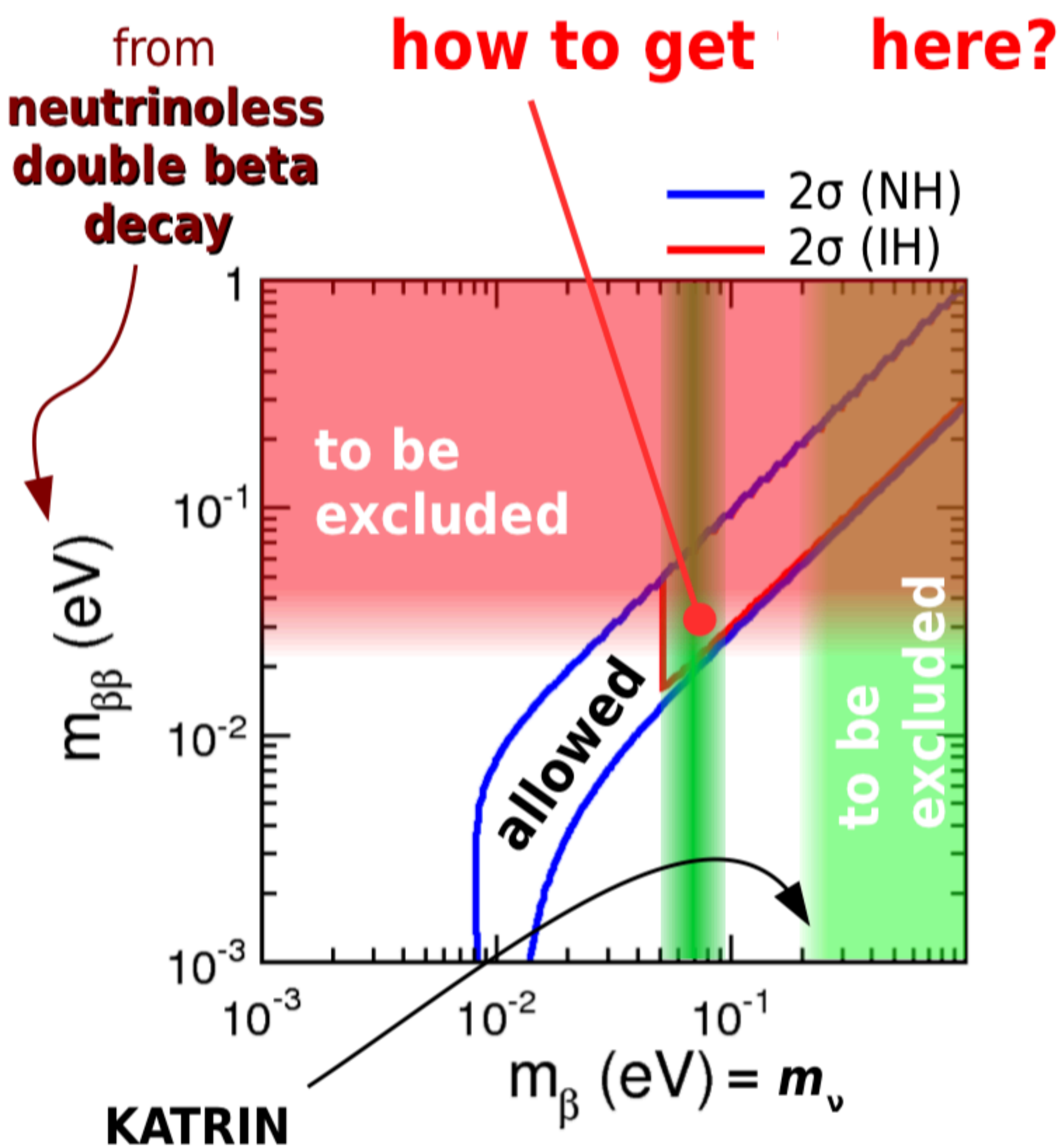

Picture: A.Nucciotti

1. Testing Neutrino Absolute Mass scale with in Laboratory with Beta decaying nucleai

2. Use of <u>Direct Calorimetric Methods</u> to overcome the artefacts of beta spectrometers

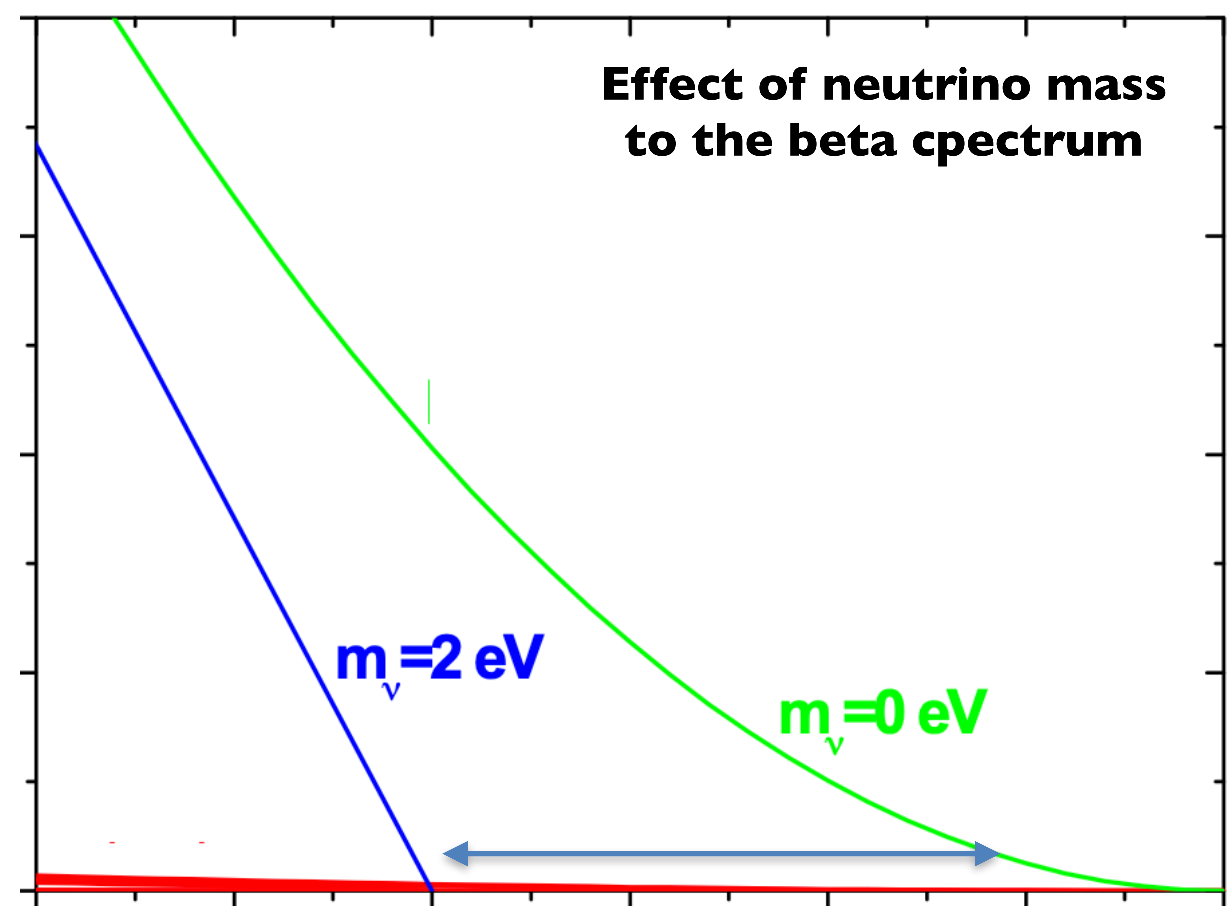

Improved Rhenium detector with Superconducting TES

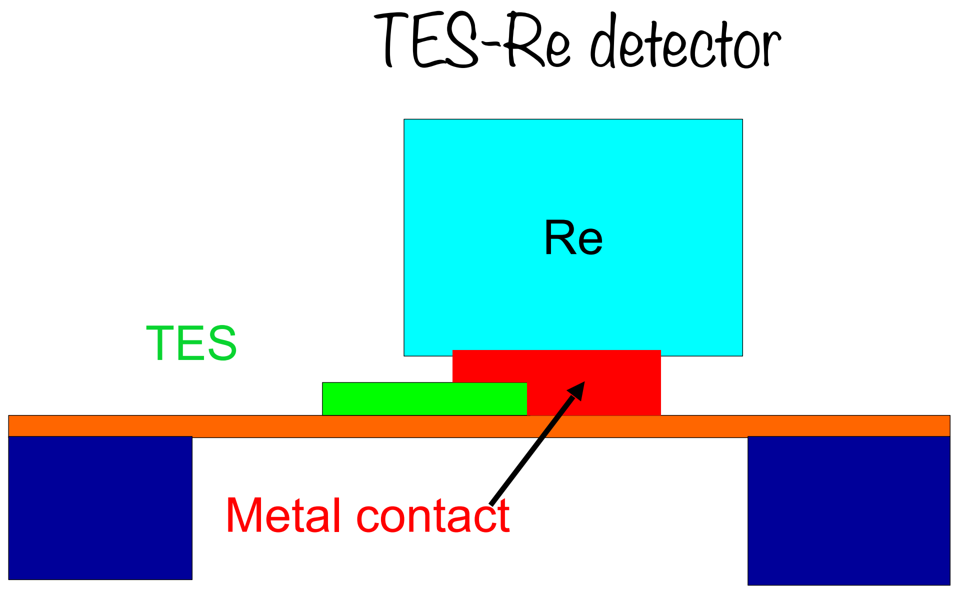

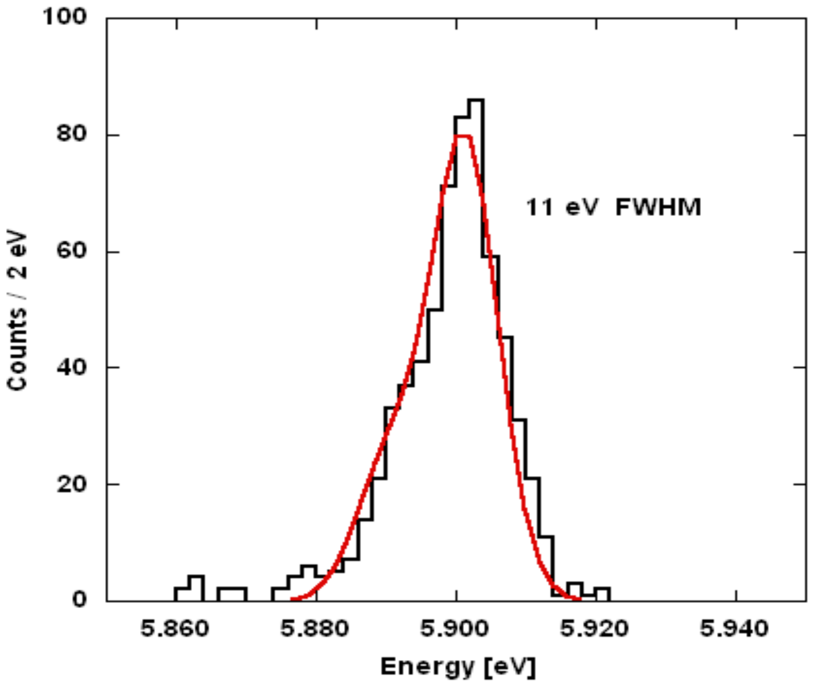

Re-crystal on epoxy-post / Ir-TES / SiN-membrane

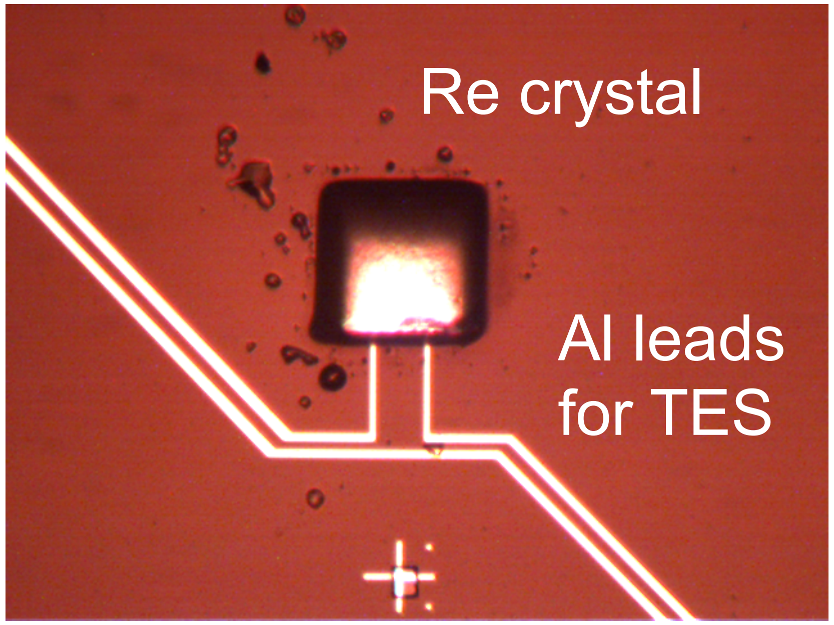

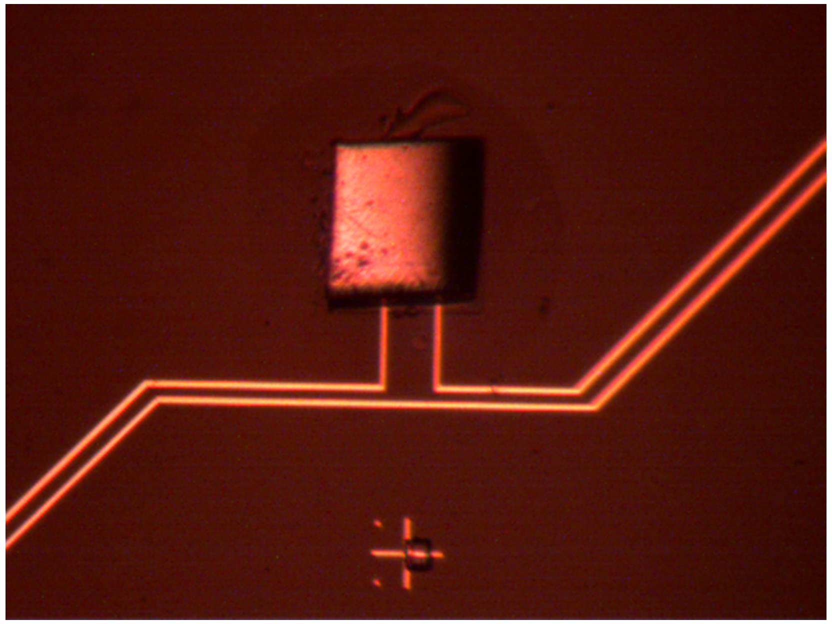

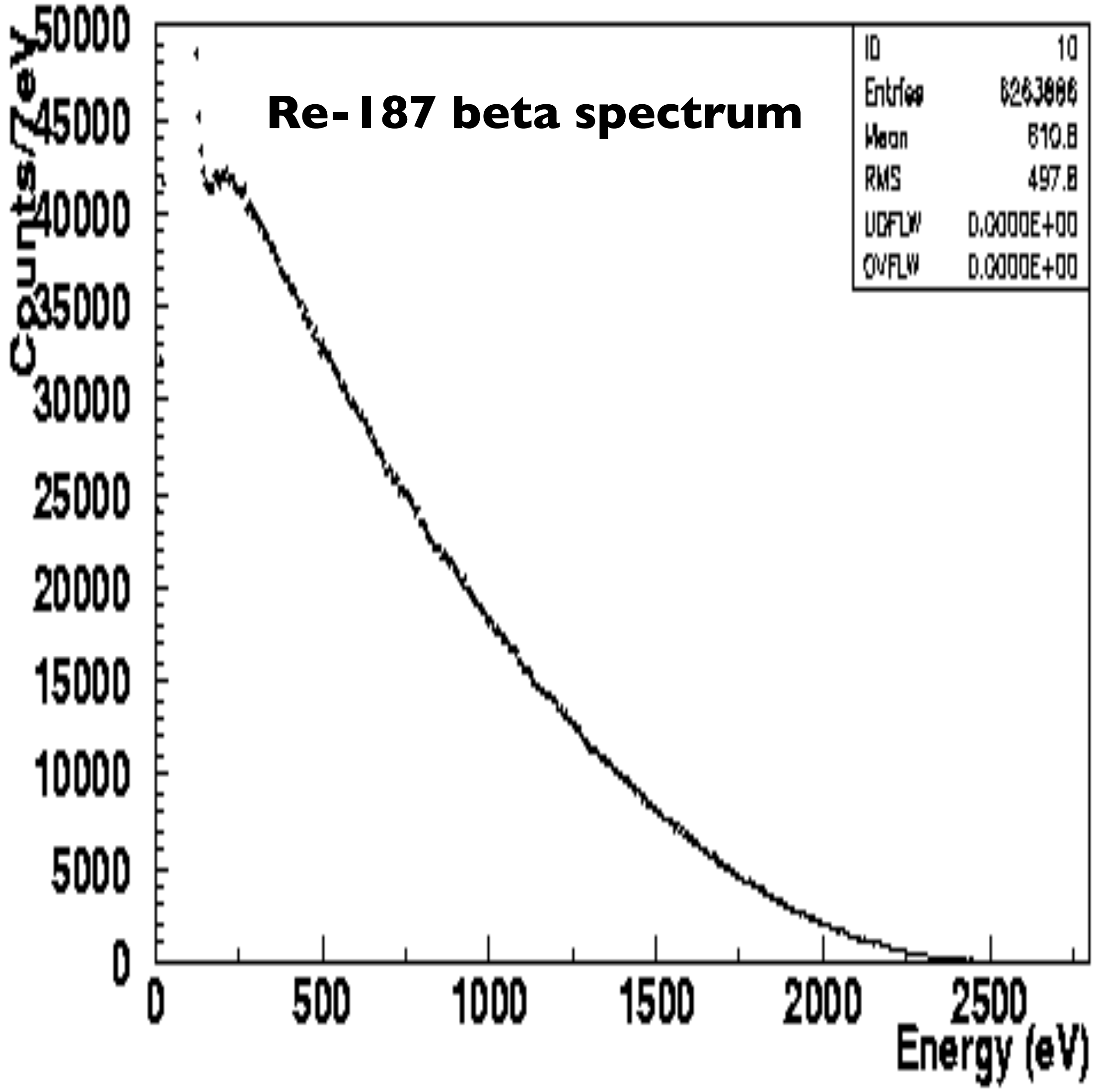
Re-187 beta spectrum
Counts/7eV
Energy (eV)
ID 10
Entries 8263886
Mean 810.8
RMS 497.8
UDFLW 0.0000E+00
OVFLW 0.0000E+00
0
500
1000
1500
2000
2500
5000
10000
15000
20000
25000
30000
35000
40000
45000
50000

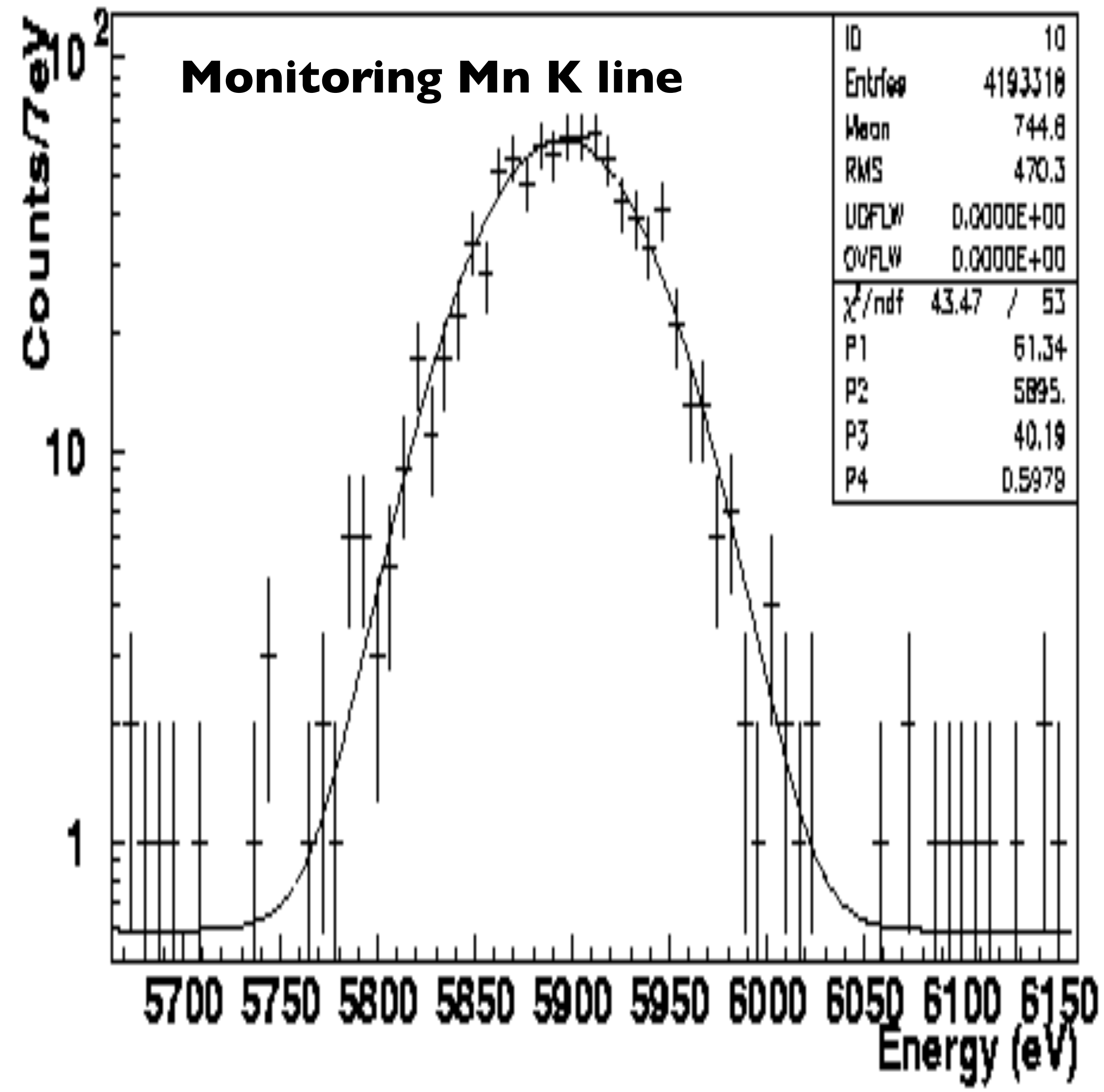
Monitoring Mn K line
Counts/7eV
Energy (eV)
ID 10
Entries 4193318
Mean 744.8
RMS 470.3
UDFLW 0.0000E+00
OVFLW 0.0000E+00
χ²/ndf 43.47 / 53
P1 61.34
P2 5895.
P3 40.19
P4 0.5979
5700 5750 5800 5850 5900 5950 6000 6050 6100 6150

Beta Environmental Fine structure(BEFS)

Residuals from theo. beta spectrum

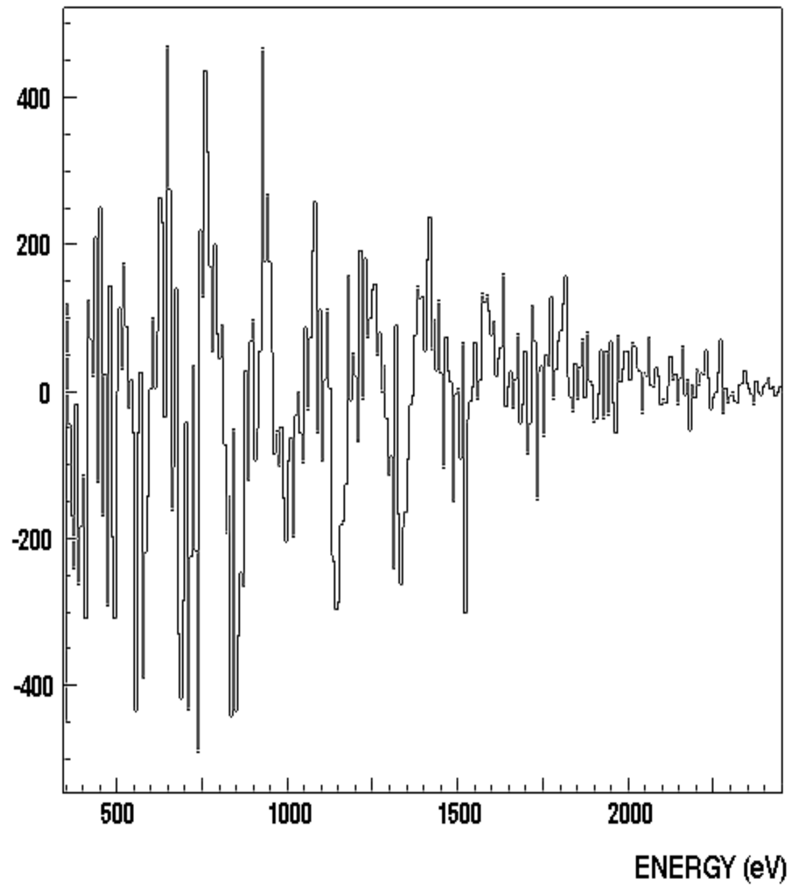

Oscillatory pattern of the Beta Spectrum

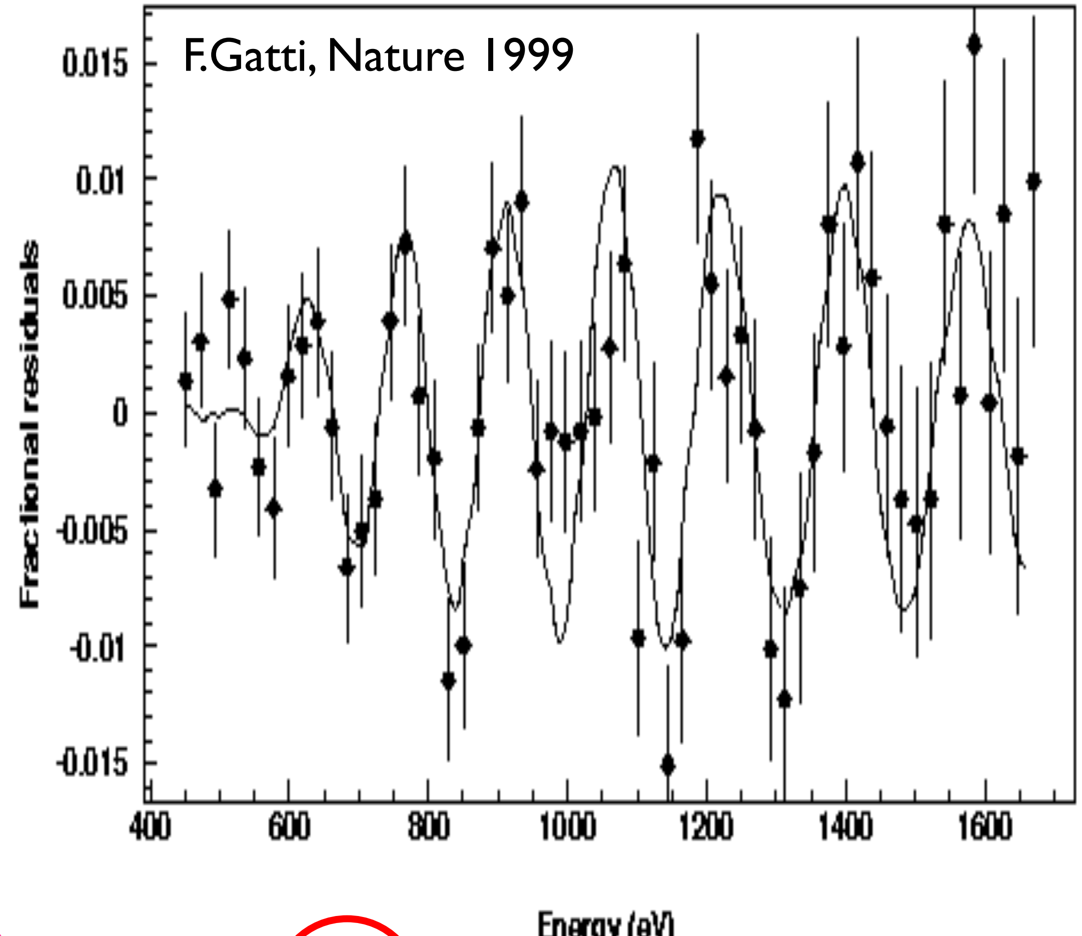

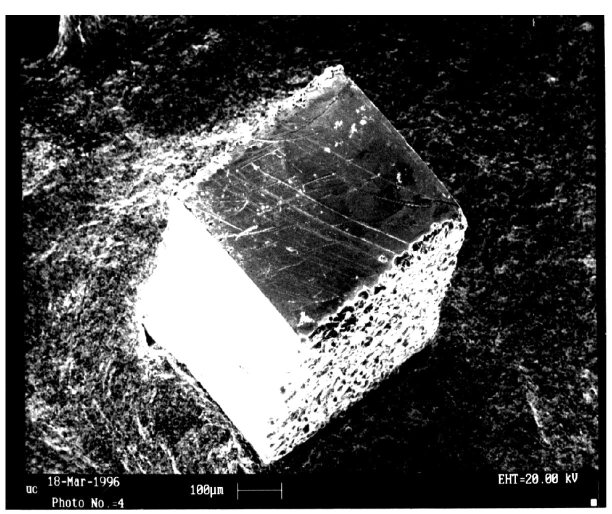

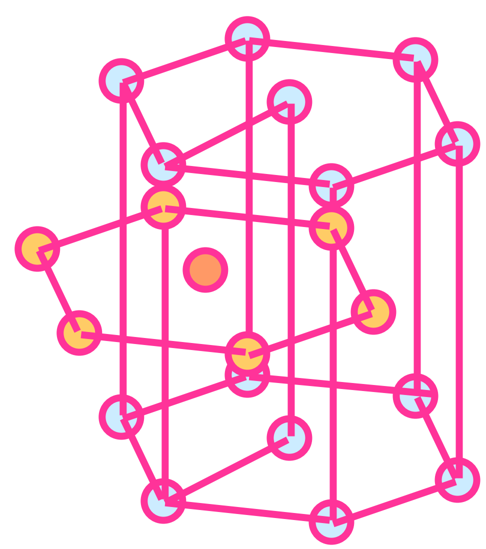

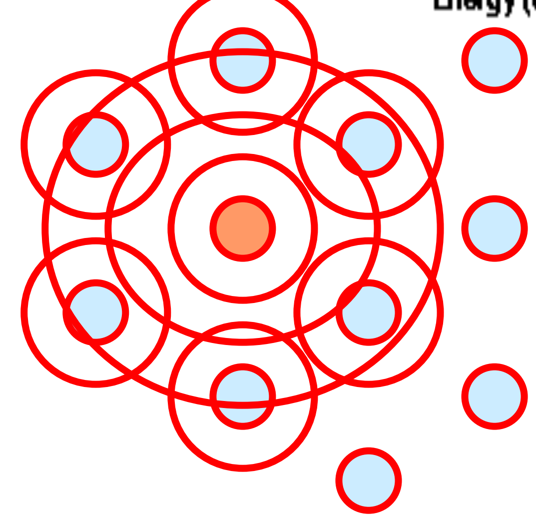

HOLMES

$^{163}\mathrm{Ho} + e^- \longrightarrow {}^{163}\mathrm{Dy}^* + \nu_e$ electron capture decay

(A. De Rujula and M.Lusignoli, Phys. Lett. 9 (1982)

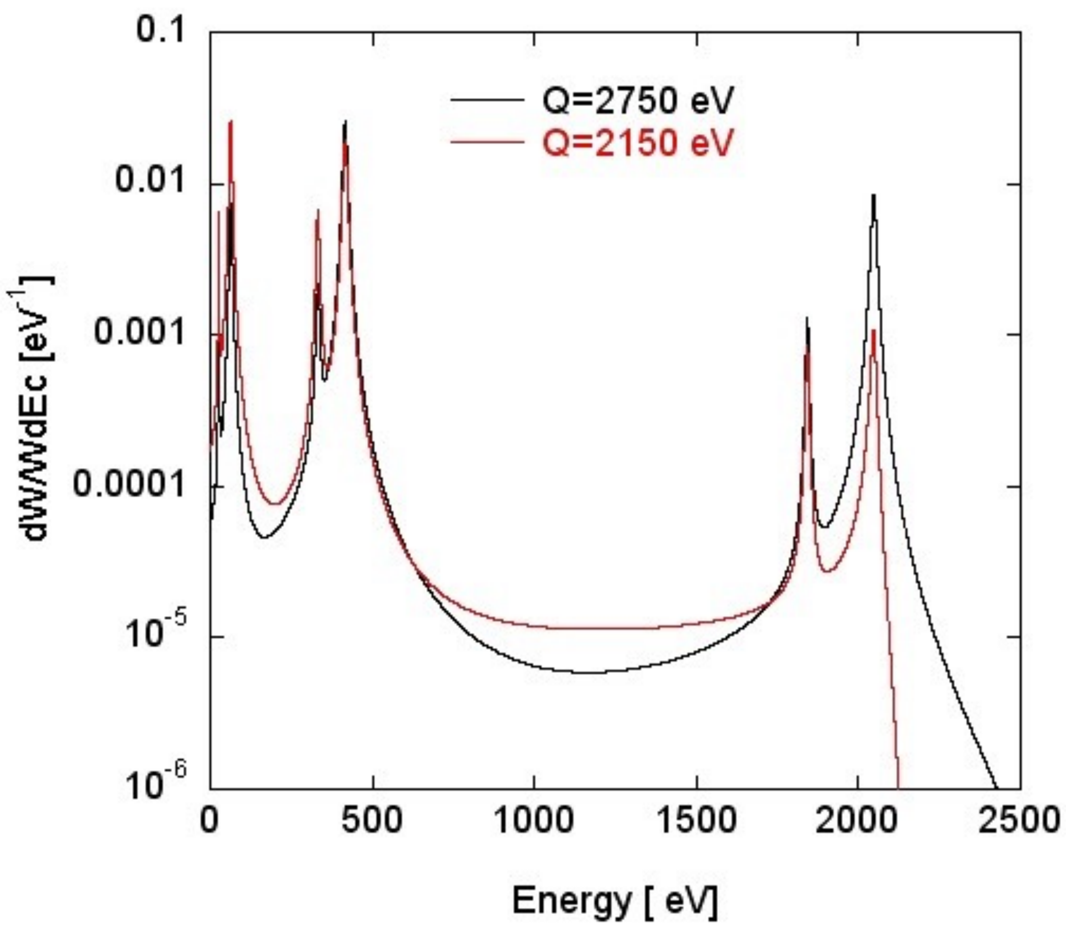

- First calorimetric measurement of ^{163}Ho endpoint energy: Q = 2.80 ± 0.05 keV (F. Gatti, et al, Physics Letters B, 1997) with Ho-oxide embedded in Sn absorber

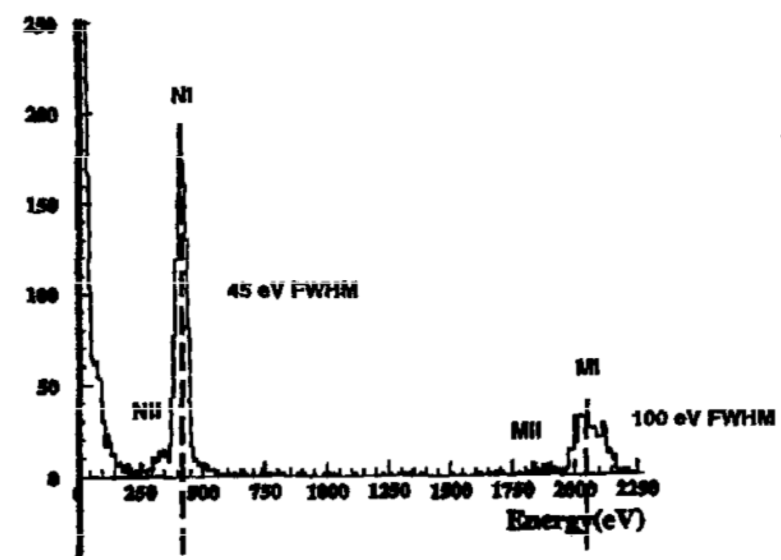

HOLMES

Univ. Milano-Bicocca
INFN Milano-Bicocca
G.Ceruti
M.Faverzani
E.Ferri
A.Giachero
A.Nucciotti
A.Orlando
G.Pessina
A.Puiu
S.Ragazzi

INFN Genova
M.Biasotti
V.Ceriale
G.Gallucci
M.De Gerone
F.Gatti
L.Parodi
F.Siccardi

INFN Roma
M.Lusignoli

INFN LNGS
S.Nisi

NIST
B.Alpert
D.Becker
D.Bennett
J.Fowler
J.Gard
J.Hays-Wehle
G.Hilton
J.Mates
C.Reintsema
D.Schmidt
D.Swetz
J.Ullom
L.Vale

PSI
R.Dressler
S.Heinitz
D.Schumann

CENTRA-IST
M.Ribeiro-Gomes

ILL
U.Koester

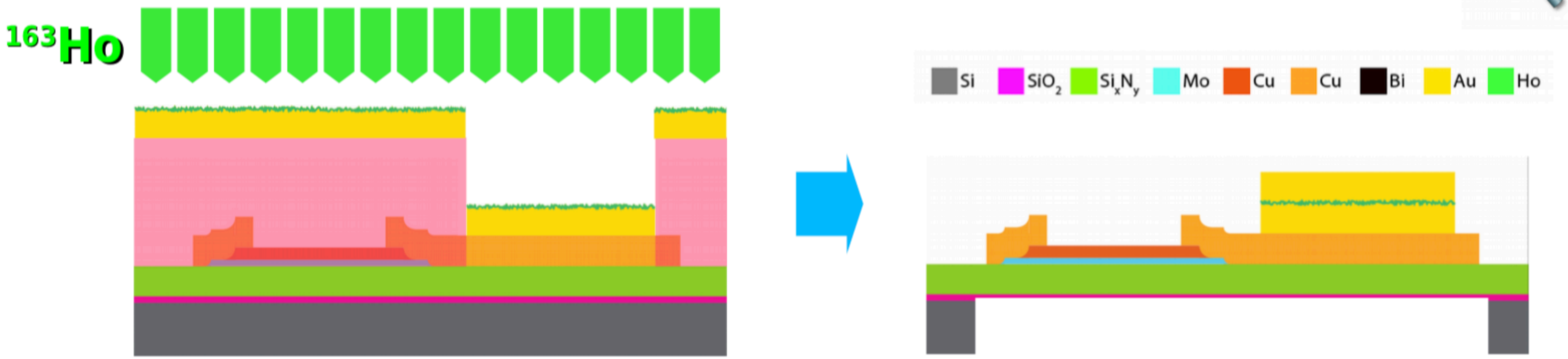

- TES array fabricated at **NIST**, Boulder, CO, USA
- ^{163}**Ho** implantation at **INFN**, Genova, Italy
- 1 μm **Au** final layer deposited at INFN Genova
- final fabrication process definition in progress
- HOLMES **4×16 linear sub-array** for low parasitic *L* and high implant efficiency

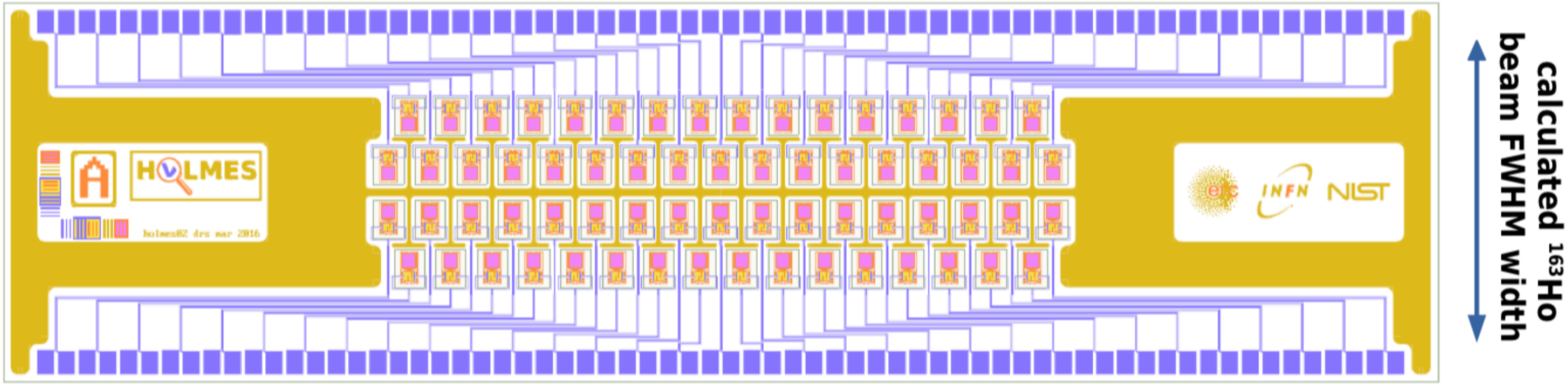

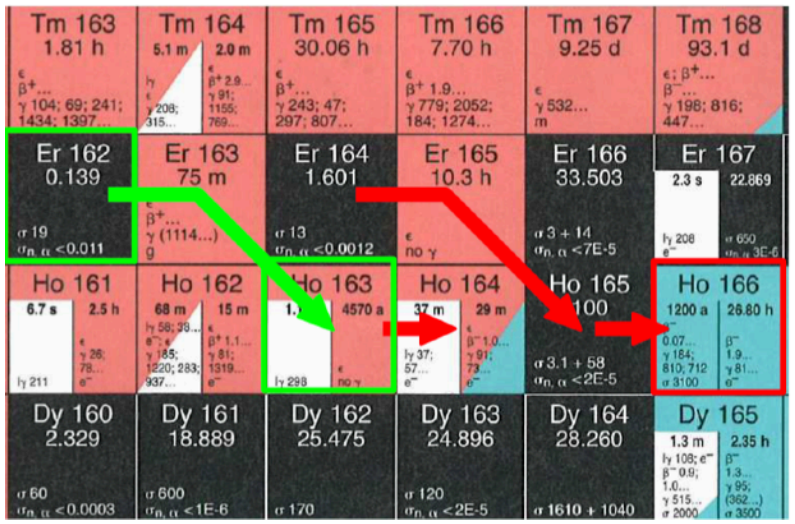
Tm 163
1.81 h
Tm 164
Tm 165
30.06 h
Tm 166
7.70 h
Tm 167
9.25 d
Tm 168
93.1 d
Er 162
0.139
Er 163
75 m
Er 164
1.601
Er 165
10.3 h
Er 166
33.503
Er 167
22.869
Ho 161
Ho 162
Ho 163
4570 a
Ho 164
Ho 165
100
Ho 166
1200 a
26.80 h
Dy 160
2.329
Dy 161
18.889
Dy 162
25.475
Dy 163
24.896
Dy 164
28.260
Dy 165
2.35 h

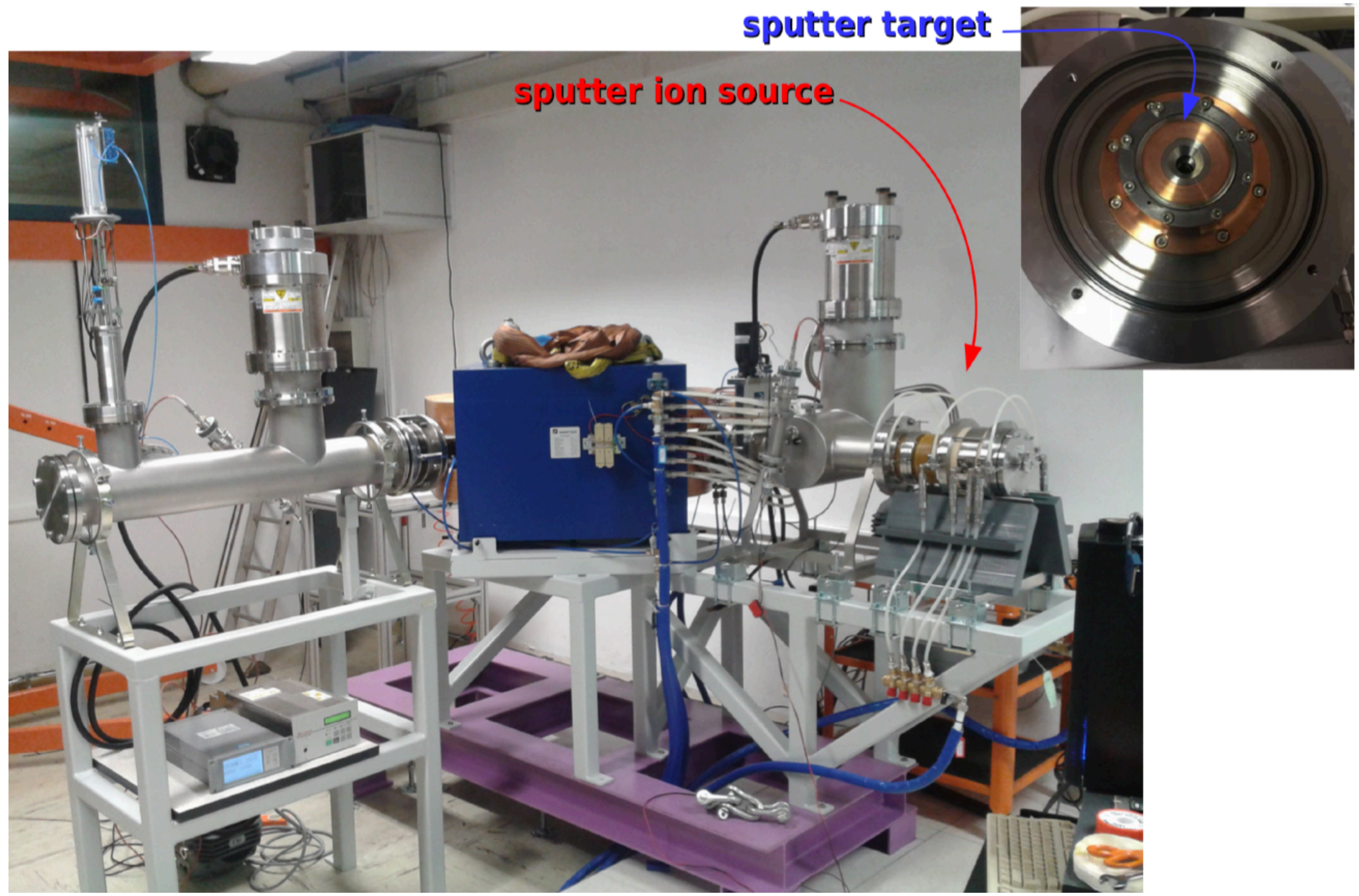
sputter target
sputter ion source

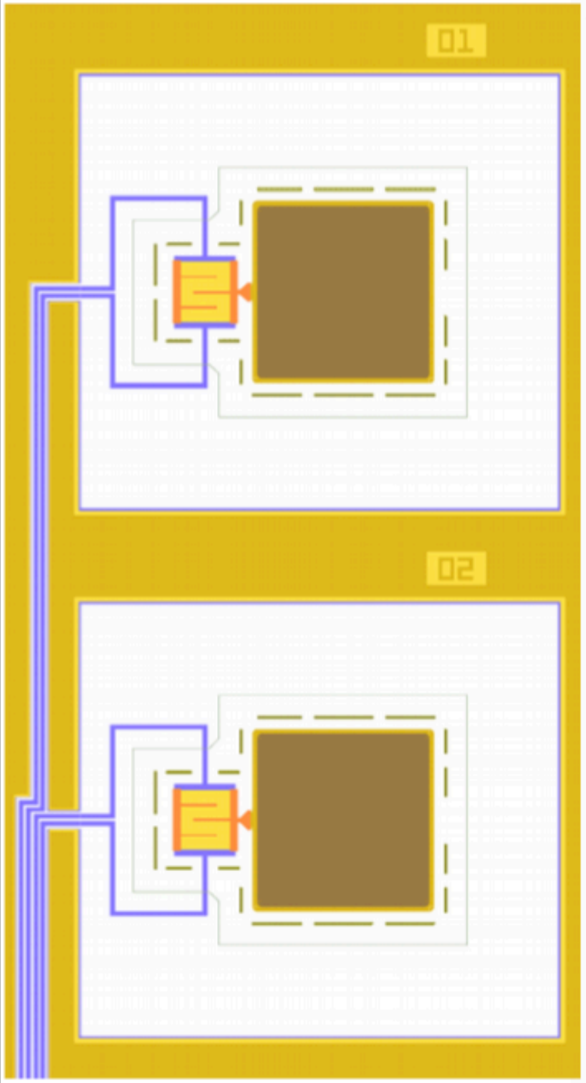

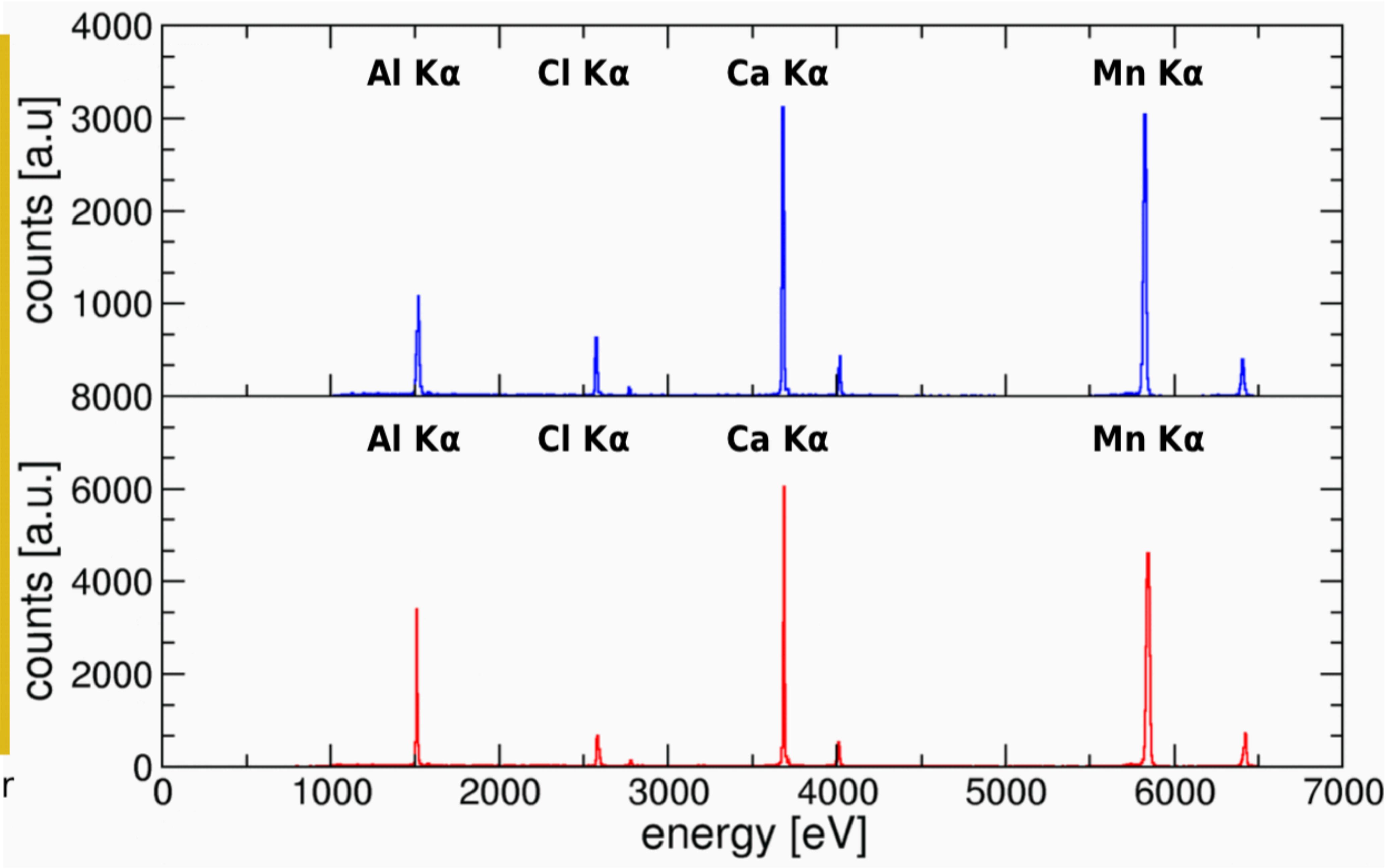

380×380 μm² absorber
C = 0.9 pJ/K
G = 480 pW/K

HOLMES-like pixels without collimator

- $\Delta E_0 \approx 5$ eV $\quad \Delta E \approx 7.5$ eV @ 2.6 keV
- $\tau_{rise} \approx 20$ μs $\quad \tau_{decay} \approx 140$ μs
- slew rate ≈ 0.1 Φ_0/S @ 2.6 keV

PTOLEMY

Capture of relic neutrinos on decaying tritium beta decay:

$$ {}^{3}_{1}H + \nu_e \rightarrow {}^{3}_{2}He + e $$

Neutrino Capture on a
Beta Decaying Nucleus (NCB)

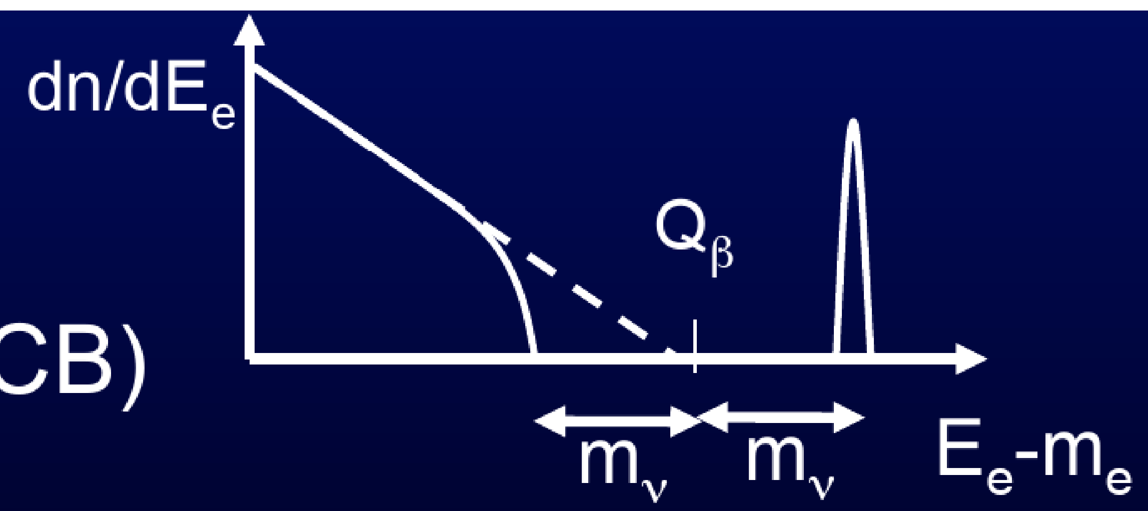

PTOLEMY conceptual design

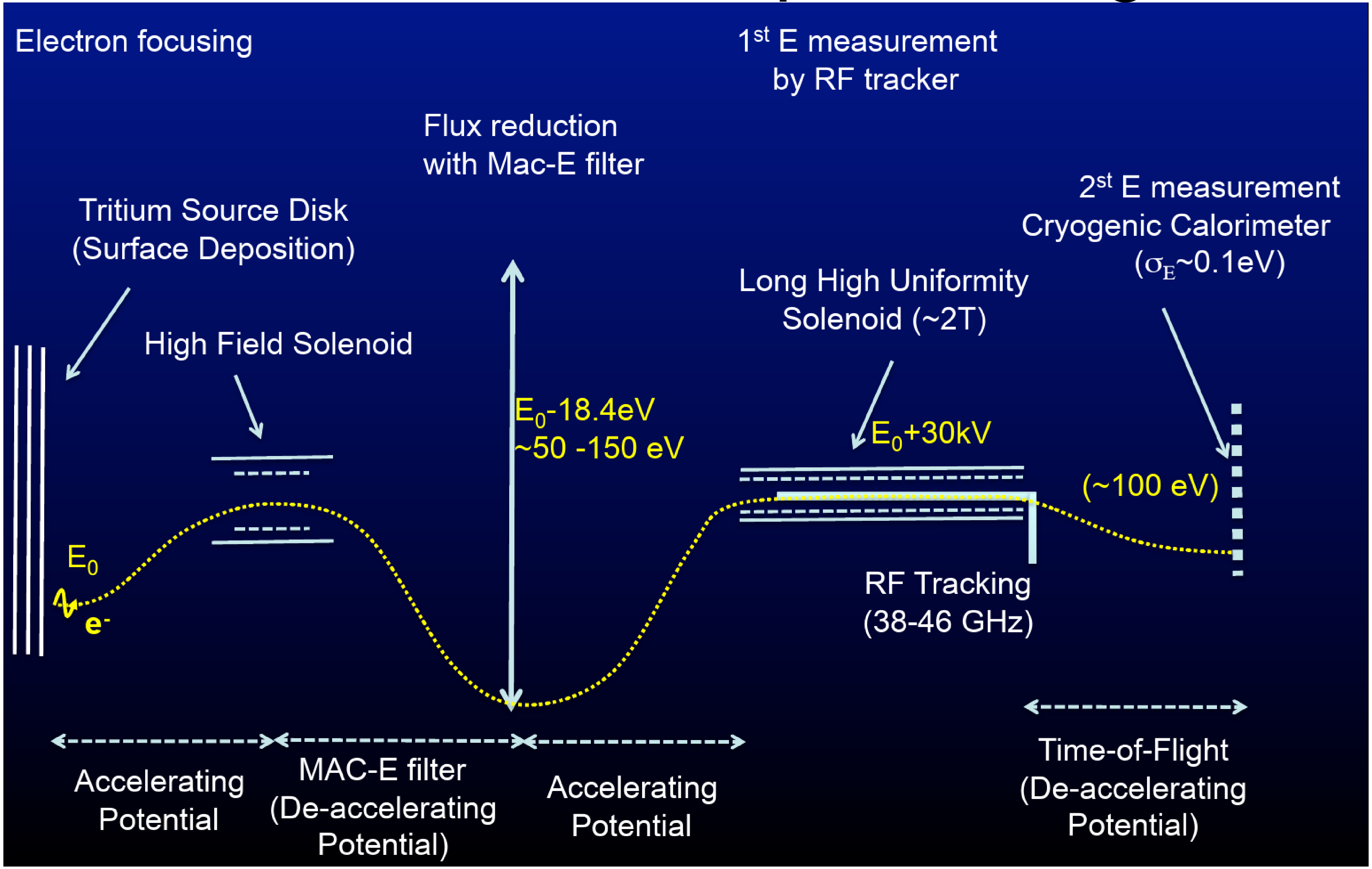

TES as electron detector with sub-eV energy resolution

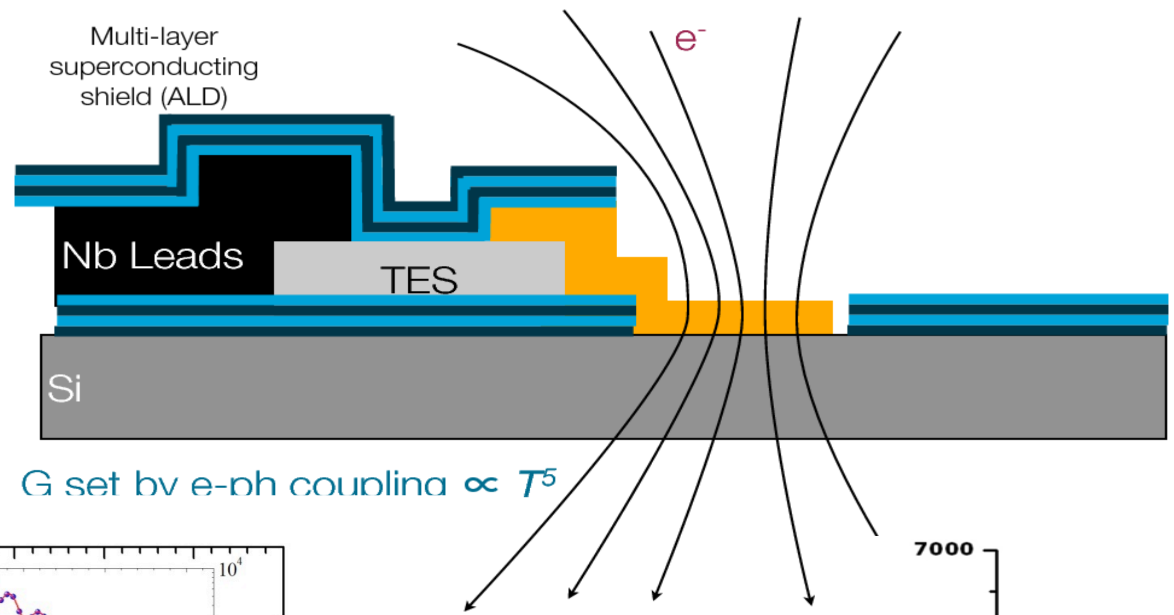

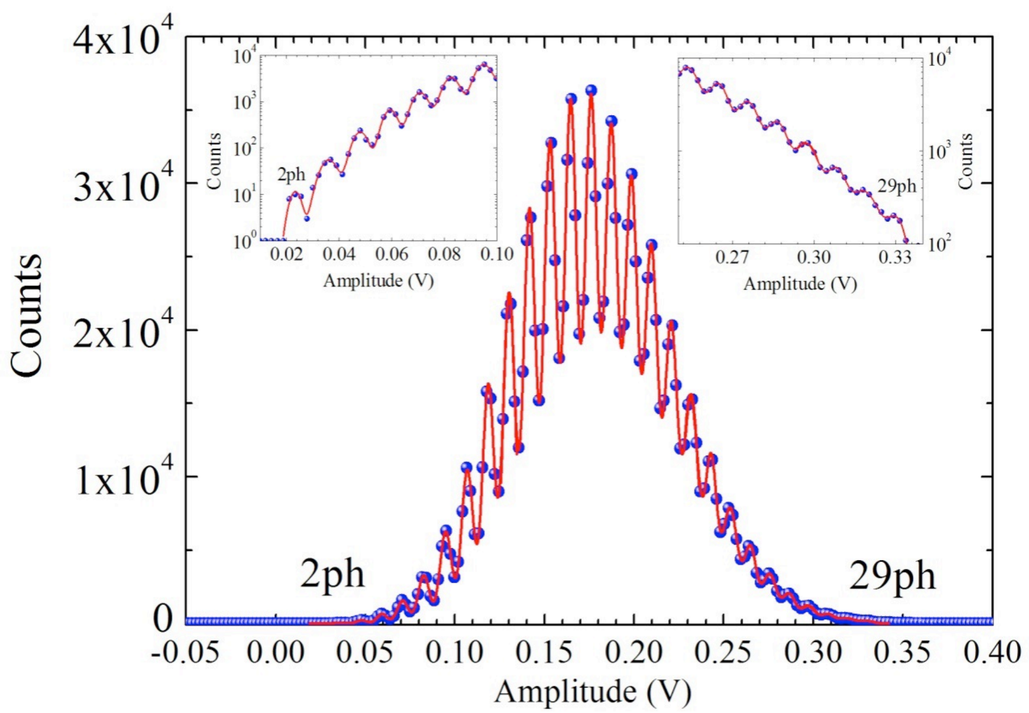

L. Lolli, et al. *J. Low Temp. Phys.*, vol. 167, pp. 803-808, 2012.

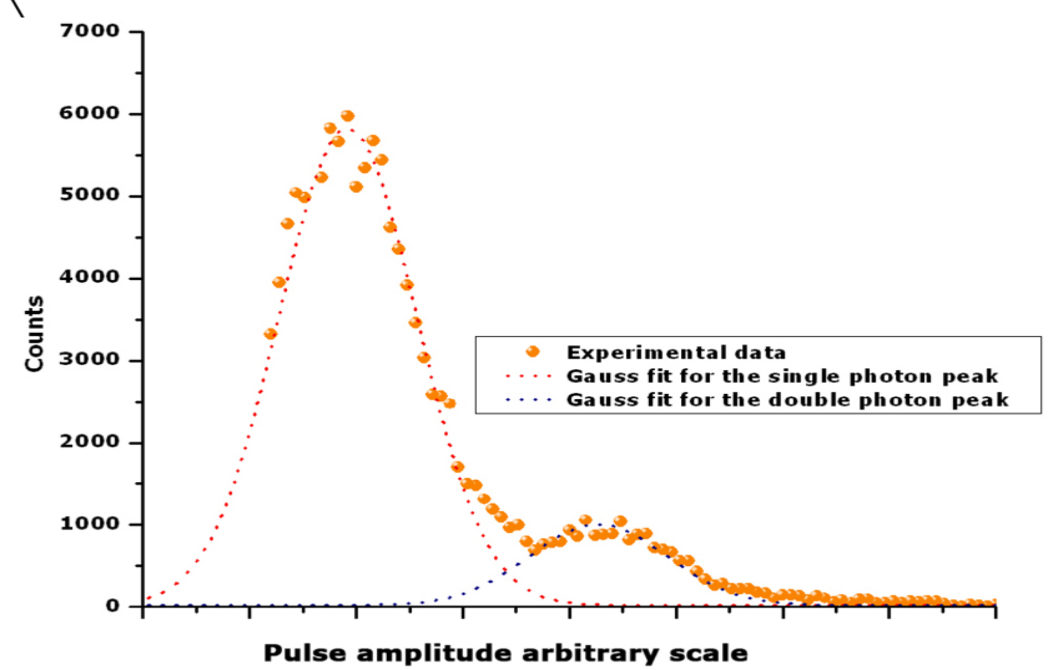

D. Bagliani et al. J. Low. Temp. Phys. 151: 234–238 (2008)

LSPE: Large Scale Polarization Explor

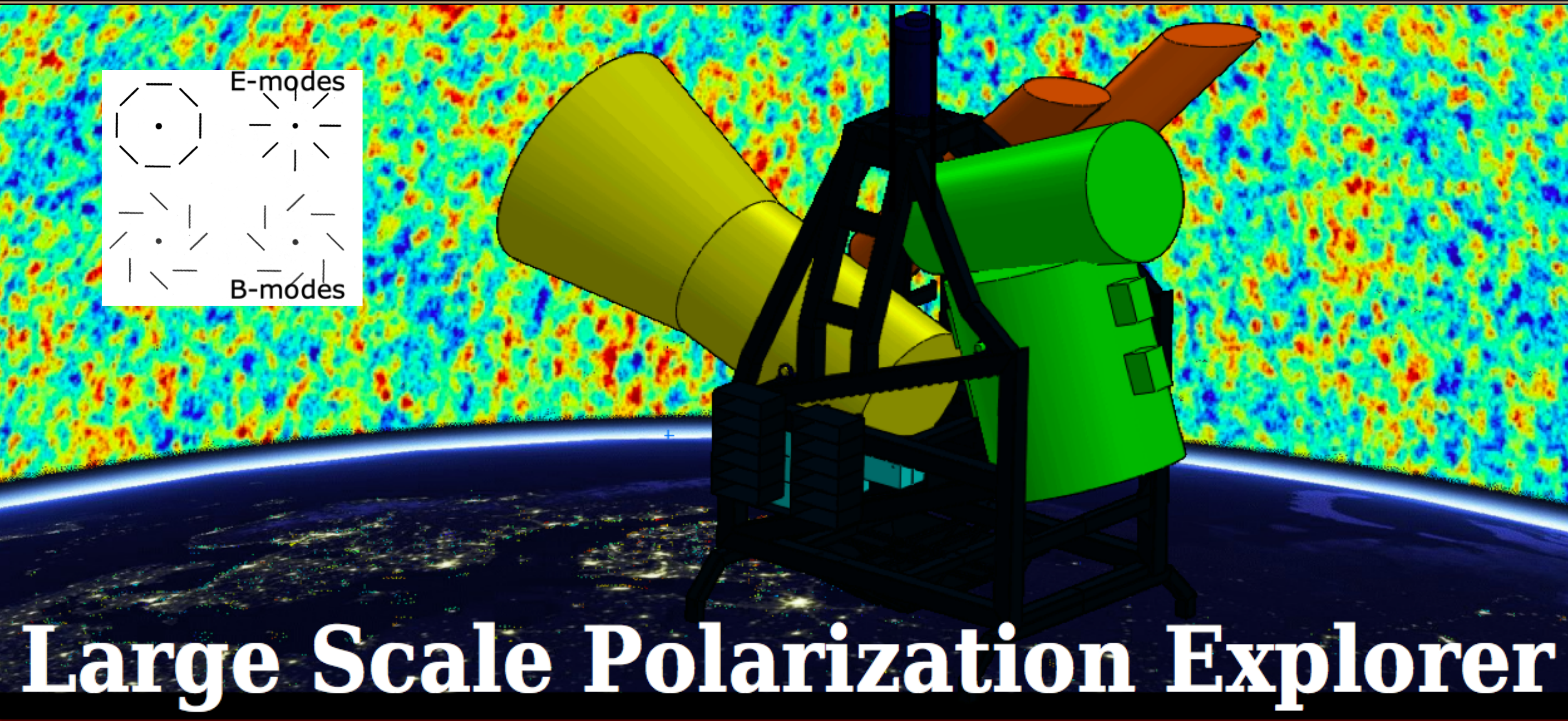

CMB measurements can probe all phases of the evolution of the Universe

Measurement of CMB polarization, Search for tensor perturbations produced during inflation. Initial quantum fluctuations and inflation. **THE TARGET OF LSPE**

Physics of the primeval fireball (acoustic oscillations of the primeval plasma). Physics of recobination

LSS (galaxy clusters, filaments) via Sunyaev-Zeldovich effect (SZ):

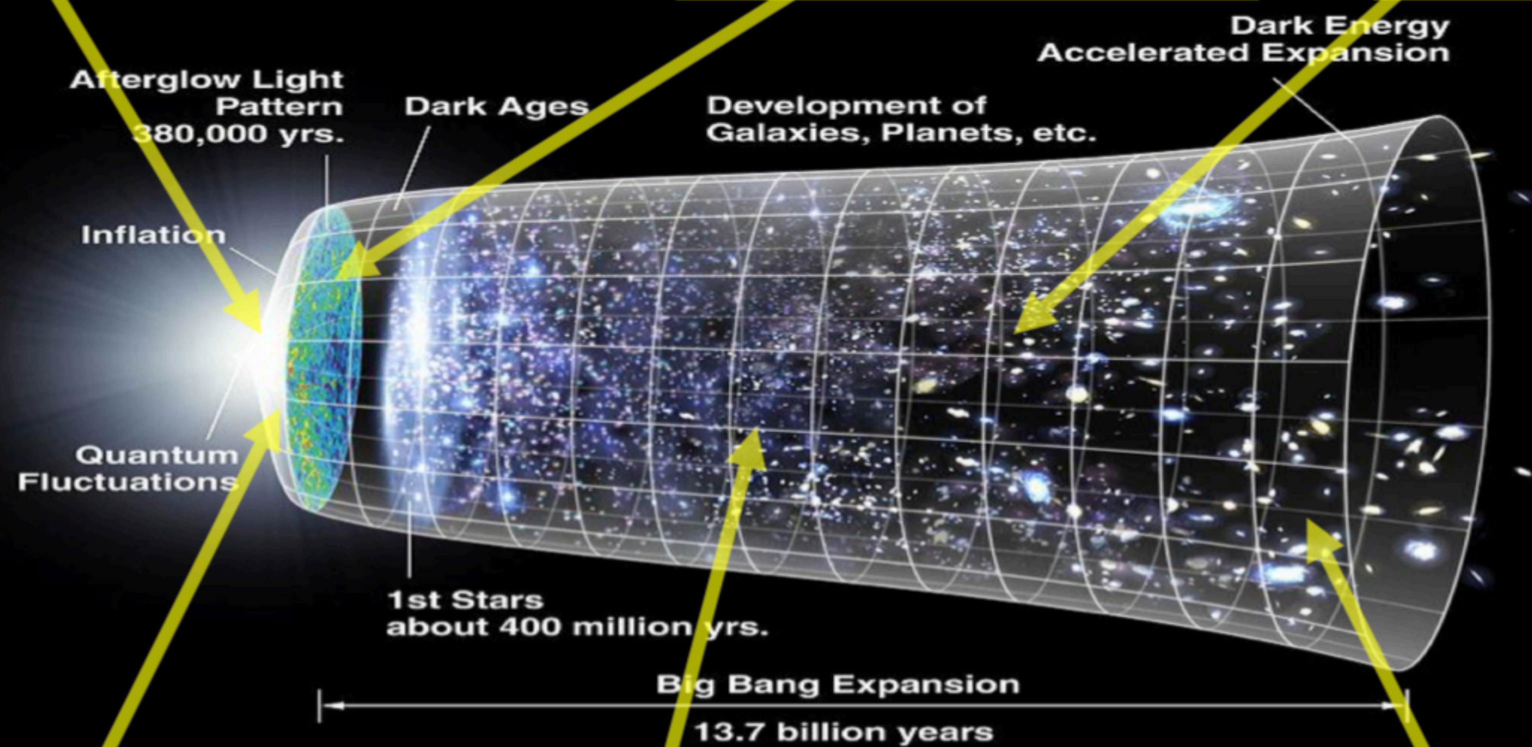

Probe epochs before recombination and new physics using CMB spectral distortion measurements

Map the gravitational potential all the way to z=1100 through CMB lensing

Dipole: our *absolute* motion in the universe

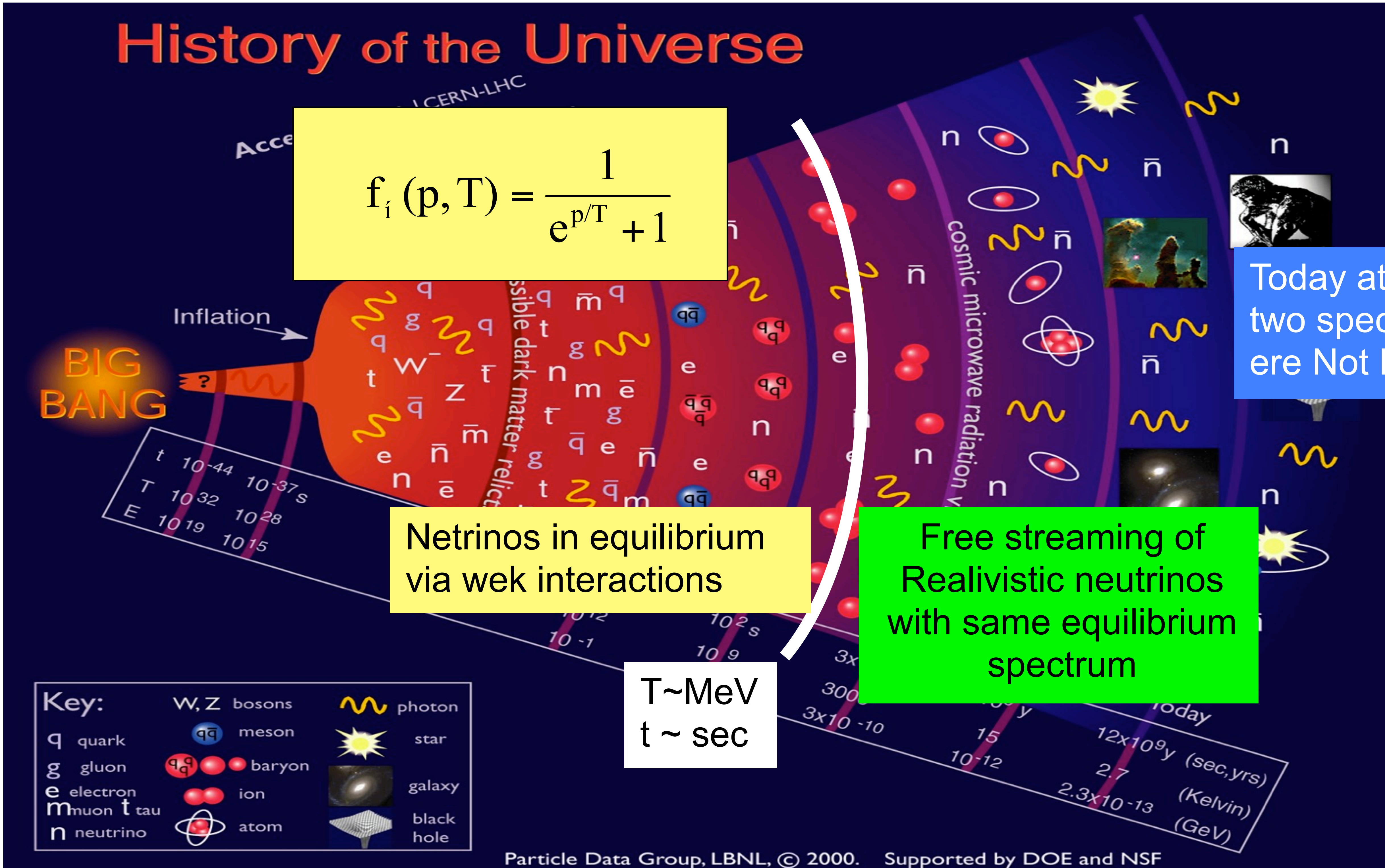

$$f_i\,(p,T) = \frac{1}{e^{p/T}+1}$$

Netrinos in equilibrium via wek interactions

T~MeV
t ~ sec

Free streaming of Realivistic neutrinos with same equilibrium spectrum

Today at least two species ere Not Rel.

- The Large-Scale Polarization Explorer is
  - a spinning stratospheric balloon payload
  - flying long-duration, in the polar night
  - aiming at CMB polarization at large angular scales
  - using polarization modulators to achieve high stability
- Frequency coverage: 40 – 250 GHz (5 channels)
- Two instruments:
  SWIPE and **STRIP**
- Angular resolution: 1.5 – 2.3 deg FWHM
- Sky coverage: 20-25% of the sky per flight
- Combined sensitivity: 10 μK *arcmin* per flight

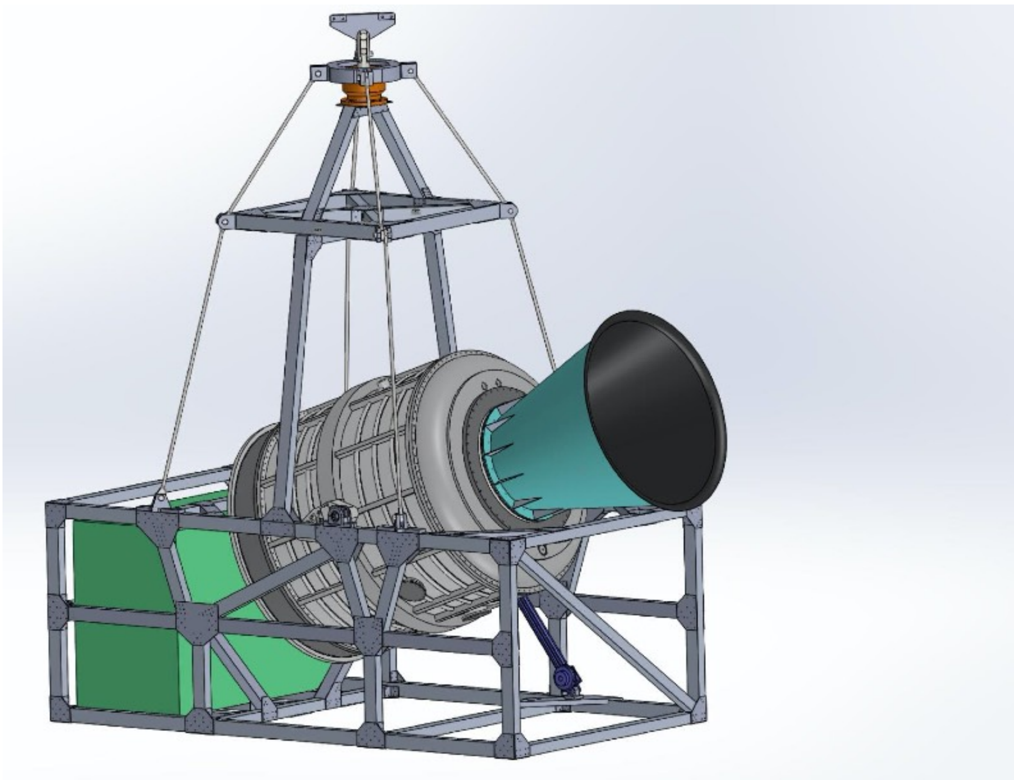

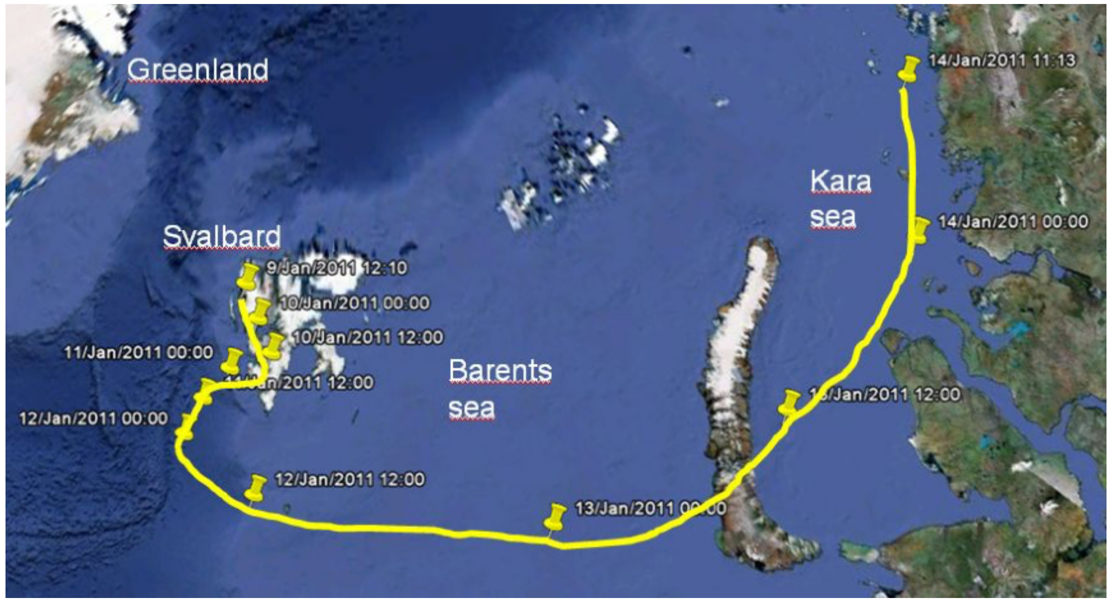

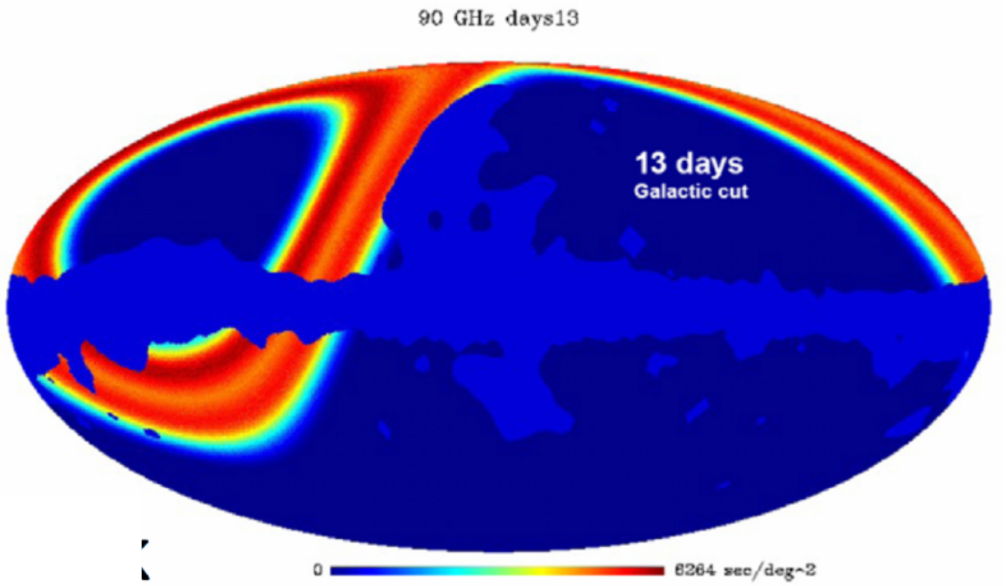

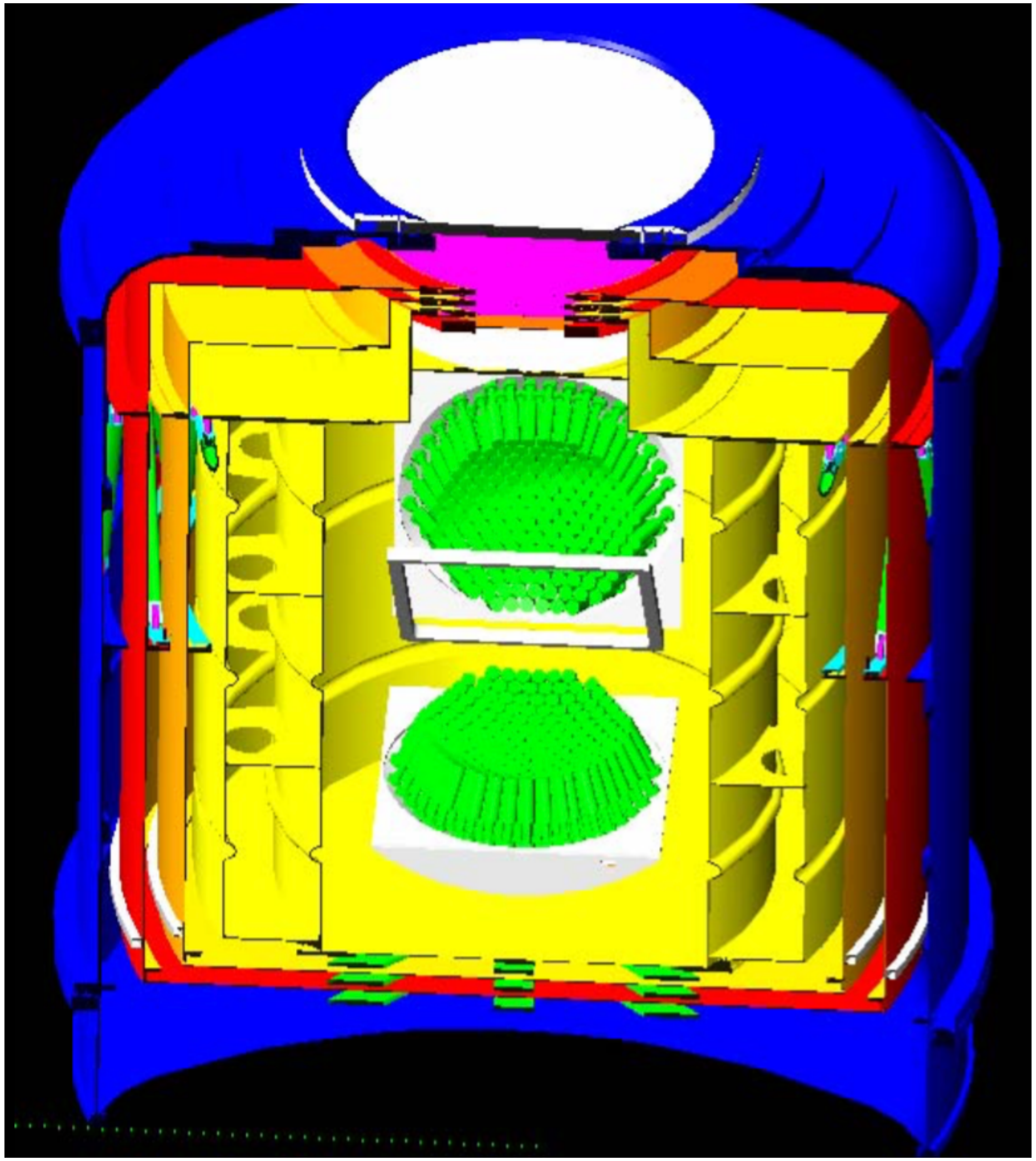

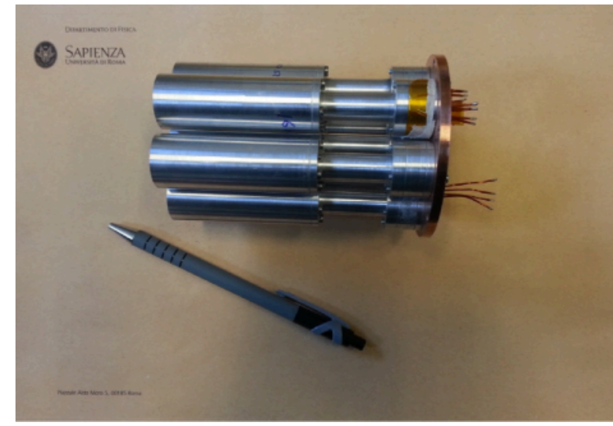
SAPIENZA

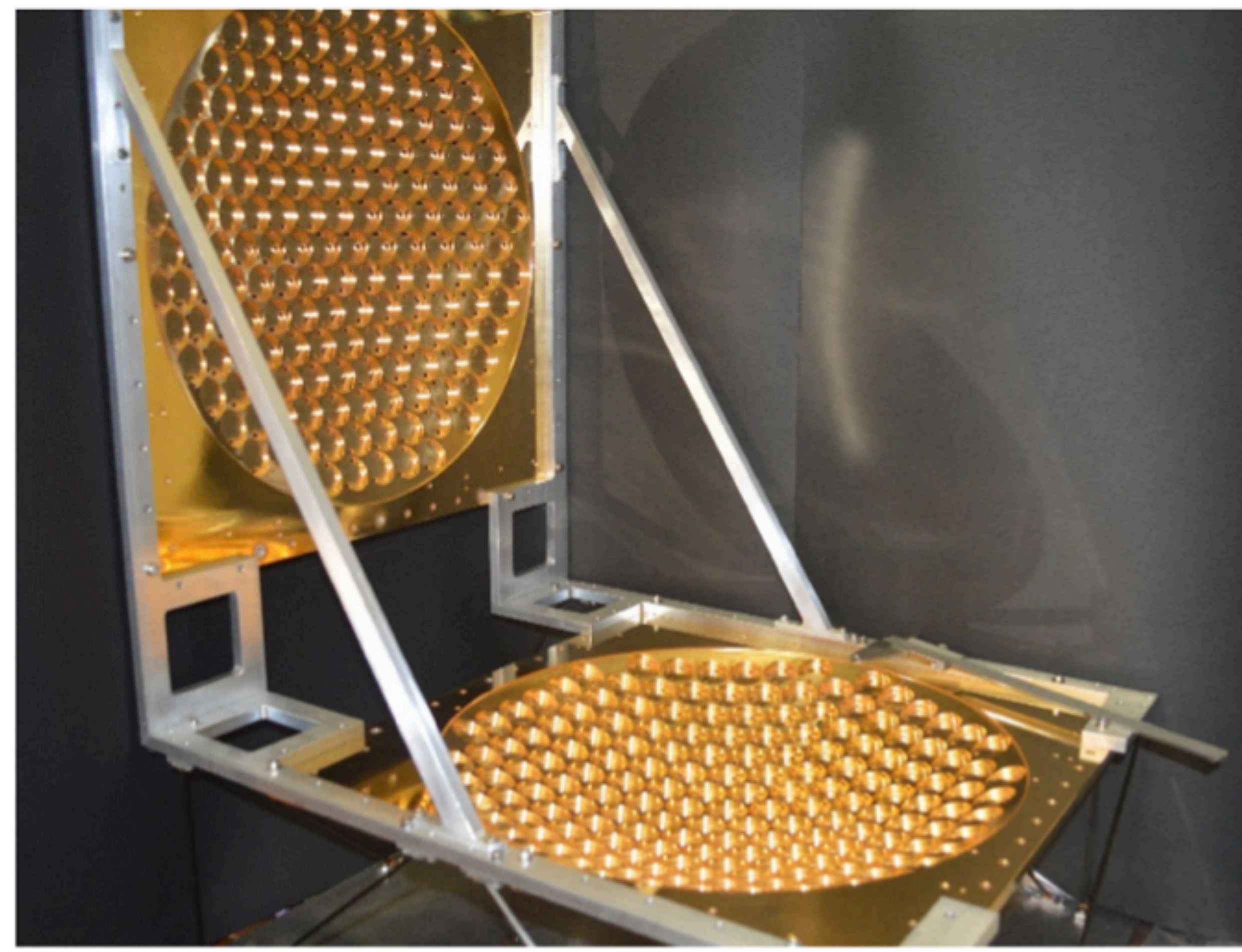

LSPE: Large Scale Polarization Explor

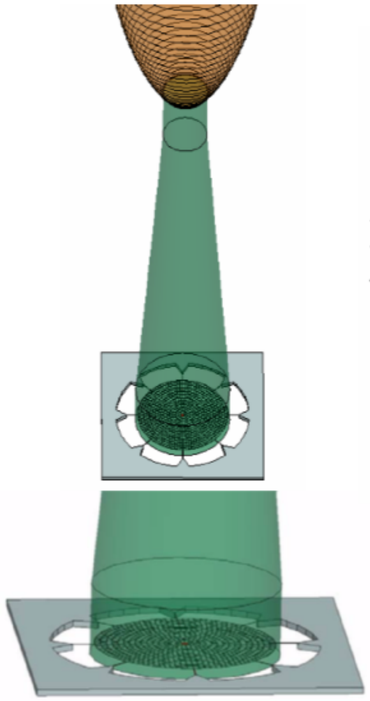

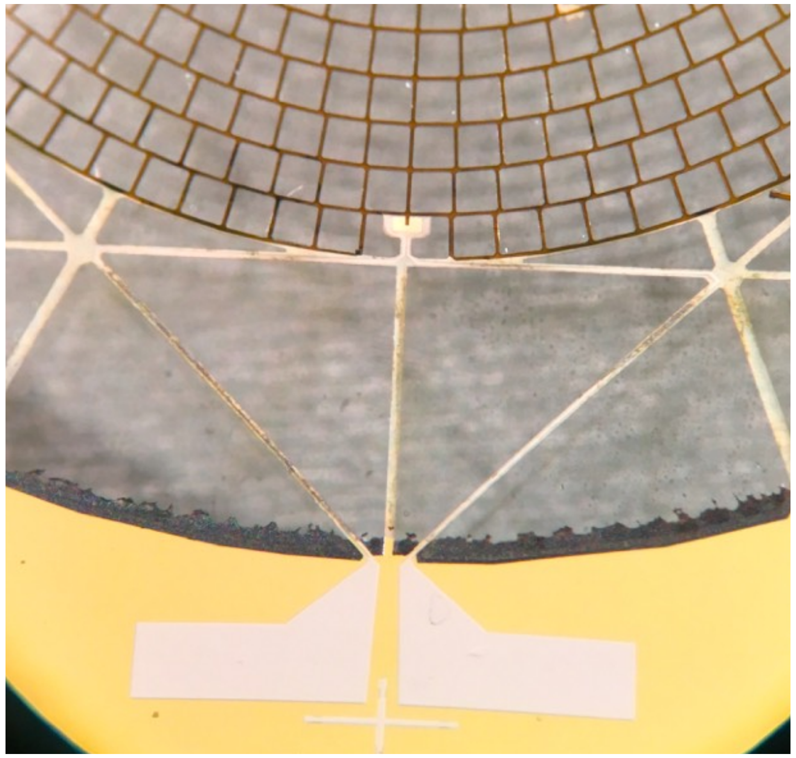

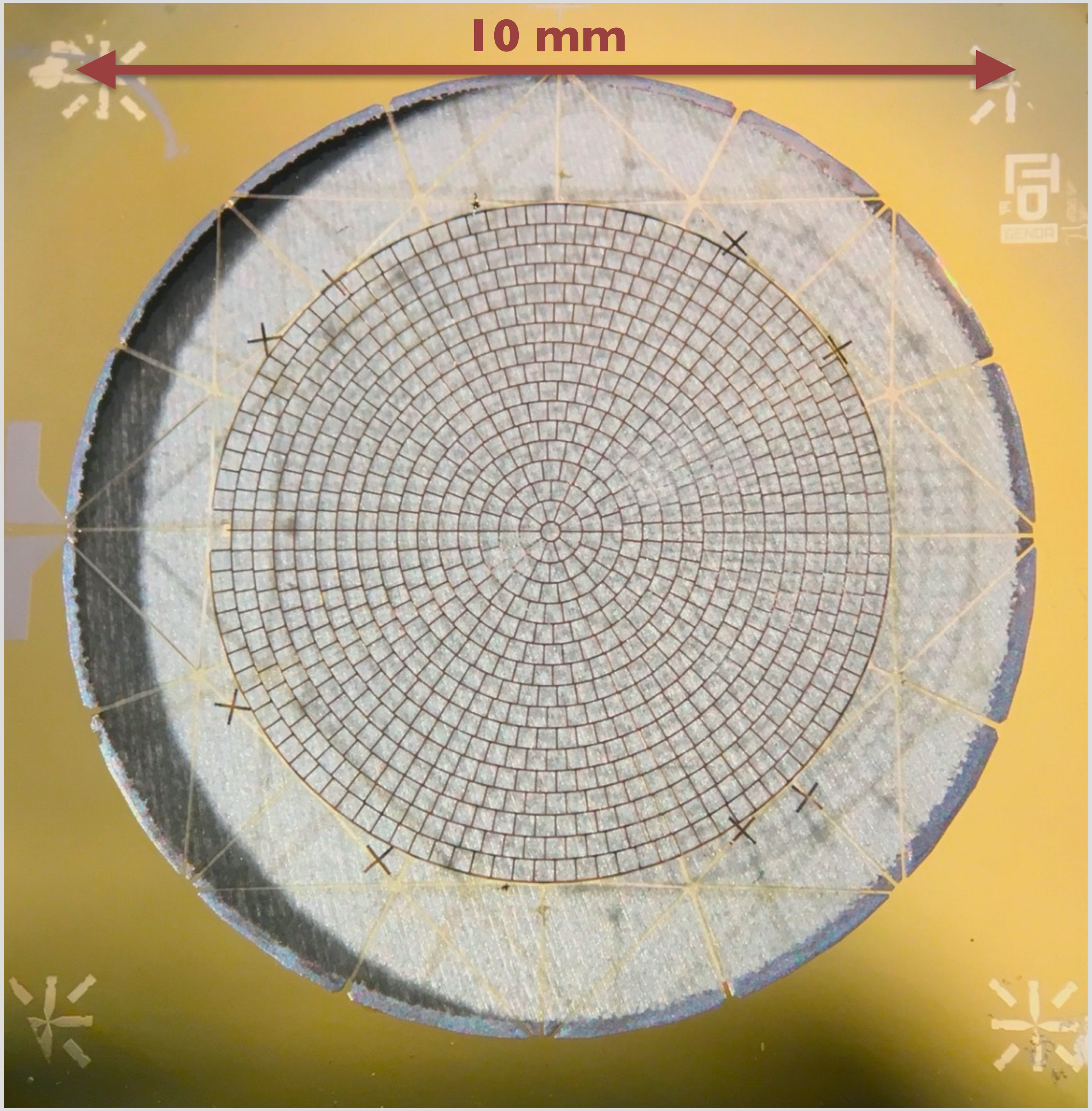

SW lateral TES type

LSPE: Large Scale Polarization Explor

Bolometer IV curves

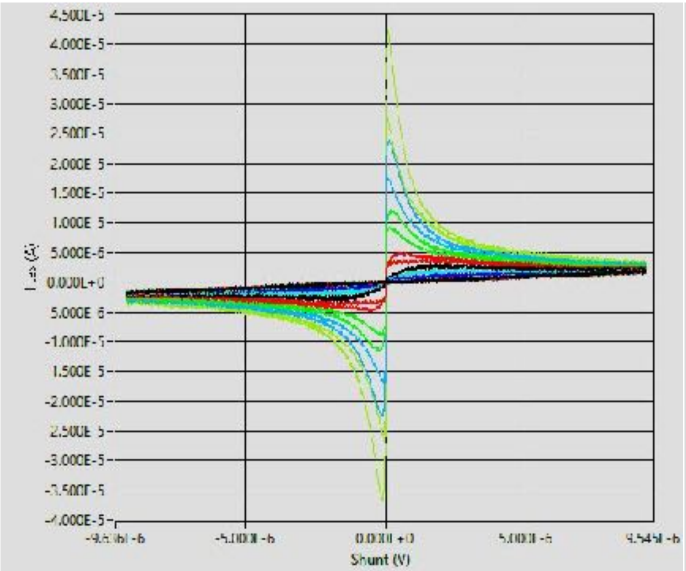

G vs V bias

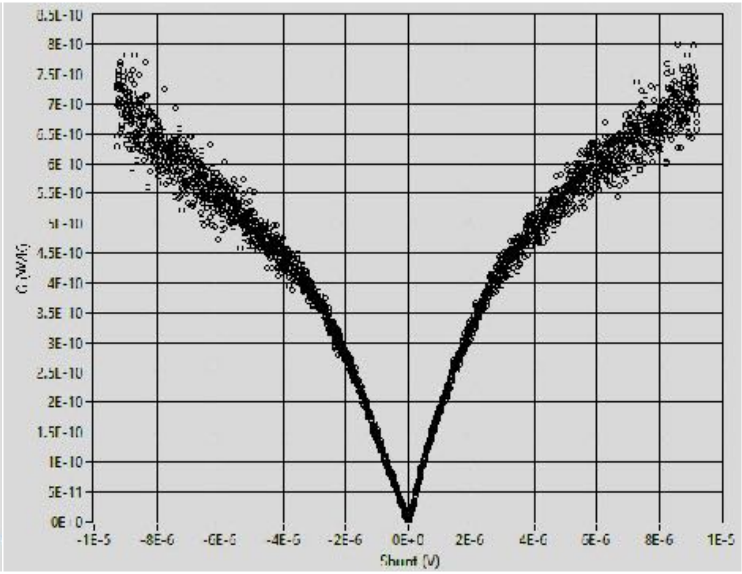

SW central TES type

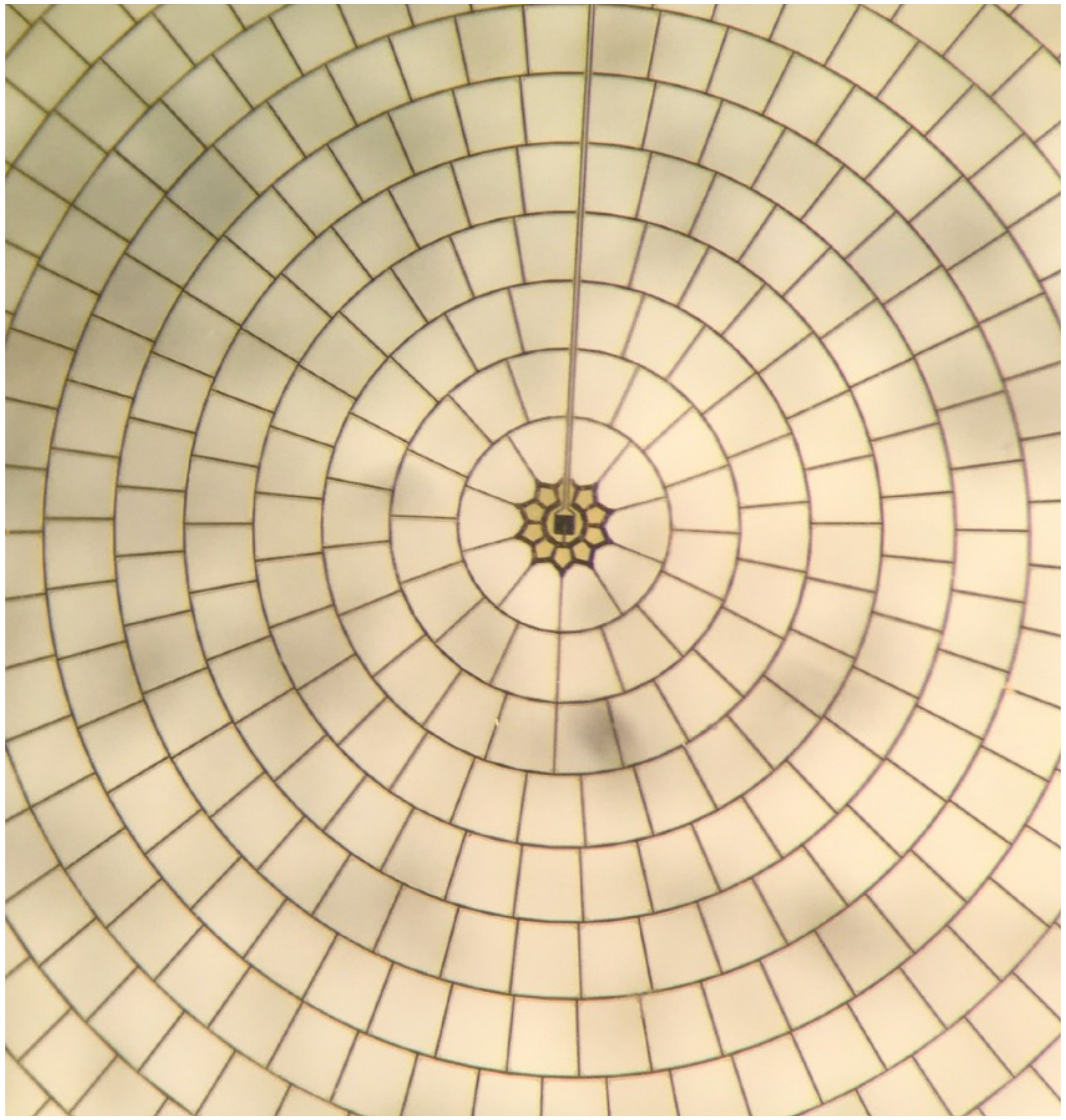

Electronics	***SQUID VTT J3***
G	***3-6 x 10^{-11} W/K***
Rn	***1-2 Ω***
NEP	***2-5 x 10^{-17} W/$Hz^{0.5}$***
T	***0.35 -0.55 K***

ATHENA : the Advanced Telescope for High ENergy Astrophysics

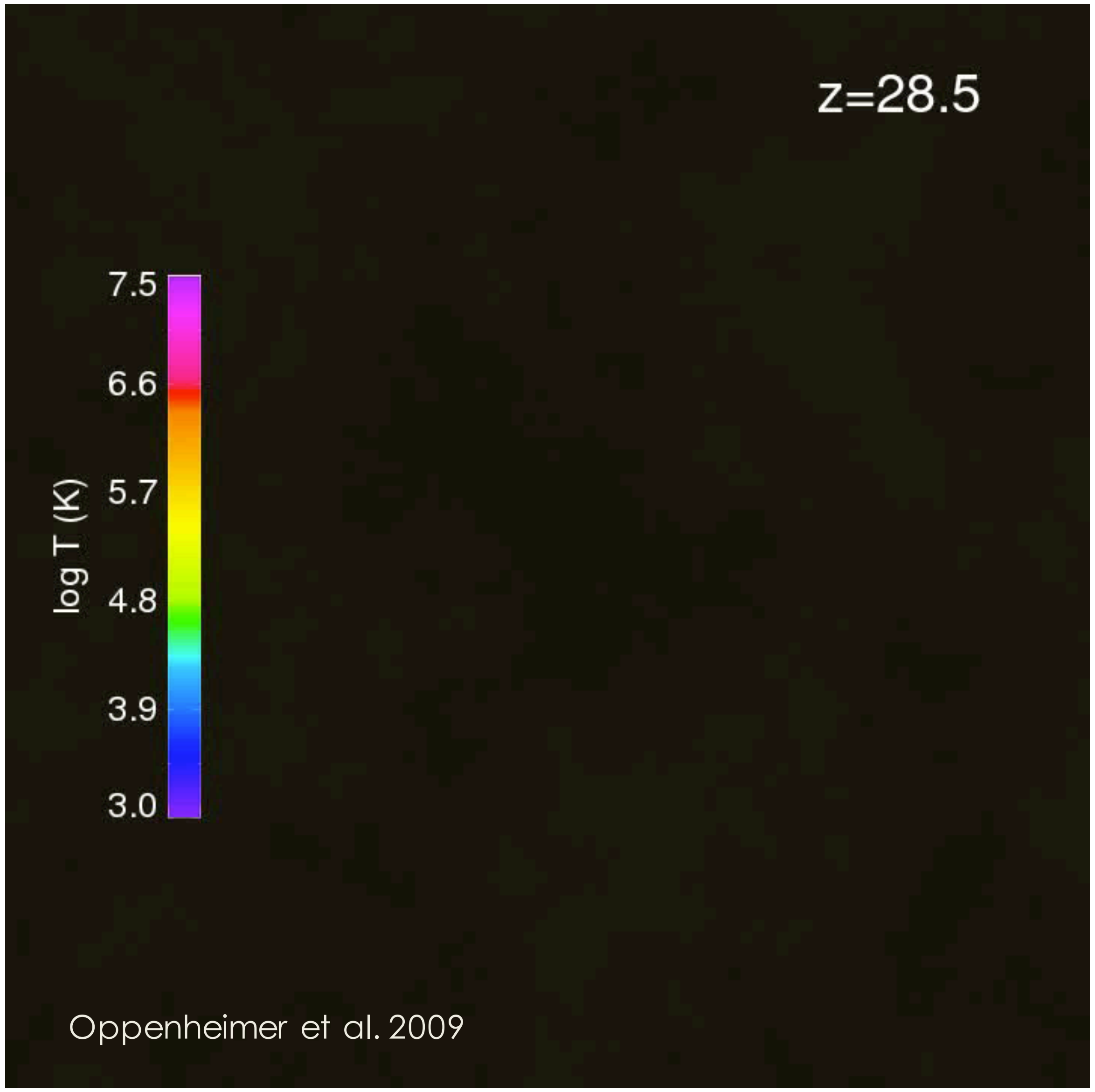
z=28.5
7.5
6.6
5.7
4.8
3.9
3.0
log T (K)
Oppenheimer et al. 2009

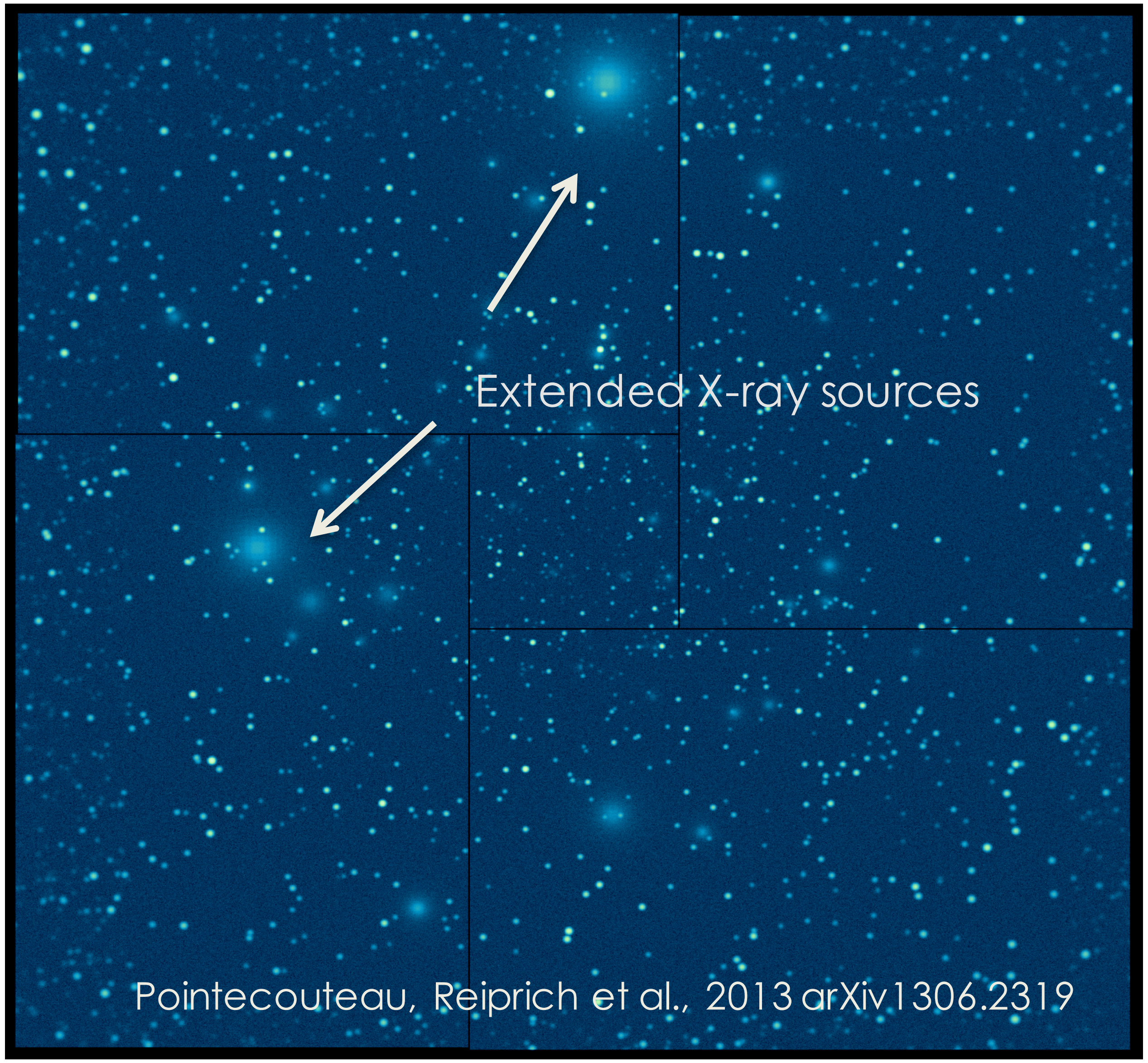
Extended X-ray sources
Pointecouteau, Reiprich et al., 2013 arXiv1306.2319

Key questions for observational astrophysics in 2028

When and how were the largest baryon reservoirs in galaxy clusters chemically enriched?

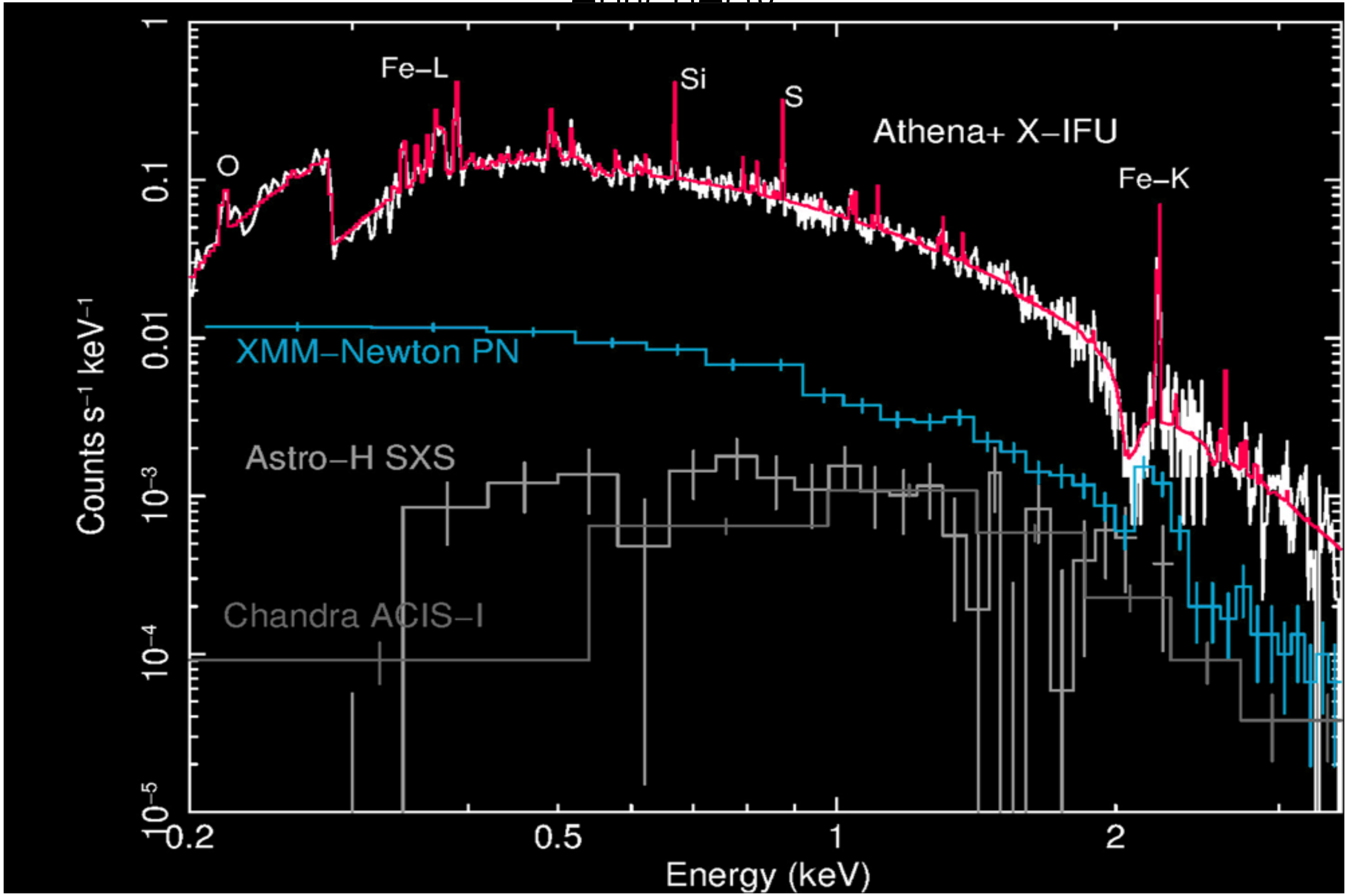

Key questions for observational astrophysics in 2028

How do black holes launch winds and outflows?
How much energy do they carry out to larger scales?

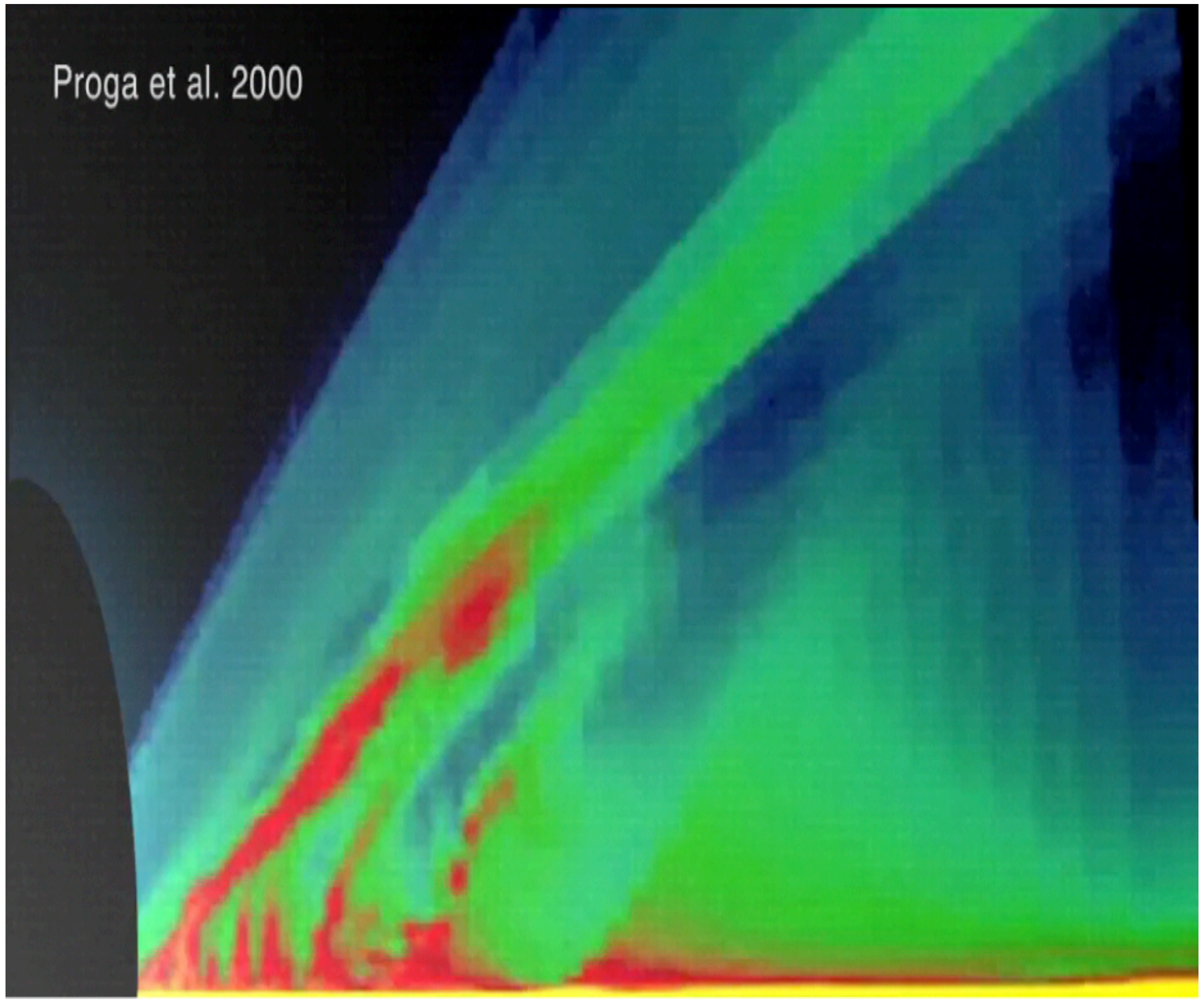

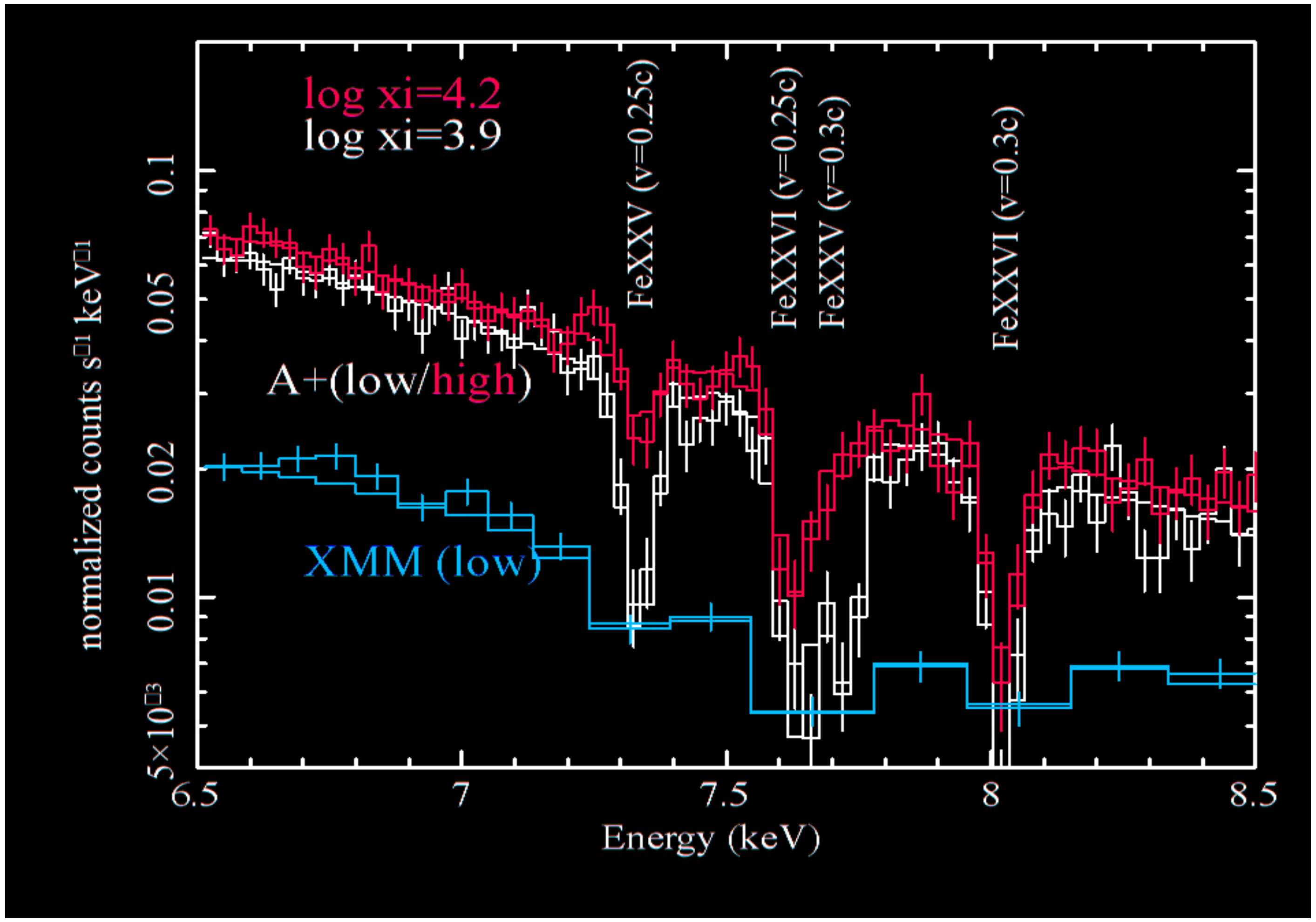

Cappi, Done et al., 2013 arXiv1306.2330
Dovciak, Matt et al., 2013 arXiv1306.2331

ATHENA : the Advanced Telescope for High ENergy Astrophysics

X-IFU

X-ray Integral Field Unit

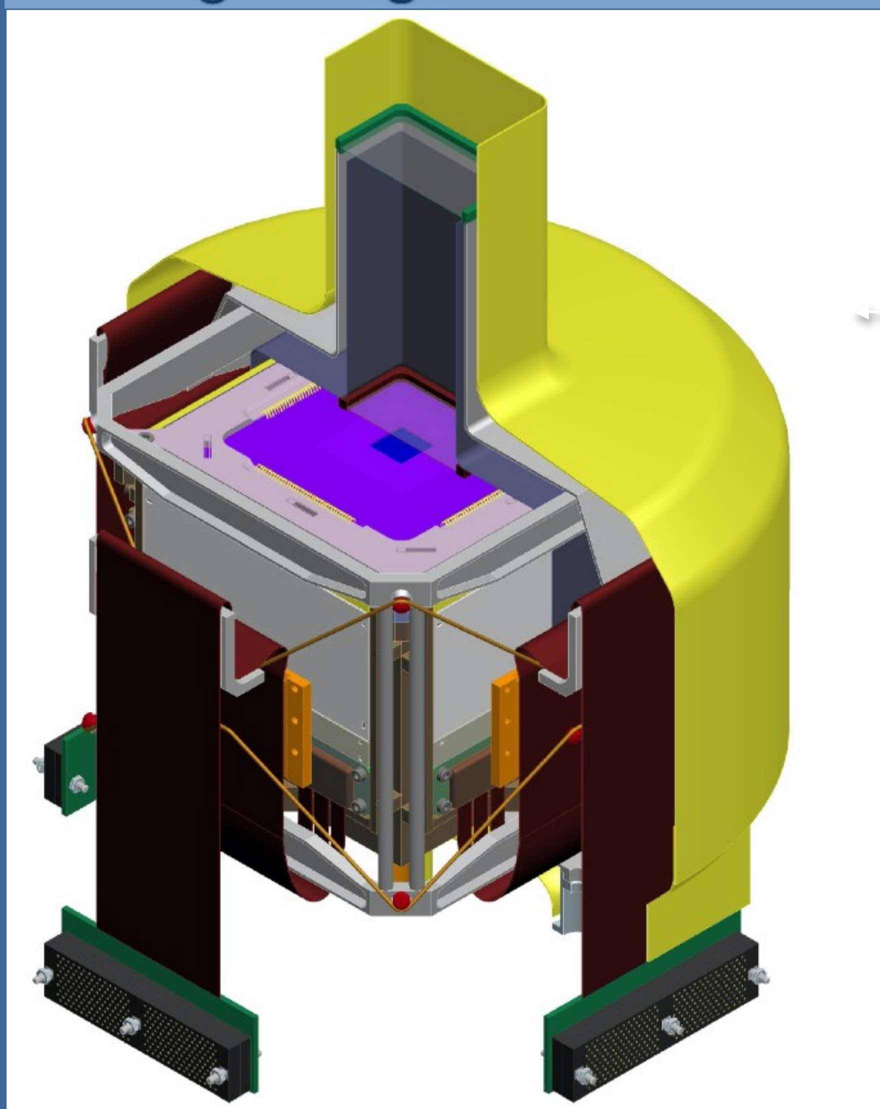

L2 orbit Ariane V
<5100 kg
power 2500 W
5 year mission

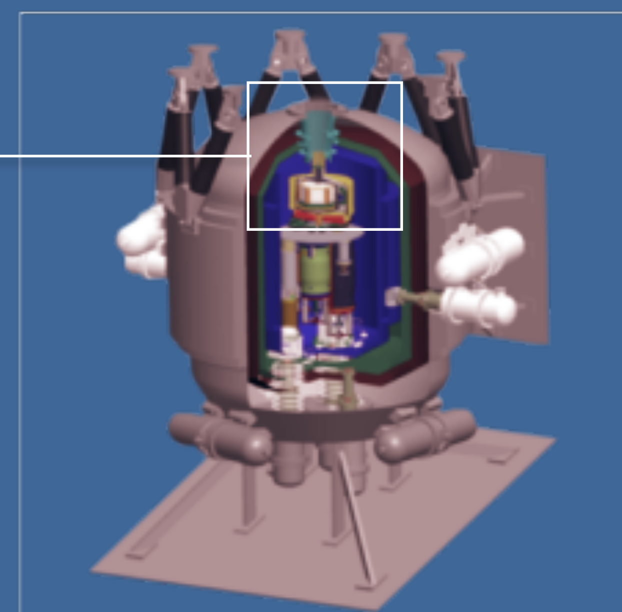

X-ray Integral Field Unit:
DE: 2.5 eV
Fielf of View: 5 arcmin
Operating temp 50 mK

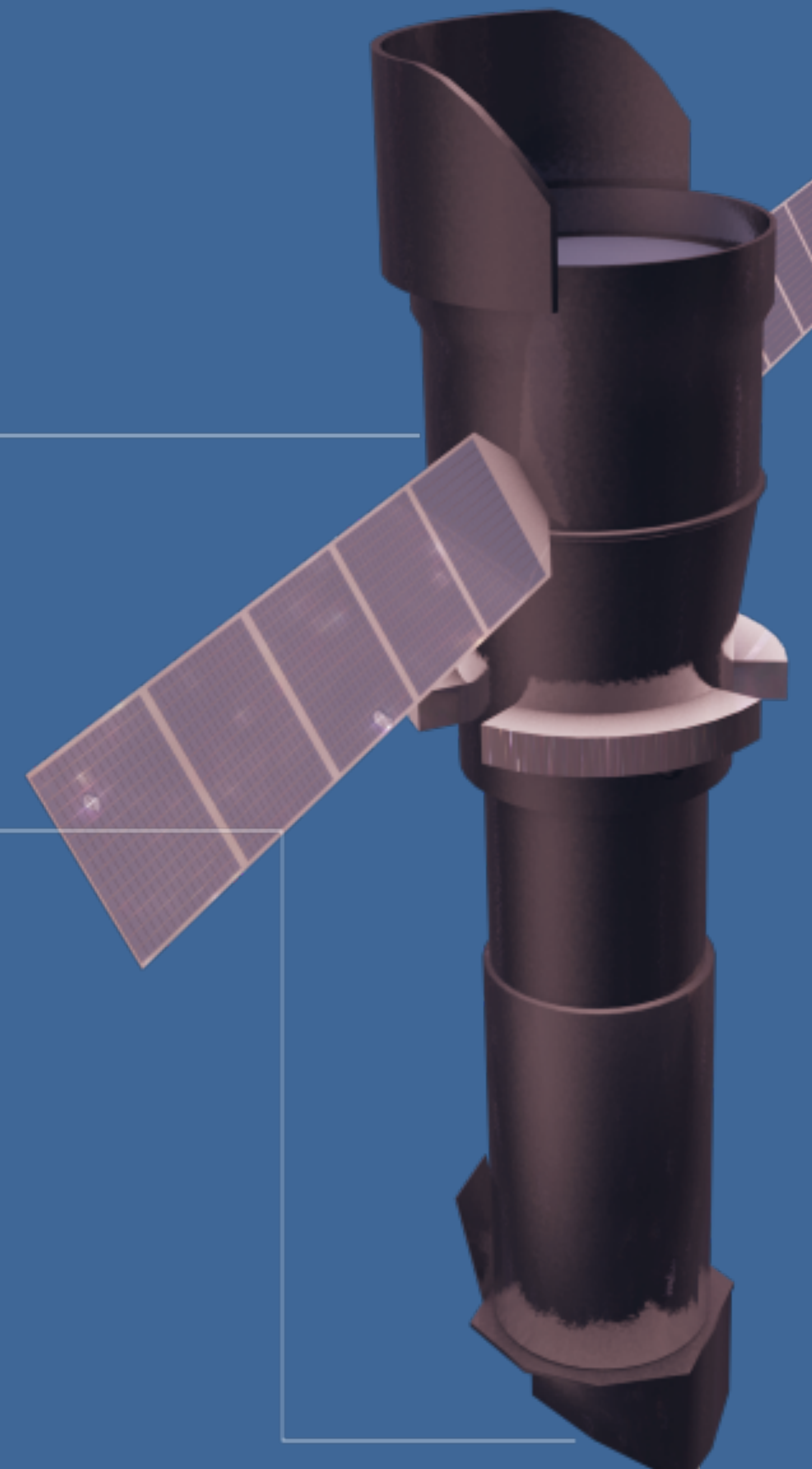

ATHENA : the Advanced Telescope for High ENergy Astrophysics

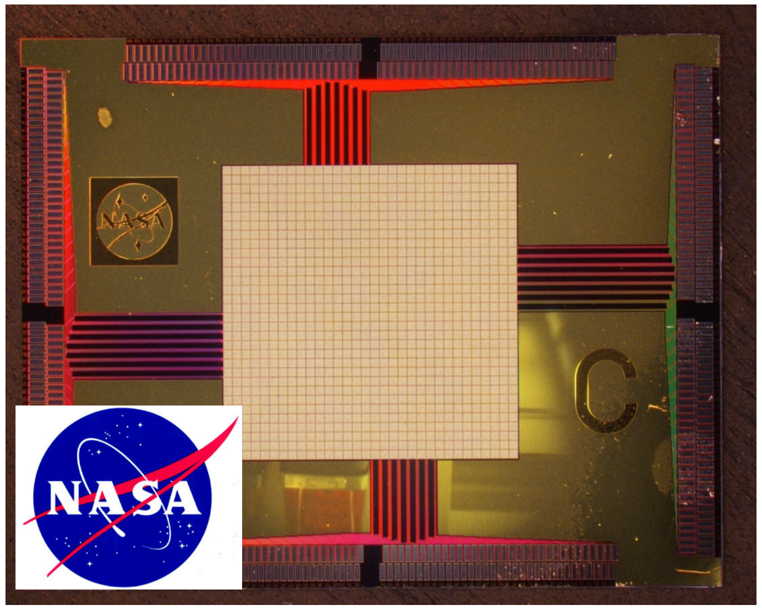

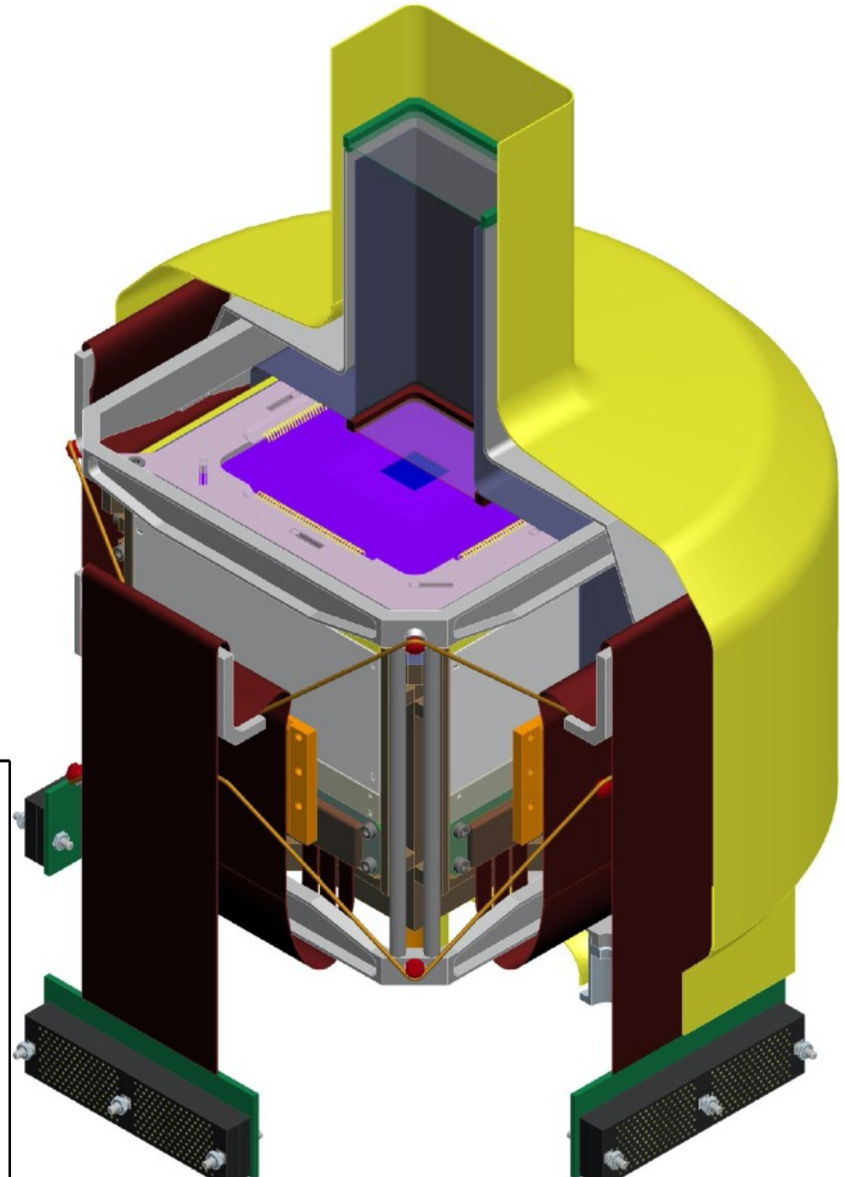

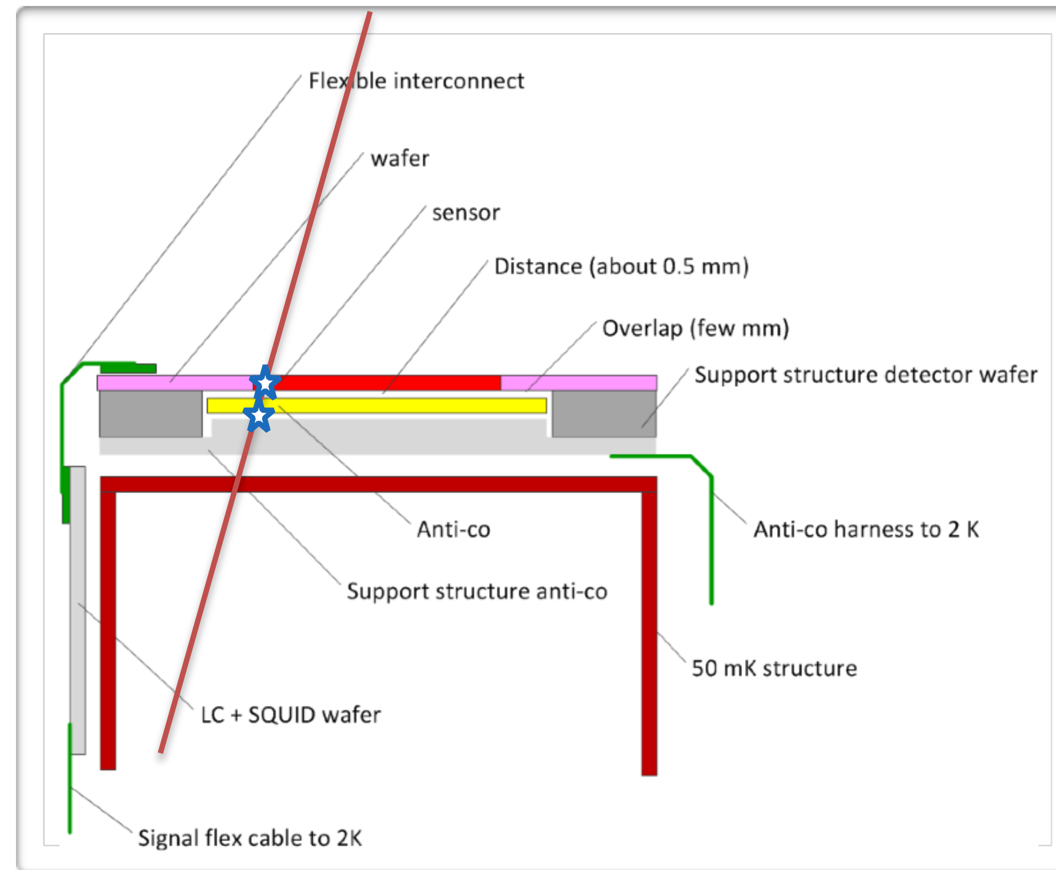

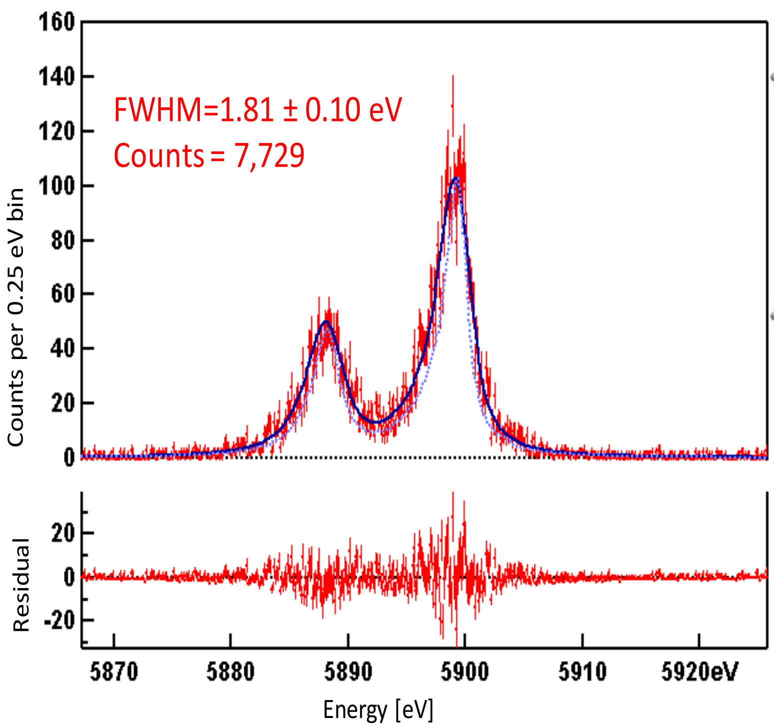

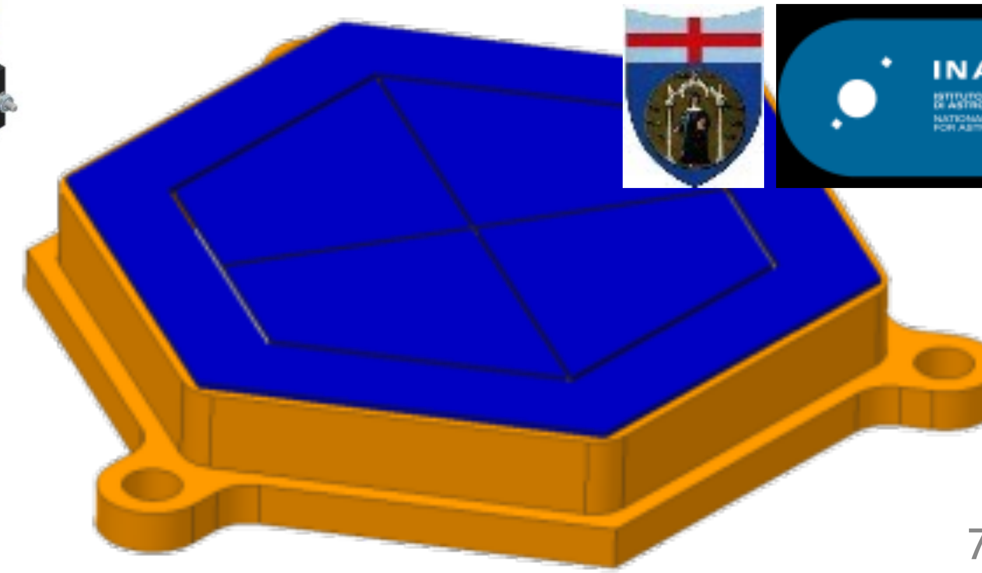

Background reduction

- Extensive simulations/design and TES AC detector

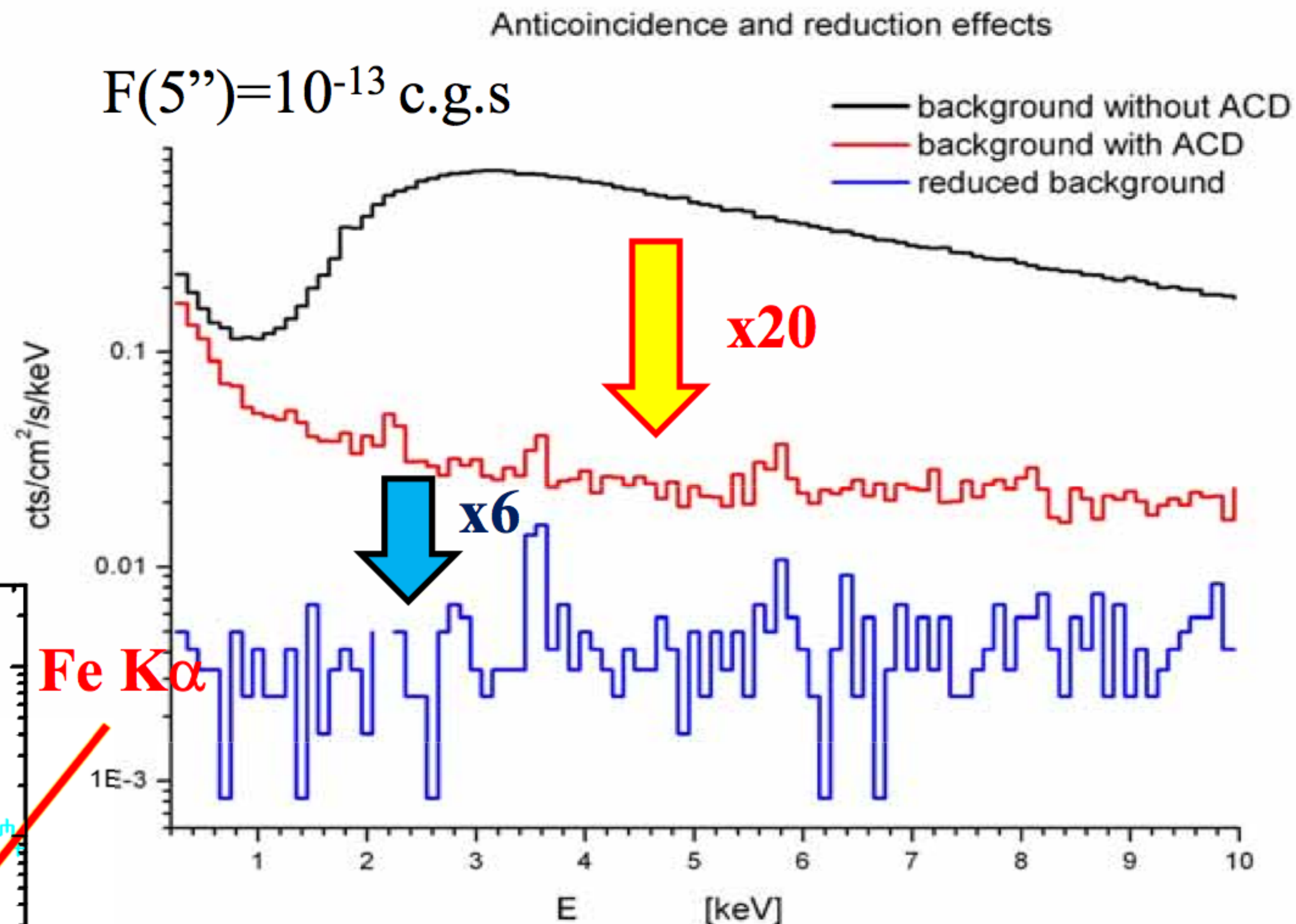

S. Lotti - IAPS-INAF

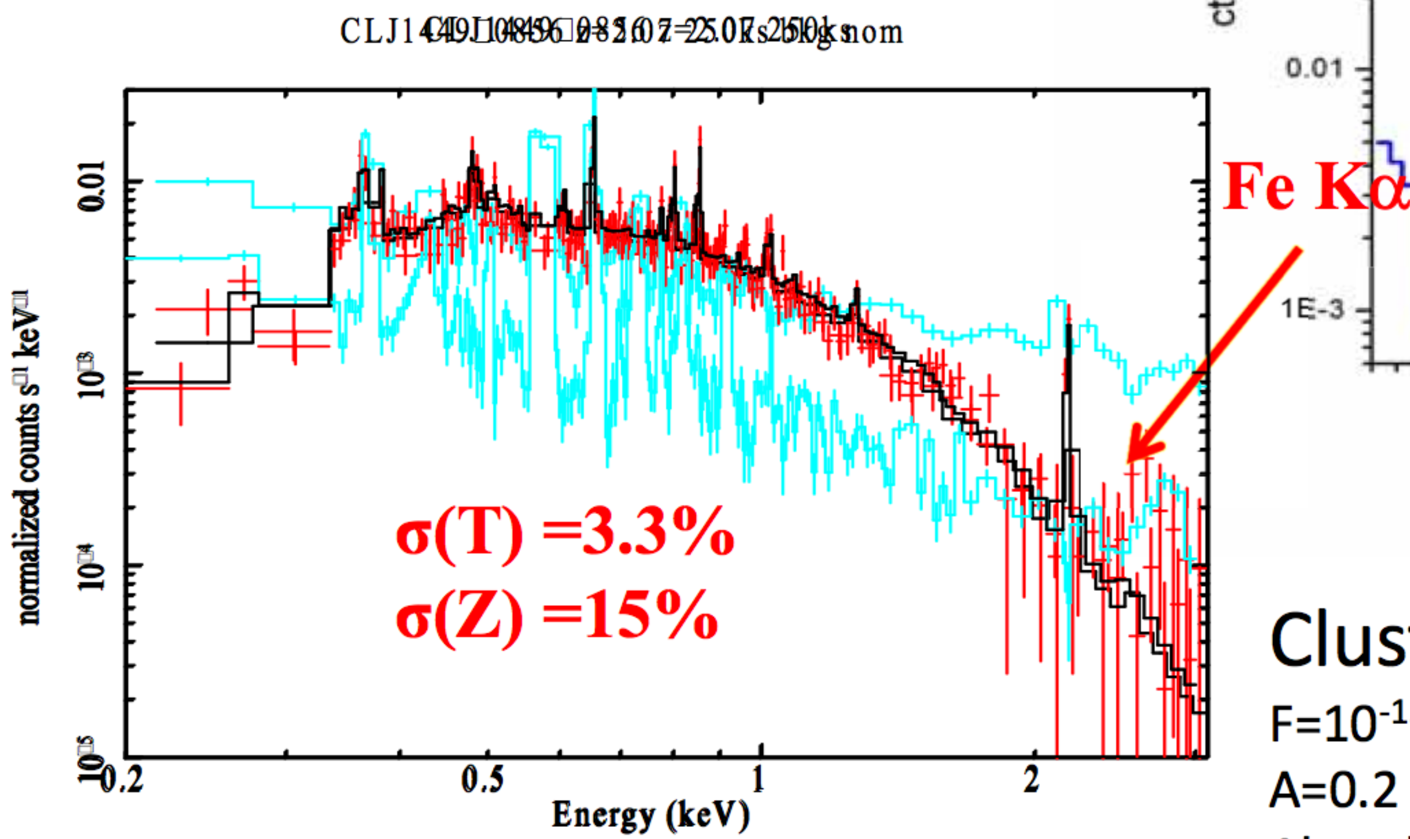

S. Lotti - IAPS-INAF

Cluster at the formation epoch (z=2)

$F=10^{-15}$ erg/cm^2/s, (Gobat et al 2011), L=7 10^{43} erg/s
A=0.2 arcmin^2, kT=2.0 keV,
Abundance 0.3, area=1m2,f/l=12m

Microscopic Detection Mechanism

1. Hot spot along the particle track
2. Quasi-diffusive heat transport
4. Efficient collection of fast A-thermal signal needs large TES coverage
5. Possible Upgrade with Phonon Collectors for larger signal uniformity

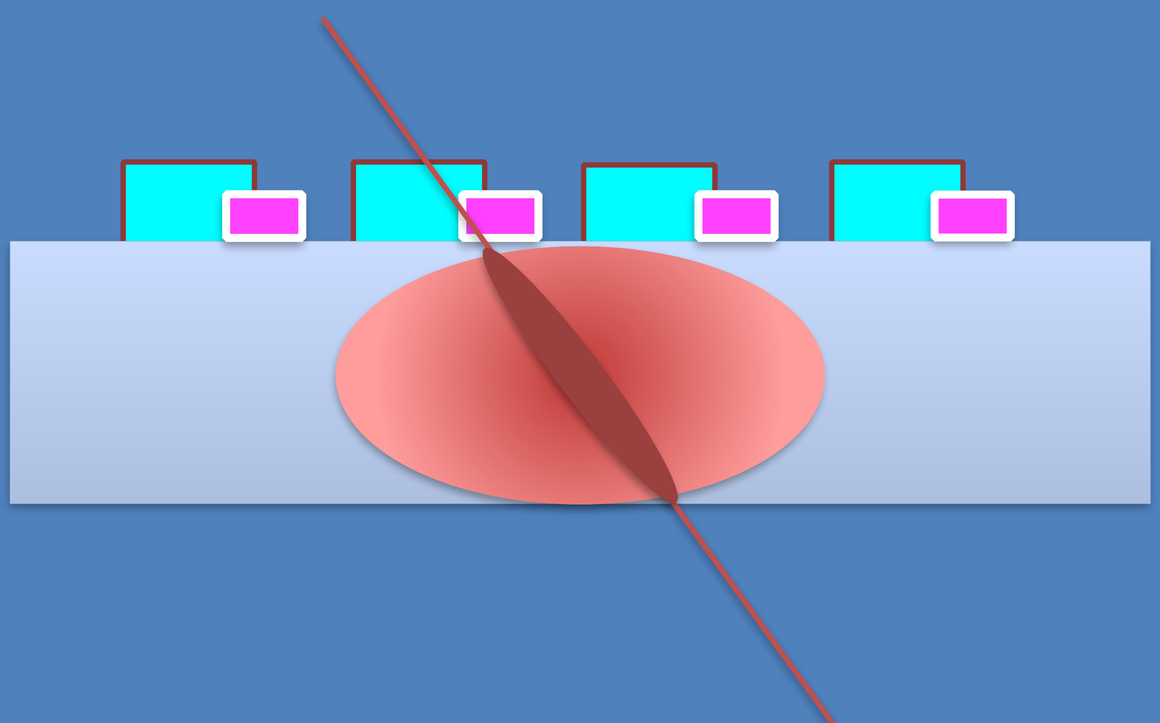

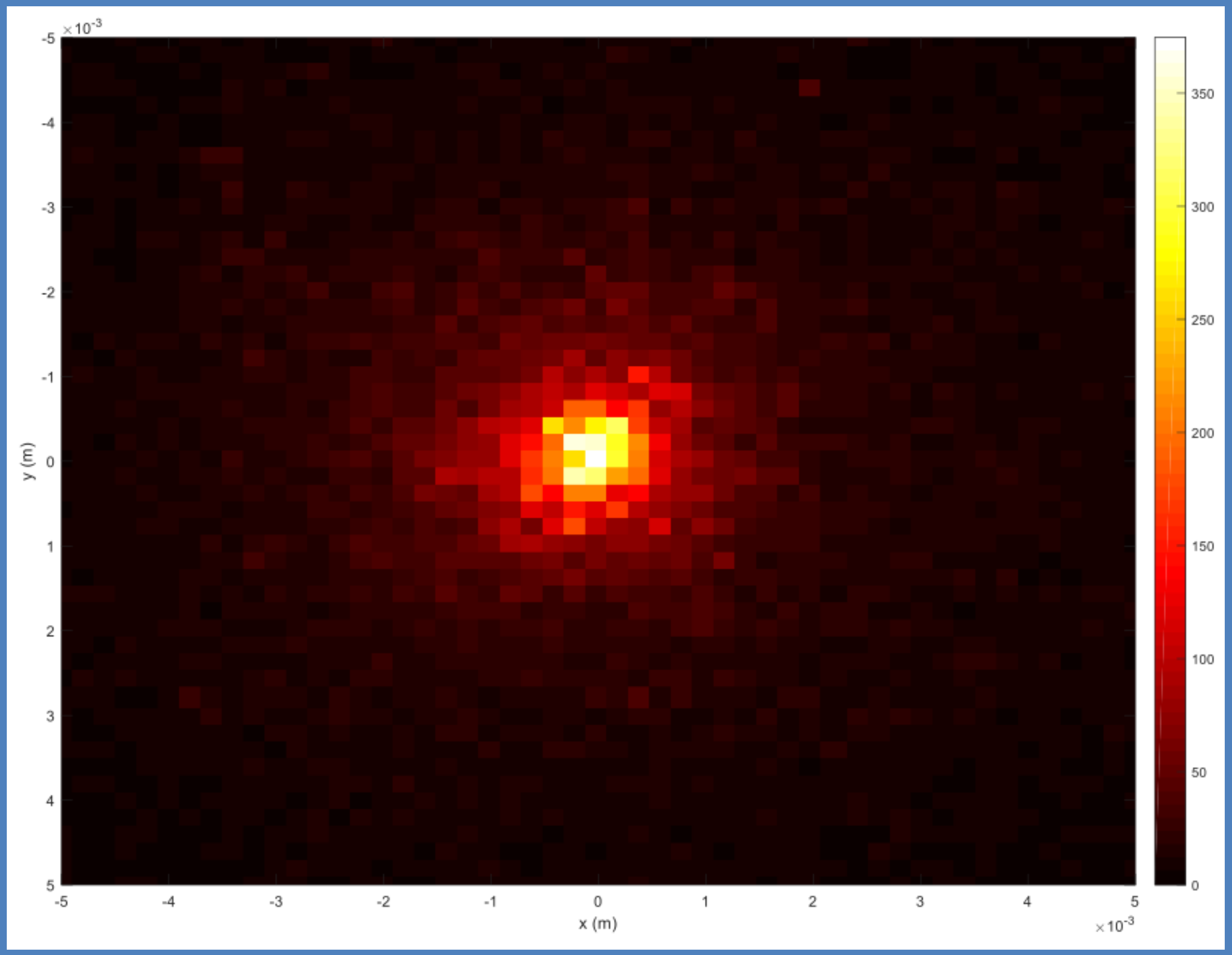

2D plot of the integrated heat flux (arbitrary unit) at the surface (pixel size=200 μm

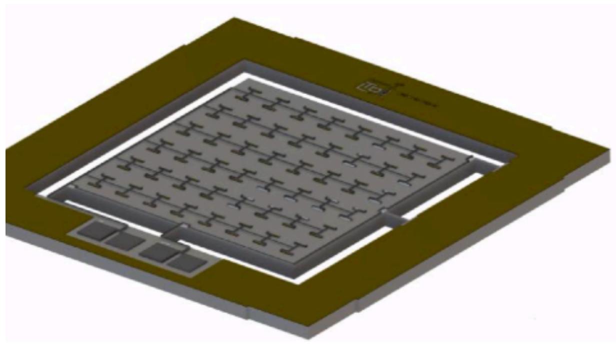

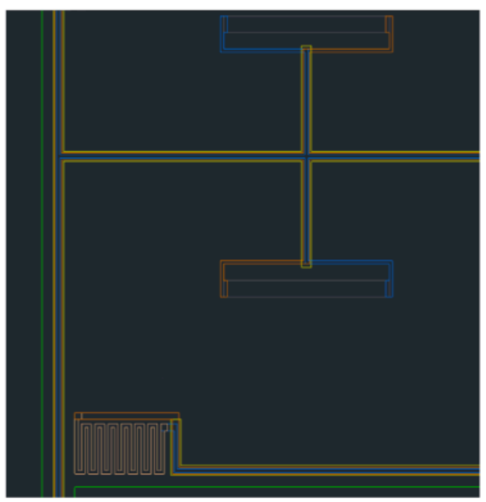

- Planar device
- Baseline: 96 TESs without aluminum fingers
- Freestanding silicon absorber 10 × 10 mm^2
- 4 silicon beams
- Silicon thickness 500 µm
- TESs Ir:Au bilayer to reduce T_c
- Anti-inductive overlapped wiring with alternate TES biasing

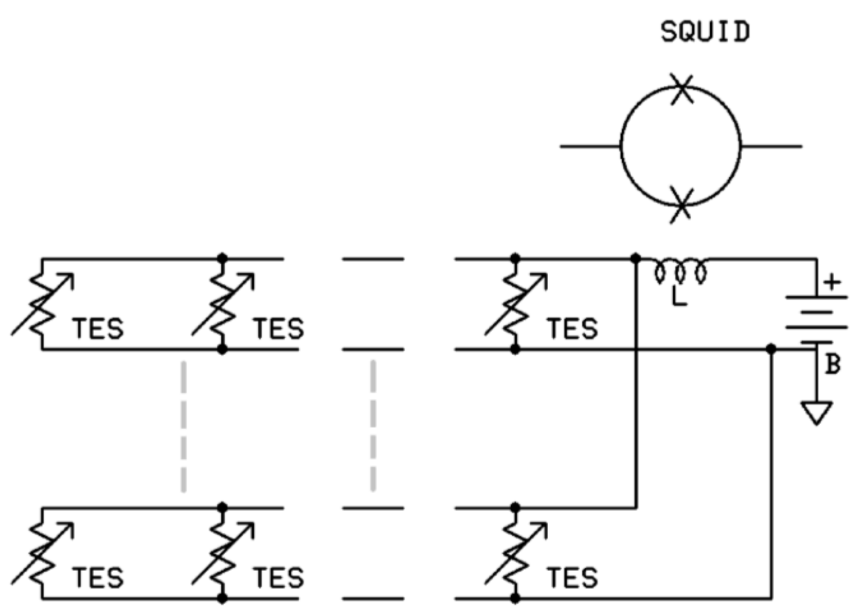

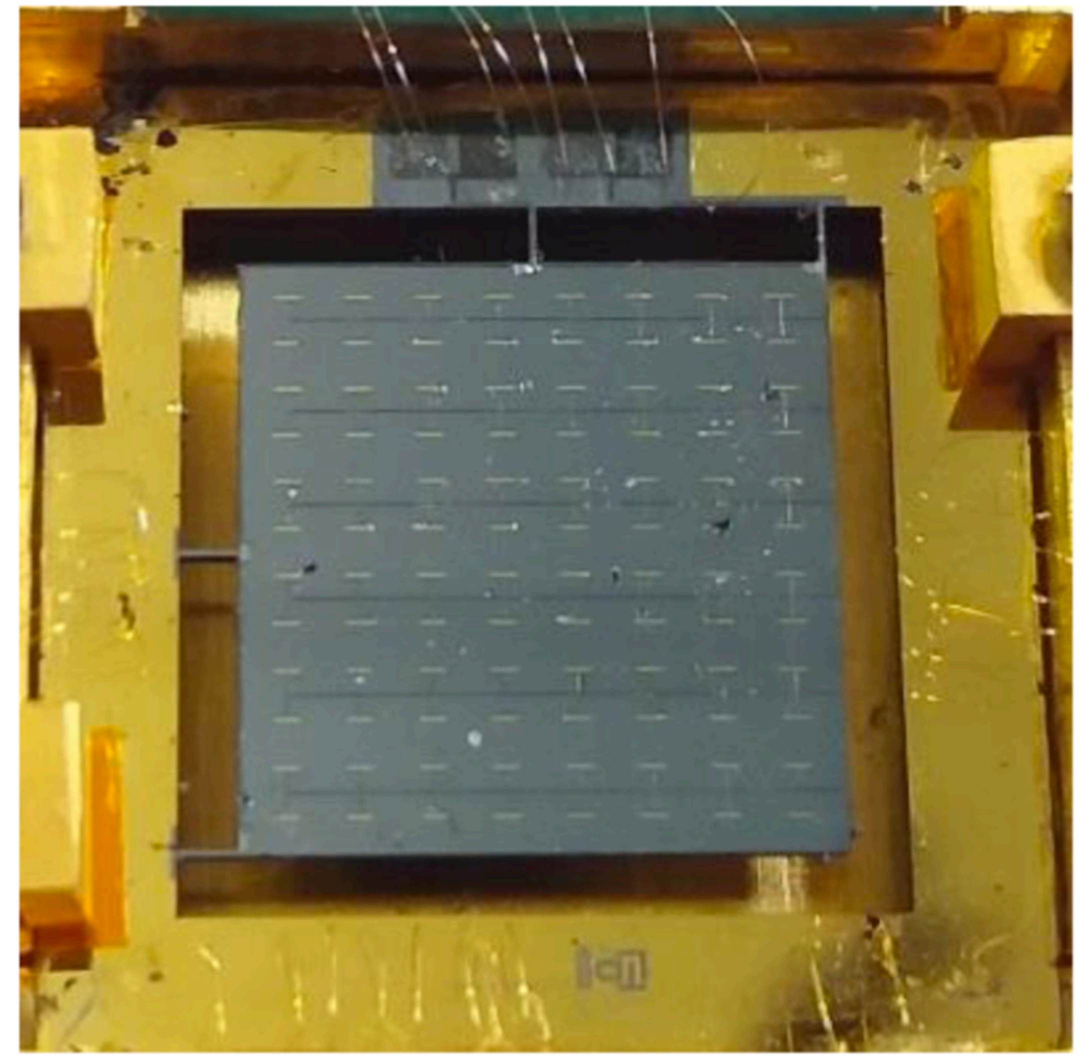

Some last snapshots of the work under way

- Amplitude of the thermal signal is of course limited by the low quality silicon of the test detector
- Decay time is also increased by the same effect
- The low resistance 1mΩ stretches the rise time
- This is a peculiarity of this detector that was not fabricated for signal —> we have already produced 1-10μs rise time and 100 μs decay time

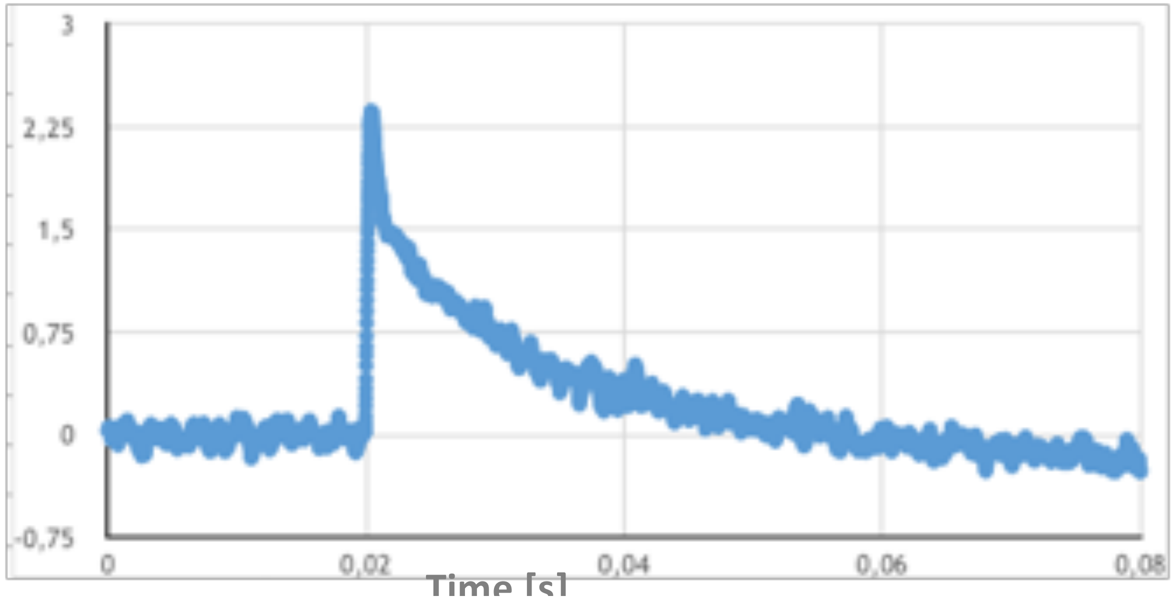

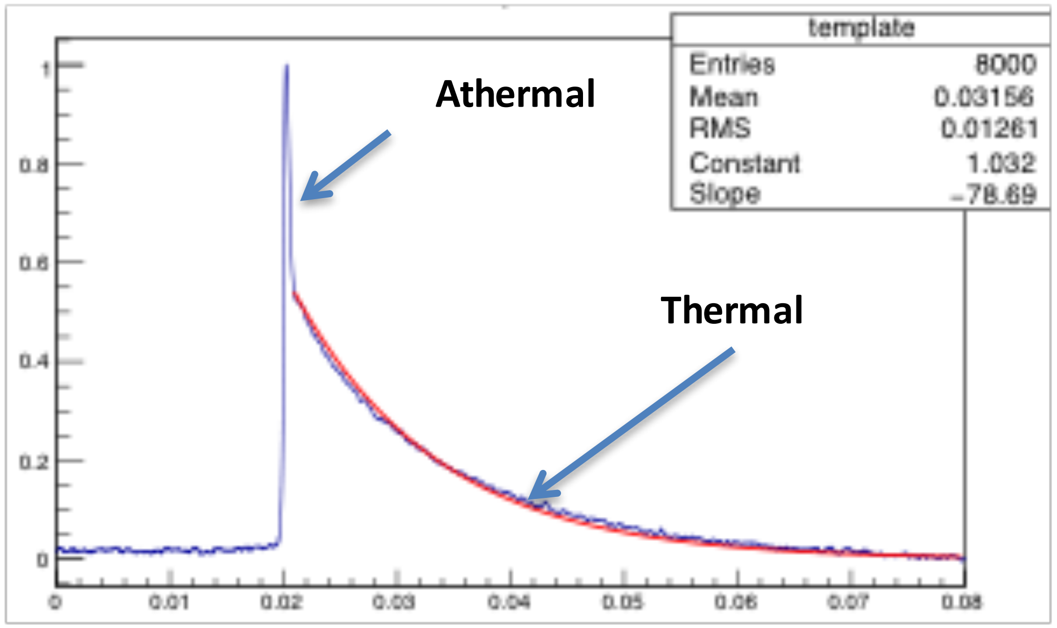

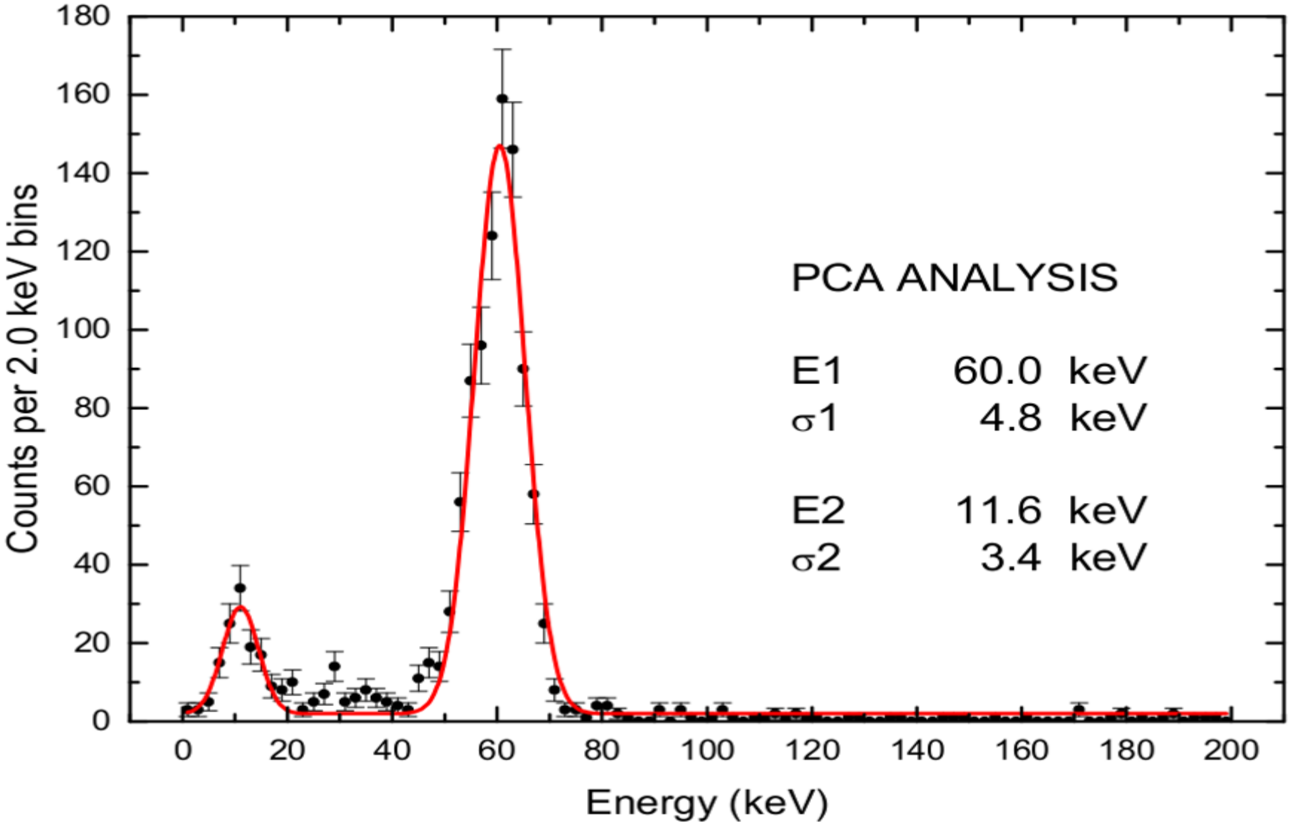

D.Corsini, M. Biasotti, F.Gatti - Uni. Genova

40Pix-B setup in SRON CTP cooler

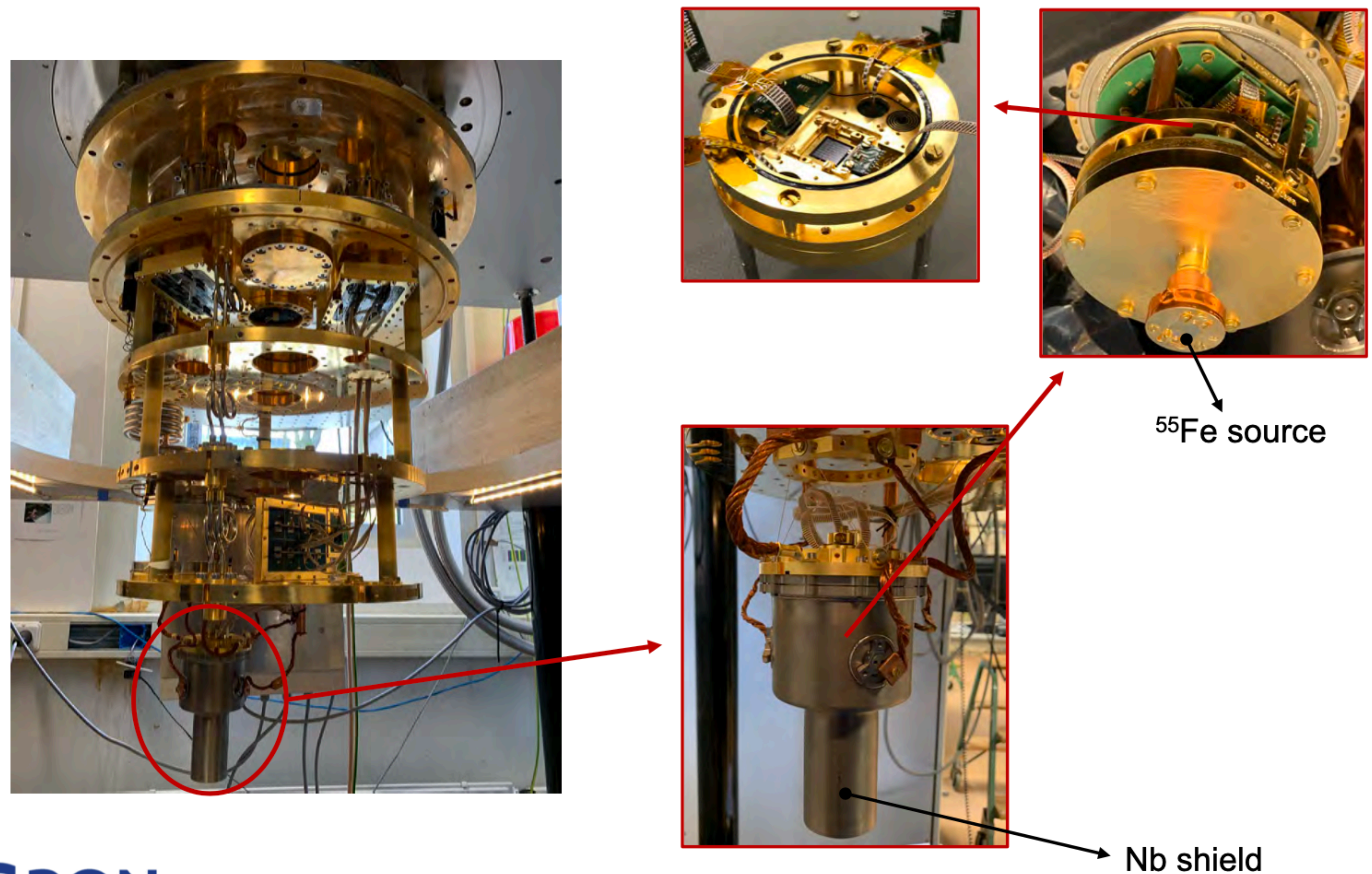

SRON

(Anti)Coincidences

- In the last weeks we have finalized the **anticoincidence capability demonstration**. We have operated simultaneously the CryoAC and 19 pixels of the TES array (**MUX mode**, 3 of 16 are blind pixels).
- In 890 ks of observation (~ 10 days), we have collected **286 coincidence events** (a factor x10 wrt last run). The observed count rate is **1.6 cts/cm^2/min**, in agreement with the expectation for cosmic muons.

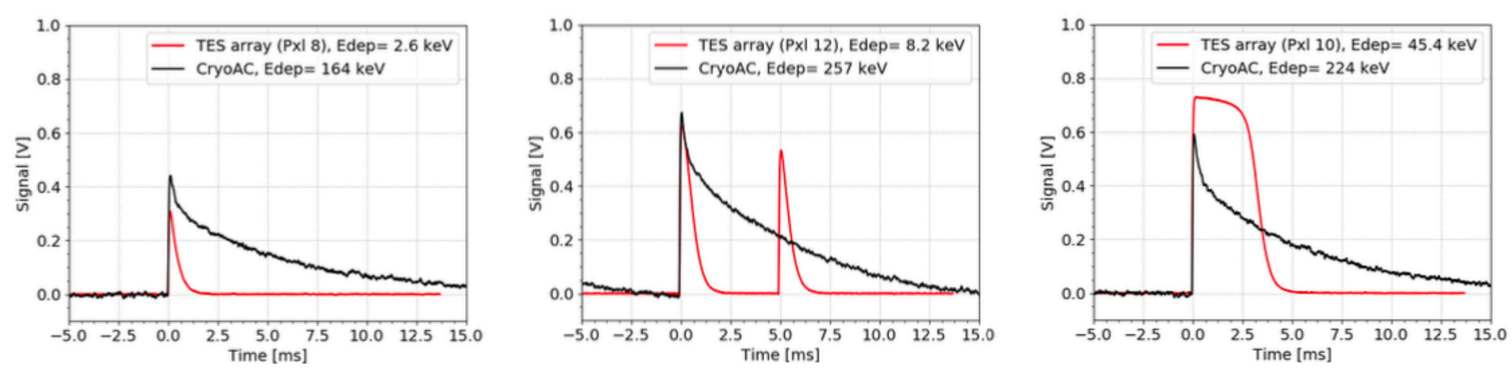

- The energy deposition on both CryoAC and TES array are consistent with the expectations for Minimum Ionizing Particles (MIPs). The **Landau distribution shape** is now more clear in the acquired spectra.

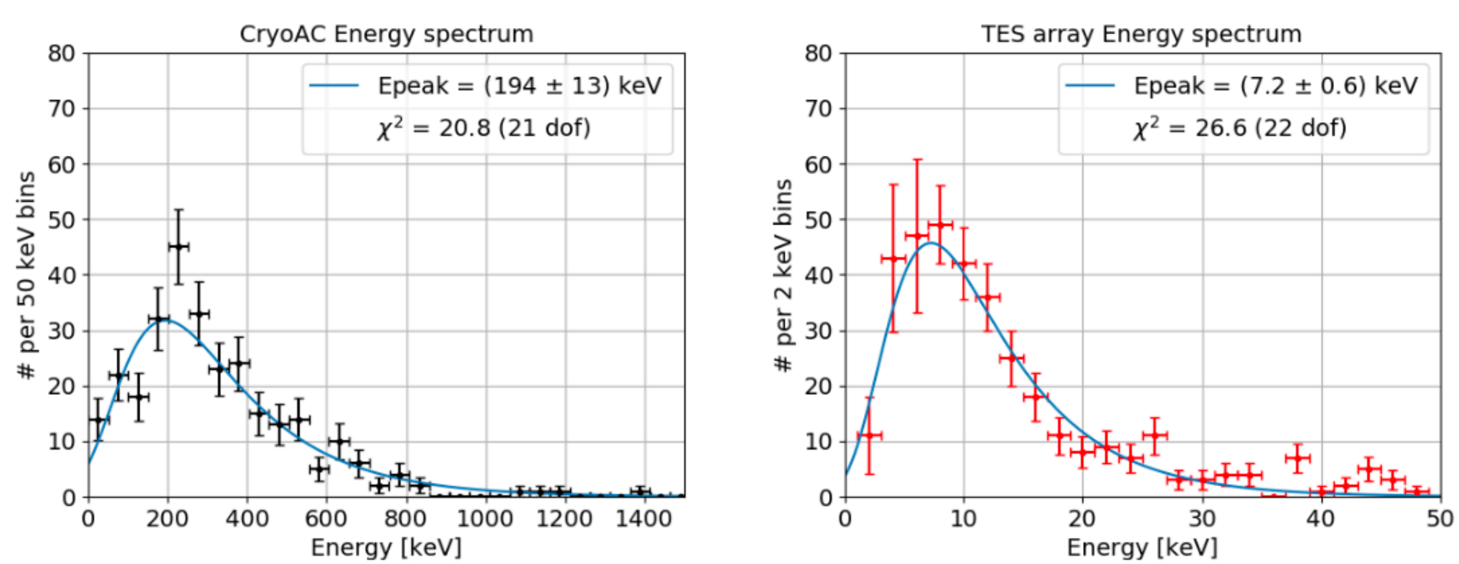

SRON

Summary

- TES is almost well know physical system presntly used in many radiation detectors,
- Nevertheless, fine physiscal effetcts (related to the superconductivity phenomena) are not fully clarified and need proper investigations.
- TES based Low T detectors offer a wide spectrum of new instruments for nuclear and particle physics, IR-UV, X-ray to gammas, microwave and THz
- Single particle/fhoton detection with VERY HIGH ENERGY RESOLUTION
- Possibility to built detector with a large variety of materials and with not “usual” geometry.
- New Sup. Electronics (SQuID Mux - M. Kiviranta talk tomorrow) allows deploying large arrays of detetctors: $O(10^4)$ bolometers and $O(10^3)$ micro-calorimeters
- Large TES-based instruments are under design for space telscopes for X-ray Astrophysics (ATHENA-ESA) and CMB (LiteBird-JAXA)
- Limitations of the cryogenics and of the MUX readout complexity are presently an affordable difficulty thanks to the huge developments in these last 10 years.
- Firts commercial LTD - EDXS systems proposed by private industries

- Suggested references: Cryogenic Particle Detection, Ed C. Enss, Springer, Handbook of applied Superconductivity. P Seidel, Wiley.